



**COLORADO**  
Department of Transportation

Applied Research and Innovation Branch

# Detention Basin Alternative Outlet Design Study

**Author:**

**Ken A. MacKenzie, P.E., Master Planning Program Manager  
Urban Drainage and Flood Control District,  
Denver, Colorado**

**Report No. CDOT-2016-04  
Oct 2016**

The contents of this report reflect the views of the author(s), who is(are) responsible for the facts and accuracy of the data presented herein. The contents do not necessarily reflect the official views of the Colorado Department of Transportation or the Federal Highway Administration. This report does not constitute a standard, specification, or regulation.

Detention Basin Alternative Outlet Design Study

**Technical Report Documentation Page**

1. Report No. CDOT-2016-04	2. Government Accession No.	3. Recipient's Catalog No.	
4. Title and Subtitle  Detention Basin Alternative Outlet Design Study		5. Report Date Oct 2016	
		6. Performing Organization Code 106.20	
7. Author(s) Ken A. MacKenzie, P.E.		8. Performing Organization Report No. CDOT-2016-04	
9. Performing Organization Name and Address  Urban Drainage and Flood Control District, Denver, Colorado		10. Work Unit No. (TRAIS)	
		11. Contract or Grant No.	
12. Sponsoring Agency Name and Address Colorado Department of Transportation - Research 4201 E. Arkansas Ave. Denver, CO 80222		13. Type of Report and Period Covered Final report	
		14. Sponsoring Agency Code	
15. Supplementary Notes Prepared in cooperation with the US Department of Transportation, Federal Highway Administration			
16. Abstract  This study examines the outlets structures CDOT has historically employed to drain water quality treatment detention basins and flood control basins, presents two new methods of metering the water quality capture volume (WQCV), namely 1) the <i>Elliptical Slot Weir</i> alternative and 2) the <i>Maximized Orifice Area</i> alternative. The study also develops new sizing guidance for the overflow outlet, and new design software that should be very helpful to CDOT and its contractors. The report documents the findings of mathematical and physical hydraulic models, presents new equations and mathematical functions to help CDOT better design these facilities, presents new design methods and software tools, and provides an overview of a new Colorado statute that CDOT must comply with regarding all stormwater detention and infiltration facilities.  Implementation			
17. Keywords Detention Basins, Extended Detention Basins, Stormwater Quality Best Management Practices, BMPs, Stormwater Control Measures, Outlet Structure Design, MS4 Compliance		18. Distribution Statement This document is available on CDOT's website <a href="http://www.coloradodot.info/programs/research/pdfs">http://www.coloradodot.info/programs/research/pdfs</a>	
19. Security Classif. (of this report) Unclassified	20. Security Classif. (of this page) Unclassified	21. No. of Pages 88	22. Price

# Detention Basin Alternative Outlet Design Study

Prepared by:

Ken A. MacKenzie, P.E., Master Planning Program Manager  
Urban Drainage and Flood Control District,  
Denver, Colorado

Submitted to:

Colorado Department of Transportation  
Research Contract (SAP # 271001746)



April 18, 2016 Draft

# **Detention Basin Alternative Outlet Design**

## **CONTENTS**

### RESEARCH STATEMENT

#### 1. INTRODUCTION

#### 2. ELLIPTICAL SLOT WEIR ALTERNATIVE

##### 2.1 Computational Fluid Dynamics (CFD) Modeling

##### 2.2 Physical Modeling at Colorado State University

##### 2.22 Weir Discharge Coefficient Analysis

##### 2.21 Development of Theoretical Rating Equation

##### 2.23 Qualitative Observations of Debris Handling Characteristics

##### 2.3 Field Installation

#### 3. MAXIMIZED ORIFICE AREA ALTERNATIVE

#### 4. NEW SIZING GUIDANCE FOR OVERFLOW OUTLET

##### 4.1 Computational Fluid Dynamics (CFD) Modeling

##### 4.2 Guo's Analysis by Comparing to CDOT Type C and D Inlet Study

##### 4.21 Weir Flow Capacity

##### 4.22 Orifice Flow Capacity

##### 4.3 Physical Modeling at the USBR Hydraulics Lab

##### 4.31 Model Setup

##### 4.32 Model Results

#### 5. DEVELOPMENT OF NEW DESIGN SOFTWARE

##### 5.1 Mathematical Model of a Detention Basin

##### 5.2 Sizing of Runoff Volumes and Required Storage Volumes

5.3 Shaping Of Inflow Hydrographs

5.4 Using the UD-Detention Workbook Model

5.41 Basin Worksheet

5.42 Outlet Structure Worksheet

6. RELEVANT NEW STATUTORY REQUIREMENTS

7. CONCLUSION

8. REFERENCES

**LIST OF FIGURES**

- Figure 1: The current standard for water quality outlet design.*
- Figure 2: Water quality metering plate with orifices spaced vertically 4" on center.*
- Figure 3: A visualization of the construction of the elliptical slot weir.*
- Figure 4: Elliptical slot weir design information.*
- Figure 5: Fluid configuration visualization.*
- Figure 6: Stage-discharge curve for elliptical slot weir having a slot width of 0.01 ft.*
- Figure 7: Stage-discharge curve for elliptical slot weir having a slot width of 0.02 ft.*
- Figure 8: Stage-discharge curve for elliptical slot weir having a slot width of 0.03 ft.*
- Figure 9: Comparison of stage-discharge family of curves for elliptical slot weirs.*
- Figure 10: Elliptical sharp-crested weir details.*
- Figure 11: Stage-discharge relationship for the 14:1 elliptical weir.*
- Figure 12: Qualitative observations on debris handling characteristics.*
- Figure 13: Extended detention basins replaced with elliptical slot weirs.*
- Figure 14: Fabrication details of water quality orifice plate and elliptical slot weir at USPS.*
- Figure 15: Fabrication details of water quality orifice plate and elliptical slot weir at Northfield.*
- Figure 16: Actual installation of water quality orifice plate and elliptical slot weir at Northfield.*
- Figure 17: Levelogger™ pressure transducer installation.*
- Figure 18: USPS detention basin storage levels for April 28, 2015 to June 10, 2015.*
- Figure 19: Northfield detention basin storage levels for April 28, 2015 to June 10, 2015.*
- Figure 20: Well screen from 1999 USDCV Vol. 3.*
- Figure 21: Bar grate from 1999 USDCV Vol. 3.*

- Figure 22 *Typical frequent clogging issues associated with well screens.*
- Figure 23 *Section showing minimized number and maximized area of water quality orifices.*
- Figure 24 *Section of outlet structure with water quality plate and overflow outlet with grate*
- Figure 25 *Basic model setup for 3:1 and 4:1 sloped overflow weirs in the CFD model.*
- Figure 26 *Outlet box model.*
- Figure 27 *Water surface cutaway.*
- Figure 28 *FLOW-3D<sup>®</sup> simulations with gradually-increasing water depths.*
- Figure 29 *FLOW-3D<sup>®</sup> resulting rating curve for the outlet box with 3:1 H:V top slope.*
- Figure 30 *FLOW-3D<sup>®</sup> resulting rating curve for the outlet box with 4:1 H:V top slope.*
- Figure 31 *Side-by-side comparison of FLOW-3D<sup>®</sup> rating curves.*
- Figure 32 *Grate dimensions.*
- Figure 33 *Weir flow overtopping submerged side along grate.*
- Figure 34 *Orifice flow through submerged area on grate.*
- Figure 35 *Physical model layout of an extended detention basin.*
- Figure 36 *Types of grates tested in USBR hydraulics lab 1/3-scale model.*
- Figure 37 *Model setup for 3:1 (H:V) and 4:1 (H:V) grate slope testing.*
- Figure 38 *Model setup for horizontal grate testing.*
- Figure 39 *Close-up of horizontal grate testing.*
- Figure 40 *100-year restrictor plate covering the final discharge pipe.*
- Figure 41 *Water quality orifice plate configurations tested in the complete EDB model.*
- Figure 42 *Data collected in the 1:0 (H:V) slope configuration for each grate.*
- Figure 43 *Data collected in the 4:1 (H:V) slope configuration for each grate.*
- Figure 44 *Data collected in the 3:1 (H:V) slope configuration for each grate.*

- Figure 45*      *Data collected on the complete EDB with micropool and 1:0 (H:V) slope.*
- Figure 46*      *Approximate boundary zones for weir flow, mixed flow, and orifice flow.*
- Figure 47*      *Sample flow oscillations that occurred when flows entered mixed zone.*
- Figure 48*      *Stage discharge plot from the 100-year orifice and overflow outlet for a 1:0 slope.*
- Figure 49*      *Locations of variables used in Table 5 equations.*
- Figure 50*      *Front view of detention basin model.*
- Figure 51*      *Side view of detention basin model.*
- Figure 52*      *Axonometric projection of detention basin model.*
- Figure 53*      *Power regression equations for ratio of stored volume to runoff volume.*
- Figure 54*      *Plot of 100-year runoff volumes and storage volumes.*
- Figure 55*      *Plot of hydrograph constants vs. shape factors for various slopes.*
- Figure 56*      *Plot of leading coefficient  $\alpha$  and exponent  $\beta$  vs. watershed slope.*
- Figure 57*      *Three hydrographs with different flow rates based on watershed shape and slope.*
- Figure 58*      *UD-Detention figure showing the three design zones.*
- Figure 59*      *“Select BMP Type” dropdown menu.*
- Figure 60*      *“Location for 1-hr Rainfall Depths” dropdown menu.*
- Figure 61*      *User-entered treatment type and watershed parameters in the Basin sheet.*
- Figure 62*      *User-entered stormwater treatment facility design parameters in the Basin sheet.*
- Figure 63*      *Stage-area-volume table created by UD-Detention program based on user inputs.*
- Figure 64*      *Graphical representation of tabulated data in Figure 63.*
- Figure 65*      *Example of built-in automation assists the user in sizing the storage volume.*
- Figure 66*      *Outlet Structure Worksheet Section 1: zones.*
- Figure 67*      *Outlet Structure Worksheet Section 2: water quality orifice placement and sizing.*

Detention Basin Alternative Outlet Design Study

- Figure 68*      *Outlet Structure Worksheet Section 3: water quality orifice table.*
- Figure 69*      *Outlet Structure Worksheet Section 4: optional vertical orifice.*
- Figure 70*      *Outlet Structure Worksheet Section 5: overflow outlet and grate.*
- Figure 71*      *Outlet Structure Worksheet Section 6: 100-year orifice and restrictor plate.*
- Figure 72*      *Outlet Structure Worksheet Section 7: emergency spillway.*
- Figure 73*      *Outlet Structure Worksheet Section 8: final output table.*
- Figure 74*      *Outlet Structure Worksheet Section 9: optional inflow hydrograph table.*
- Figure 75*      *Outlet Structure Worksheet: Graph of inflow and outflow hydrographs.*
- Figure 76*      *Outlet Structure Worksheet: Graph of ponding over time within the facility.*

**LIST OF TABLES**

<i>Table 1</i>	<i>Physical-modeling data, computed theoretical flow rates, predicted flows, and percent errors.</i>
<i>Table 2</i>	<i>Summary of equations by Guo et al. for calculating discharge.</i>
<i>Table 3</i>	<i>Summary of test configurations that were modeled.</i>
<i>Table 4</i>	<i>Discharge coefficients for each slope and grate.</i>
<i>Table 5</i>	<i>Equations to determine discharge from the EDB overflow outlet.</i>
<i>Table 6</i>	<i>Leading coefficient <math>\alpha</math> and exponent <math>\beta</math>.</i>

## Detention Basin Alternative Outlet Design

### RESEARCH STATEMENT

Extended detention and full-spectrum detention basins improve the quality of stormwater runoff through settling of sediment. This is achieved by detaining and slowly releasing the stormwater over a prescribed time duration of generally 40-72 hours. The metering of the impounded stormwater through the outlet structure is accomplished through one or more vertical columns of orifices in a steel plate that is affixed to the face of the structure, such that the orifices span the depth of the water quality impoundment. These orifices are protected from debris clogging with a well screen, as shown in Figure 1. While this practice has been proven to reduce TSS and related pollutants, maintenance of the orifices and the well screen is significant. An alternative outlet that is less susceptible to clogging and therefore requires less frequent maintenance would be of great benefit to the Colorado Department of Transportation (CDOT) and others.



*Figure 1. The current standard for water quality outlet design includes a column of small orifices, protected from clogging by a well screen (shown removed for maintenance). The well screen was added after earlier installations demonstrated a great propensity for clogging. Unfortunately, the well screen also becomes clogged and is considered a significant maintenance issue for CDOT field personnel.*

Key Words: Stormwater Detention Practices, Water Quality Capture Volume, Excess Urban Runoff Volume, Extended Detention Basin, Outlet Structure, Micropool, Stormwater Maintenance.

## 1. INTRODUCTION

All new construction and redevelopment sites in the CDOT MS4 (Municipal Separate Storm Sewer System) permit area are required to evaluate whether stormwater controls are required per CDOT's NDRD (New Development and Redevelopment) Program requirements to address higher runoff volumes and pollutant loads associated with an increase in impervious surfaces. These controls are here referred to as Permanent Water Quality Control Measures (also known as permanent Best Management Practices or BMPs). Water quality control measures must be periodically maintained to ensure functionality. Therefore, CDOT requires facility inspections to identify any maintenance needs such as sediment or weed removal.

The Urban Drainage and Flood Control District (UDFCD) promulgates regional stormwater quality criteria including design standards for extended detention basins to remove sediment by settling action. For many highway projects, extended detention basins represent the default water quality BMP and there are thousands of these basins in service across the Colorado. As recently as 2010, the UDFCD's *Urban Storm Drainage Criteria Manual (USDCM) Volume 3* recommended an outlet structure for detention basins that included a water quality plate having orifices spaced 4" vertically on center and being sized such that the water quality capture volume (WQCV) drain out in 40 hours or longer, as shown in Figure 2.

The problem with this guidance is that smaller water quality orifices clog more quickly, and the UDFCD guidance often resulted in very small orifices. CDOT has followed the UDFCD guidance in numerous detention basin outlet structure designs. In September 2012, UDFCD and CDOT partnered to jointly fund a study to examine alternatives to the columns of small orifices and accompanying well screens which represent the state of practice for water quality, and also to examine the hydraulic characteristics of detention basin overflow outlets and develop equations, methods, and tools to better design stormwater quality extended detention basins.

## Detention Basin Alternative Outlet Design Study

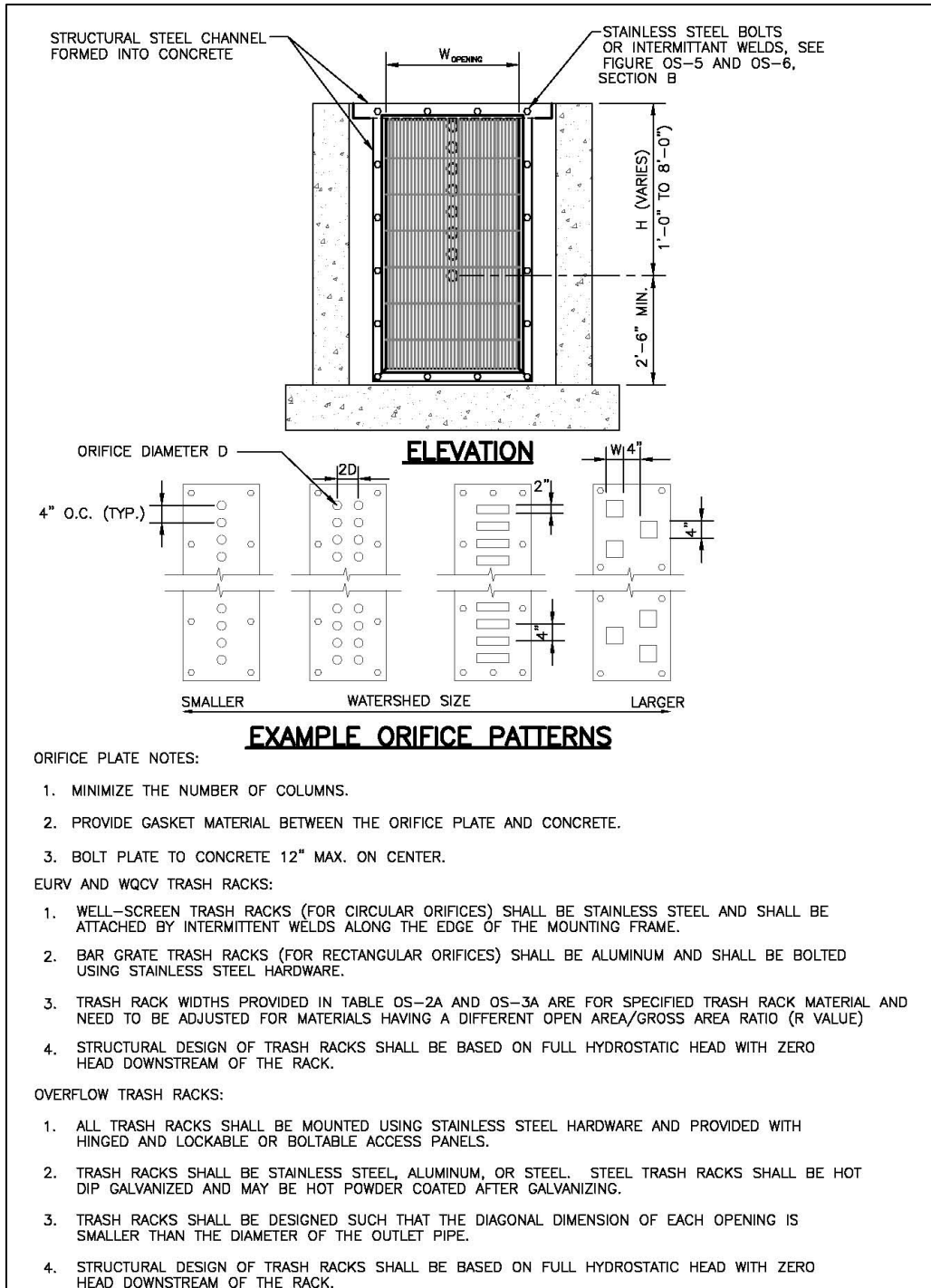


*Figure 2. As recently as 2010, the USDCM recommended a water quality metering plate with orifices spaced vertically 4" on center. This guidance often resulted in very small water quality orifices that were prone to clogging and created nuisance ponding of water and maintenance problems.*

## 2. ELLIPTICAL SLOT WEIR ALTERNATIVE

In order to provide the slow metering of the WQCV necessary to remove sediment through settling, a V-notch weir was analyzed. It was apparent that the slot would have to be very narrow in order to not drain too quickly and an adjustment to the shape of the V-notch resulted in an elliptical slot. The principal benefit of the elliptical shape over the simple V shape is that it drains the top zone more quickly and the lower zone more slowly, allowing better settling of the storage volume and resulting in cleaner stormwater discharges. A schematic is shown as Figure 3.

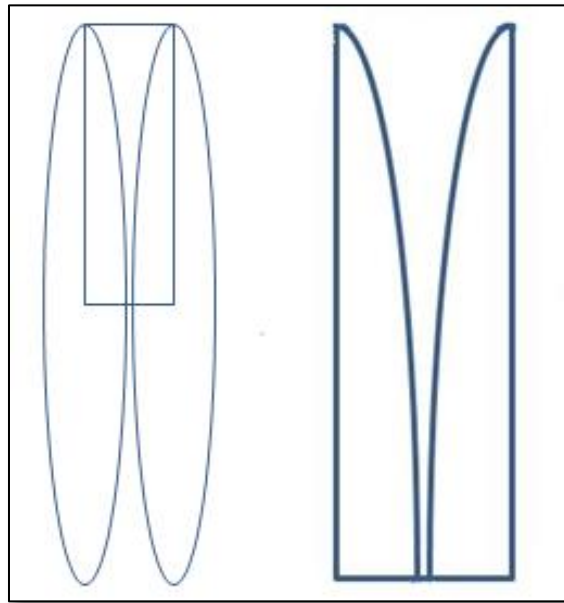


*Figure 3. A visualization of the construction of the elliptical slot weir from the gap between the upper halves of two vertical ellipses having a large major-to-minor axis ratio.*

### 2.1 Computational Fluid Dynamics (CFD) Modeling

In May 2011 UDFCD contracted with ARCADIS U.S., Inc. to perform Computational Fluid Dynamics (CFD) modeling of the weir. This modeling was based on a design where the major axis of the ellipse was ten times greater than the minor axis of the ellipse used to construct the profile of the weir. The gap width at the bottom of the notch was equal to 0.04 ft, and the total height of the weir was equal to 3.0 ft as shown in Figure 4.

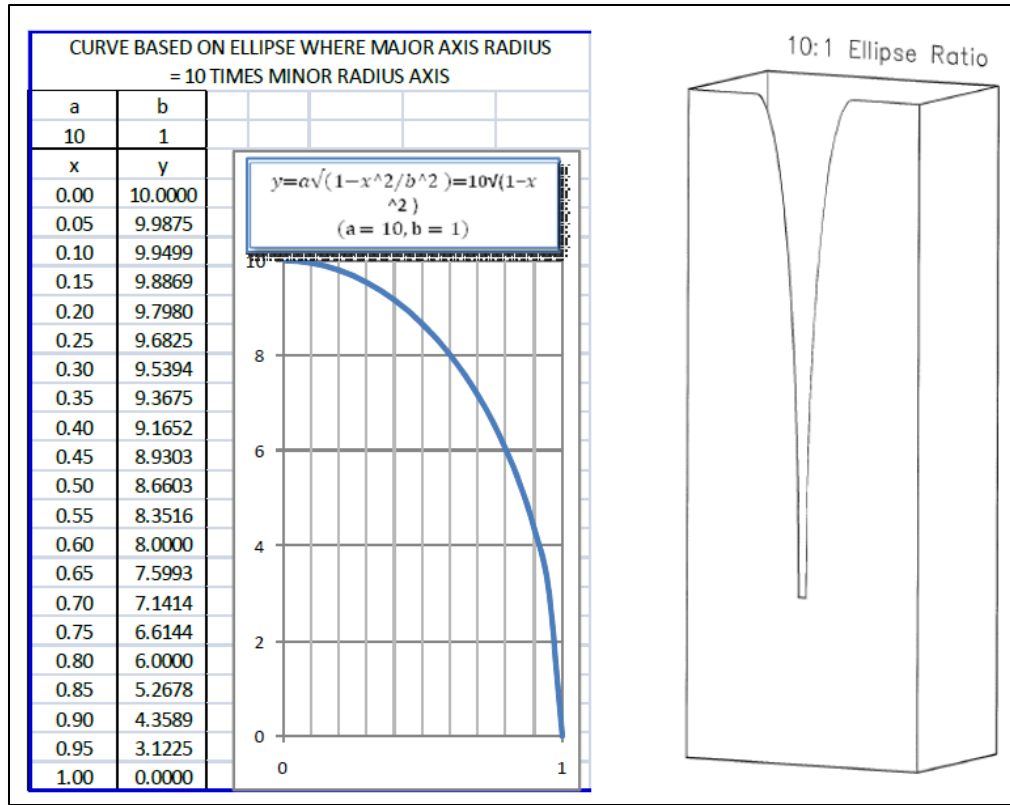


Figure 4. Elliptical slot weir design information.

Three different CFD models of the weir were constructed. The first model contained 216,000 control volumes (40 x 60 x 70) and the other models contained 25% more total control volumes and 25% less total control volumes. Comparison tests, based on results provided by these different models, were used to assess grid sensitivity. Other tests were also carried out to determine the sensitivity of model results to turbulence closure and program version. In all of the simulations carried out, an \*.stl file was used to define the weir structure inside of the model grid.

In each of the calculations flow was introduced at the model boundary upstream of the weir (specified water surface elevation) and flow left the domain downstream of the weir (continuative boundaries at the at the bottom and downstream side of the grid). No-slip boundary conditions were specified at all solid walls, and two different turbulence closure schemes were invoked (the Renormalized Group (RNG) model for turbulence was used in some of the calculations and the standard k-e model for turbulence was used in others). Sample graphics

showing the calculated fluid configuration for flows with head elevations equal to 1.0 ft and 2.0 ft are provided in Figure 5. In these visualizations the fluid free-surface is defined as the location of the three-dimensional contour where the volume fraction is equal to 0.5. In frames (c) and (d), the fluid body has been colored by pressure - a hydrostatic distribution exists upstream of the weir and pressures in the nappe are atmospheric.

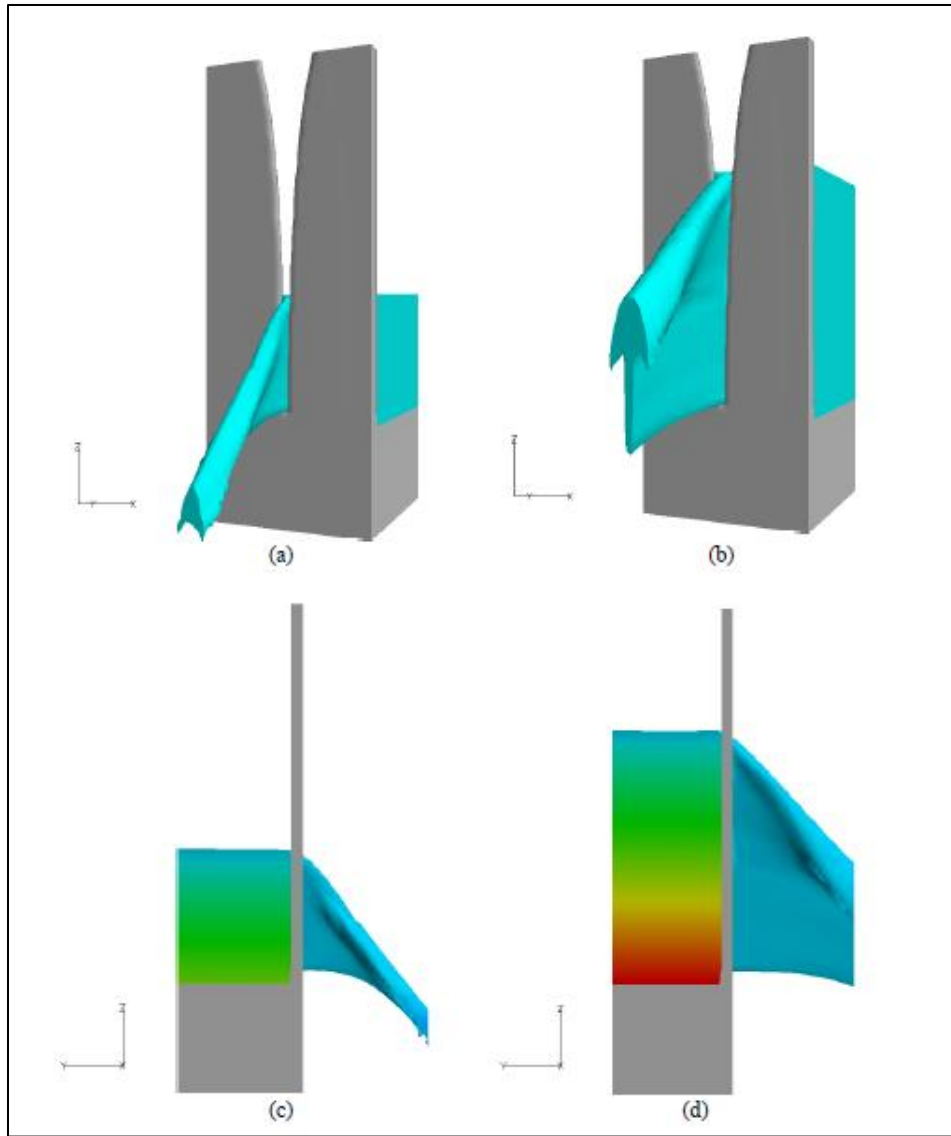


Figure 5. Fluid configuration: (a) 1.0 ft Head, (b) 2.0 ft Head, (c) 1.0 ft Head, Side View, Colored by Pressure – Common Scale, (d) 2.0 ft Head, Side View, Colored by Pressure – Common Scale.

Stage-discharge curves for an elliptical slot weirs having a 10:1 major-to-minor axis ratio and slot gaps of 0.01, 0.02, and 0.03 ft were developed from the CFD model and are shown in Figures 6 through 9.

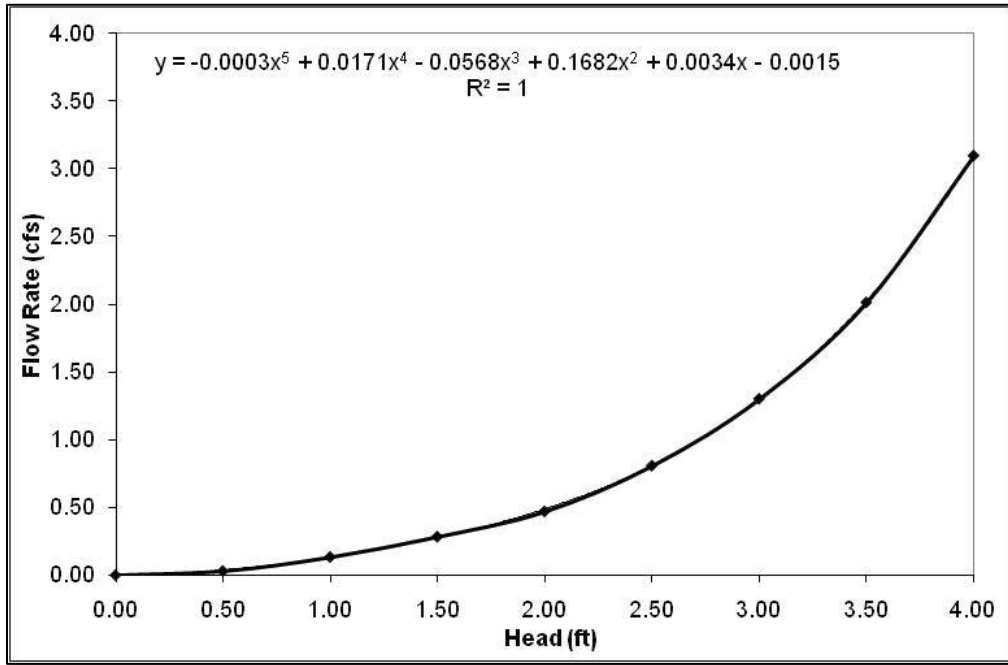


Figure 6. Stage-discharge curve for elliptical slot weir having a 10:1 major-to-minor axis and a slot width of 0.01 ft.

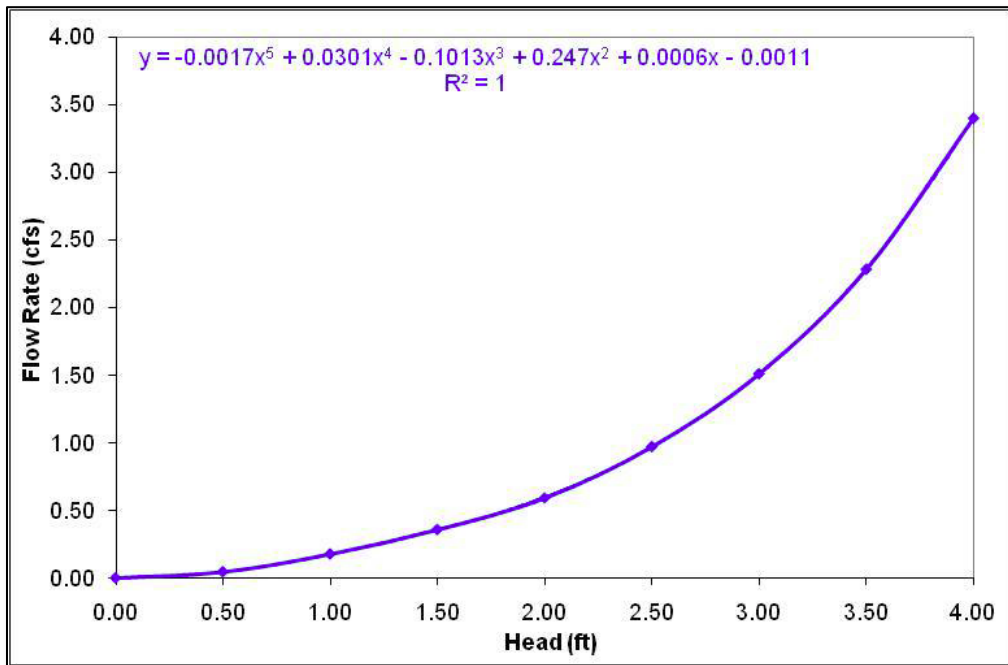


Figure 7. Stage-discharge curve for elliptical slot weir having a 10:1 major-to-minor axis and a slot width of 0.02 ft.

Detention Basin Alternative Outlet Design Study

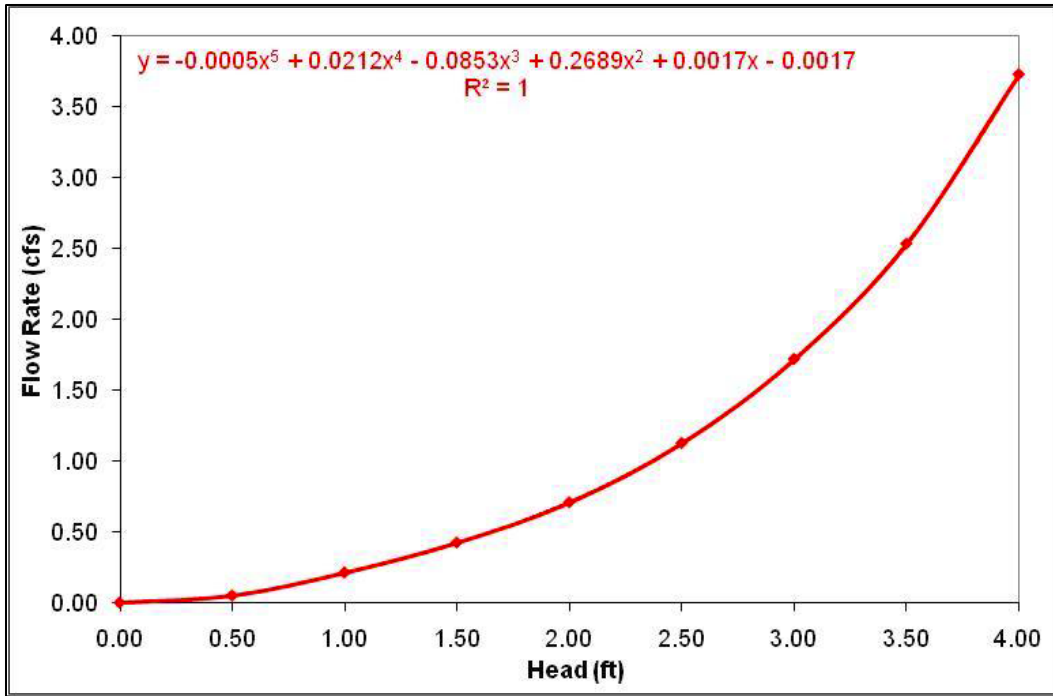


Figure 8. Stage-discharge curve for elliptical slot weir having a 10:1 major-to-minor axis and a slot width of 0.03 ft.

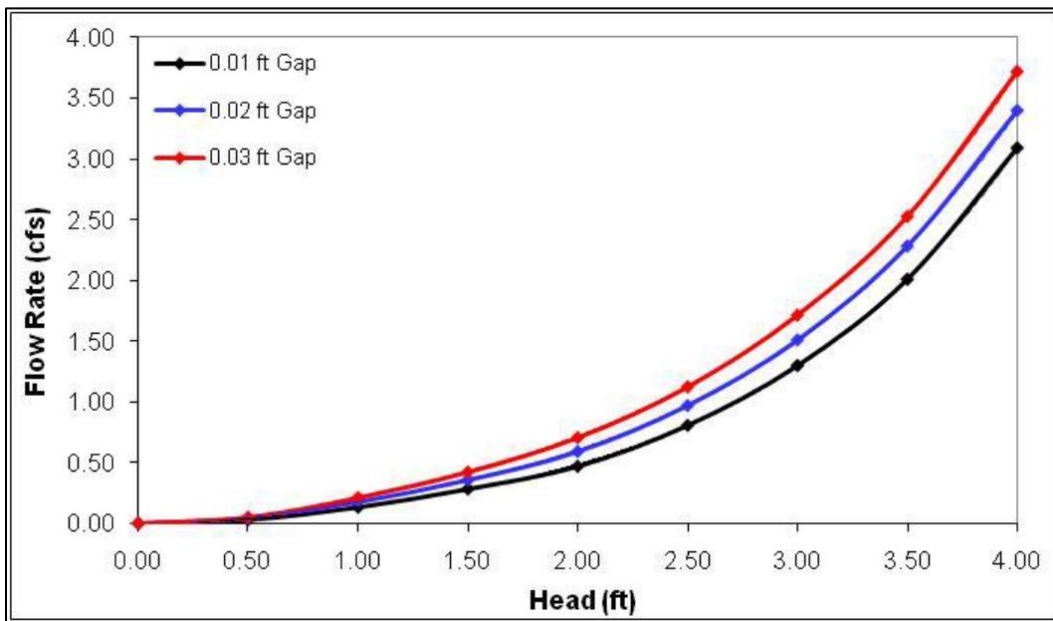


Figure 9. Comparison of stage-discharge family of curves for elliptical slot weirs having a 10:1 major-to-minor axis ratio and slot gaps of 0.01, 0.02, and 0.03.

## 2.2 Physical Modeling at Colorado State University

In December 2011 UDFCD contracted with Colorado State University to perform physical modeling of the elliptical slot weir. The results of that study were reported by Cox et al. in the ASCE Journal of Irrigation and Drainage Engineering in June 2014 (Volume 140, Issue 6) and are repeated here. A 2:1 Froude-scale physical model was constructed and stage-discharge data were collected to analyze the stage-discharge relationship of the new weir. A total of 45 steady-state tests were conducted encompassing nine unique weir geometric configurations. The ellipse ratio varied from 12 to 16, and the gap width varied from 1.5 to 9.1 mm (0.005 to 0.030 ft). A theoretical rating equation was derived for the elliptical weir and a discharge coefficient of 0.642 was determined from analyzing the physical-model data. Trapezoidal integral approximation was used to develop an explicit approximate solution for the theoretical rating equation. By using the trapezoidal integral approximation, measured discharges were predicted with a mean absolute percent error of 3.55% for the data set, excluding discharges lower than 2.83 L/s (0.10 cfs).

The objective of this research was to develop a rating equation for the elliptical sharp-crested weir. The elliptical sharp-crested weir was fabricated and tested to provide data for validation of a theoretical rating equation and calibration of discharge coefficients.

A common approach for developing theoretical stage-discharge relationships for weirs is integrating the flow velocity over elementary flow layers as shown by Eq. 1:

$$Q = \int_0^h U dA = \int_0^h \sqrt{2gy'} L dy \quad (1)$$

Where  $Q$  = outlet discharge [ $L^3T^{-1}$ ];  $U$  = flow velocity [ $LT^{-1}$ ];  $dA$  = elementary flow area [ $L^2$ ];  $g$  = gravitational acceleration [ $LT^{-2}$ ];  $y'$  = distance measured from the water surface (see Figure 10(a)) [ $L$ ];  $L$  = weir-opening length [ $L$ ];  $h$  = head above the horizontal sill [ $L$ ]; and  $dy$  = elementary flow vertical distance [ $L$ ]. Discharge coefficients are generally a function of weir geometry, approach velocity, fluid viscosity, and surface tension. The FHWA HEC-22 presented the rating equation for a proportional weir with a linear head-discharge relationship and a 0.62 coefficient of discharge (FHWA 2009).

Sharp-crested weirs were constructed with 16:1, 12:1, and 14:1 ellipse ratios at the Engineering Research Center (ERC) of CSU using computer numeric control (CNC) technology with linear positional tolerance of  $12.7\ \mu\text{m}$  (0.0005 inch). Each ellipse ratio was tested with three different gap widths ranging from 1.5 to 9.1 mm (0.005 to 0.030 ft) to provide laboratory data for the development of a stage-discharge prediction equation. Gap widths were verified using a caliper with an accuracy of  $\pm 50.8\ \mu\text{m}$  (0.002 inch).

The physical model was constructed within an existing facility that measured 2.44-m (8-ft) wide, 10.82-m (35.5-ft) long, and 0.91-m (3-ft) deep with a constant longitudinal slope of 0.0135 m/m as shown in Figure 10. The model consisted of a supply pipe network, a flume headbox, a flume/reservoir section containing the weir outlet, a tailbox to capture returning flow, and the supporting superstructure. The ellipse weir was located inside the flume section and was the only flow outlet. The vertical distance measured from the bottom of the approach channel to the weir crest was constant at 0.1524 m (0.5 ft) for all tests. A diffuser screen was installed at the junction between the headbox and the reservoir section to provide quiescent approach-flow conditions. A 2:1 exact Froude scale was chosen for the model study based on maximizing the model size with the available laboratory space. Additionally, the weir crest incorporated a 1-mm horizontal section followed by a  $45^\circ$  taper on the downstream side of the weir which is consistent with sharp-crested weir specifications.

## Detention Basin Alternative Outlet Design Study

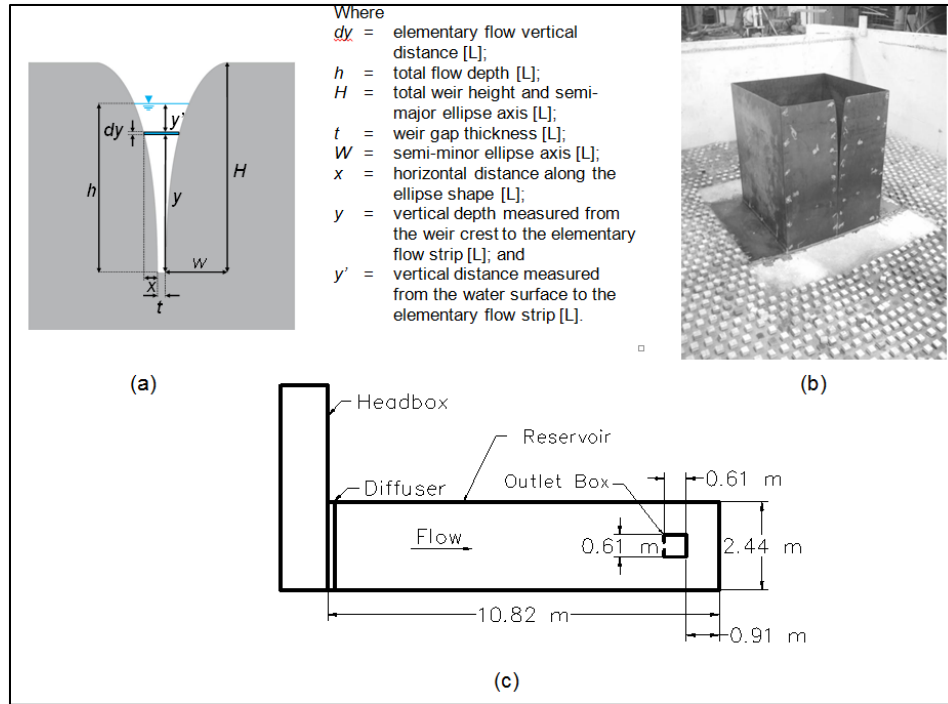


*Figure 10. Elliptical sharp-crested weir: (a) cross-section sketch of elliptical-weir parameters; (b) photograph of the elliptical sharp-crested weir; (c) plan-view sketch of the test flume setup.*

For all tests, water was gravity-fed into the flume directly from Horsetooth Reservoir. Discharge to the flume was controlled with two gate valves on a 76-mm (3-inch) pipeline and was measured using a Venturi meter with an accuracy of  $\pm 2.5\%$ . Water-surface elevations were recorded approximately 0.6 m (2 ft) upstream of the outlet using a Vernier point gage (accurate to  $\pm 0.30$  mm ( $\pm 0.001$  ft)). The point-gage measurement location was chosen to ensure the elevation was not within the draw-down section at the outlet. Additionally, water-surface elevations were measured using a pressure transducer located on the side of the outlet box away from the outlet draw-down section.

Initially, the discharge was set to achieve a flow depth corresponding to the top of the 0.61-m (2-ft) weir to determine the maximum capacity of the weir before overtopping the entire outlet box. Subsequently, steady-state discharge tests were conducted using 15, 26, 42, 65, and 100% of maximum flow capacity for each of the nine configurations resulting in a total of forty-five steady-state tests. Steady-state conditions were achieved for each test, where the discharge was set at a constant value and the water-surface elevation was monitored over time using the

pressure transducer with LabVIEW software. Data collected for each test included water temperature, water-surface elevations, and discharge. Figure 11 provides the stage-discharge relationship for the 14:1 tests to illustrate the general stage-discharge trends for the elliptical weir. Stage-discharge data for the 16:1, 12:1, and 14:1 configurations are provided in Table 2.

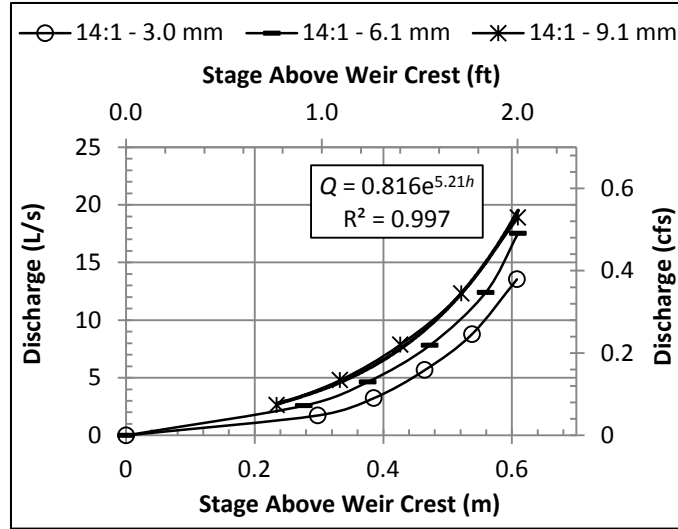


Figure 11. Stage-discharge relationship for the 14:1 elliptical weir with 3.0, 6.1, and 9.1 mm (0.010, 0.020, and 0.030 ft) gap widths, and exponential trend for 9.1 mm.

Detention Basin Alternative Outlet Design Study

Table 1. Physical-modeling Data, Computed Theoretical Flow Rates, Predicted Flow Rates, and Percent Errors

	Test ID	$t$		$h$		$Q_{meas}$		$Q_{int}$		$Q_{app}$		$Q_{pred}$		% Error
		(cm)	(ft)	(m)	(ft)	(L/s)	(cfs)	(L/s)	(cfs)	(L/s)	(cfs)	(L/s)	(cfs)	
16:1 Ellipse Ratio	1	0.152	0.005	0.314	1.031	1.13	0.040	2.04	0.072	2.03	0.072	1.30	0.046	15%
	2	0.152	0.005	0.394	1.292	2.55	0.090	3.91	0.138	3.91	0.138	2.51	0.089	-1%
	3	0.152	0.005	0.469	1.538	4.39	0.155	6.76	0.239	6.79	0.240	4.36	0.154	-1%
	4	0.152	0.005	0.536	1.760	6.80	0.240	10.60	0.375	10.68	0.377	6.85	0.242	1%
	5	0.152	0.005	0.610	2.000	10.73	0.379	16.84	0.595	16.91	0.597	10.85	0.383	1%
	6	0.305	0.010	0.300	0.985	1.44	0.051	2.54	0.090	2.51	0.089	1.61	0.057	12%
	7	0.305	0.010	0.384	1.261	3.00	0.106	4.71	0.166	4.69	0.166	3.01	0.106	0%
	8	0.305	0.010	0.476	1.563	5.61	0.198	8.60	0.304	8.60	0.304	5.52	0.195	-2%
	9	0.305	0.010	0.546	1.791	8.44	0.298	13.08	0.462	13.11	0.463	8.41	0.297	0%
	10	0.305	0.010	0.610	2.000	13.11	0.463	18.98	0.670	19.00	0.671	12.19	0.430	-7%
	11	0.457	0.015	0.294	0.963	1.64	0.058	3.12	0.110	3.07	0.109	1.97	0.070	20%
	12	0.457	0.015	0.377	1.238	3.28	0.116	5.53	0.195	5.48	0.193	3.51	0.124	7%
	13	0.457	0.015	0.459	1.507	5.52	0.195	9.13	0.323	9.08	0.321	5.83	0.206	6%
	14	0.457	0.015	0.539	1.768	8.64	0.305	14.33	0.506	14.30	0.505	9.18	0.324	6%
	15	0.457	0.015	0.610	2.000	13.37	0.472	21.12	0.746	21.08	0.744	13.52	0.478	1%
12:1 Ellipse Ratio	16	0.152	0.005	0.317	1.039	1.76	0.062	2.51	0.089	2.51	0.089	1.61	0.057	-8%
	17	0.152	0.005	0.395	1.297	3.51	0.124	4.91	0.174	4.93	0.174	3.16	0.112	-10%
	18	0.152	0.005	0.467	1.531	5.78	0.204	8.41	0.297	8.46	0.299	5.43	0.192	-6%
	19	0.152	0.005	0.539	1.767	9.09	0.321	13.74	0.485	13.86	0.489	8.89	0.314	-2%
	20	0.152	0.005	0.610	2.000	13.93	0.492	21.73	0.767	21.86	0.772	14.03	0.495	1%
	21	0.305	0.010	0.314	1.031	1.90	0.067	3.25	0.115	3.22	0.114	2.07	0.073	9%
	22	0.305	0.010	0.391	1.284	3.54	0.125	5.86	0.207	5.85	0.207	3.75	0.132	6%
	23	0.305	0.010	0.468	1.537	5.97	0.211	9.96	0.352	9.97	0.352	6.40	0.226	7%
	24	0.305	0.010	0.539	1.770	9.17	0.324	15.61	0.551	15.67	0.553	10.06	0.355	10%
	25	0.305	0.010	0.610	2.000	14.41	0.509	23.87	0.843	23.94	0.845	15.36	0.542	7%
	26	0.457	0.015	0.277	0.908	2.12	0.075	3.02	0.107	2.98	0.105	1.91	0.067	-10%
	27	0.457	0.015	0.370	1.215	4.13	0.146	6.04	0.213	5.99	0.212	3.84	0.136	-7%
	28	0.457	0.015	0.446	1.462	6.51	0.230	9.89	0.349	9.86	0.348	6.33	0.223	-3%
	29	0.457	0.015	0.531	1.742	10.56	0.373	16.55	0.584	16.56	0.585	10.62	0.375	1%
	30	0.457	0.015	0.610	2.000	16.28	0.575	26.02	0.919	26.02	0.919	16.70	0.590	3%
14:1 Ellipse Ratio	31	0.914	0.03	0.234	0.769	2.63	0.093	3.57	0.126	3.48	0.123	2.24	0.079	-15%
	32	0.914	0.03	0.333	1.092	4.79	0.169	6.93	0.245	6.81	0.240	4.37	0.154	-9%
	33	0.914	0.03	0.427	1.400	7.87	0.278	11.82	0.418	11.67	0.412	7.49	0.264	-5%
	34	0.914	0.03	0.522	1.711	12.32	0.435	19.23	0.679	19.07	0.673	12.24	0.432	-1%
	35	0.914	0.03	0.610	2.000	18.89	0.667	29.64	1.047	29.44	1.040	18.89	0.667	0%
	36	0.610	0.02	0.276	0.907	2.58	0.091	3.52	0.124	3.45	0.122	2.22	0.078	-14%
	37	0.610	0.02	0.376	1.234	4.64	0.164	6.87	0.243	6.78	0.240	4.35	0.154	-6%
	38	0.610	0.02	0.472	1.550	7.82	0.276	12.10	0.427	12.02	0.424	7.71	0.272	-1%
	39	0.610	0.02	0.559	1.835	12.40	0.438	19.40	0.685	19.34	0.683	12.41	0.438	0%
	40	0.610	0.02	0.610	2.000	17.53	0.619	25.36	0.896	25.28	0.893	16.22	0.573	-7%
	41	0.305	0.01	0.298	0.978	1.73	0.061	2.64	0.093	2.62	0.092	1.68	0.059	-3%
	42	0.305	0.01	0.385	1.264	3.23	0.114	5.11	0.181	5.09	0.180	3.27	0.115	1%
	43	0.305	0.01	0.465	1.524	5.66	0.200	8.72	0.308	8.72	0.308	5.60	0.198	-1%
	44	0.305	0.01	0.538	1.765	8.78	0.310	13.76	0.486	13.80	0.487	8.85	0.313	1%
	45	0.305	0.01	0.608	1.994	13.54	0.478	20.85	0.736	20.89	0.738	13.40	0.473	-1%

Where  $Q_{meas}$  = discharge measured in the physical model [ $L^3T^{-1}$ ];  $Q_{int}$  = discharge computed by implicitly solving the integral in Eq. (5) [ $L^3T^{-1}$ ];  $Q_{app}$  = discharge computed using the trapezoidal integral approximation [ $L^3T^{-1}$ ];  $Q_{pred}$  = predicted discharge [ $L^3T^{-1}$ ]; and all other variables have been previously defined.

## 2.21 Development of Theoretical Rating Equation

The elliptical weir stage-discharge data exhibited an exponential trend as illustrated by the exponential trend line for the 9.1-mm configuration shown in Figure 7. Although an exponential trend fits the measured data well, the discharge does not approach a value of zero when the stage value approaches zero. To accurately predict discharge throughout the entire range of stage values, a theoretical rating equation was developed for the elliptical weir following the method described by Horton (1906) and presented in Eq. 1. Figure 10(a) provides a sketch identifying the variables used in the derivation. To determine an explicit solution for the elliptical weir using the integral in Eq. 1, expressions were derived for the flow velocity ( $U$ ) and the weir opening length ( $L$ ) as a function of the vertical depth measured from the weir crest to the elementary flow strip ( $y$ ). Eq. 2 provides the expression for flow velocity as a function of the total flow depth ( $h$ ) and the vertical depth from the weir crest to the elementary flow layer ( $y$ )

$$U = \sqrt{2gy'} = \sqrt{2g(h-y)} \quad (2)$$

where all variables have been previously defined. To determine  $L$  as a function of  $y$ , initially the expression for the horizontal distance along the ellipse shape ( $x$ ) was determined as Eq. 3:

$$x = \frac{H}{R} - \frac{H}{R} \sqrt{1 - \frac{y^2}{H^2}} \quad (3)$$

Accordingly, the weir-opening length ( $L$ ) is equal to the sum of twice the horizontal distance along the ellipse shape ( $x$ ) and the weir-gap thickness ( $t$ ) as shown by Eq. 4:

$$L = 2x + t = 2 \left( \frac{H}{R} - \frac{H}{R} \sqrt{1 - \frac{y^2}{H^2}} \right) + t \quad (4)$$

Typically, end contractions are considered when computing the weir-opening length ( $L$ ) and an effective length is determined by subtracting the product of 0.1 times the number of contractions and the head above the horizontal sill ( $h$ ) (Horton 1906); however, for the ellipse weir, using that expression to compute effective weir-opening length resulted in negative weir-opening lengths for even the largest value of  $h$  (0.610 m (2.0 ft)). Therefore, the effect of end contractions was

not included in the computation of the weir-opening length for the ellipse weir. Substitution of Eq. 2 and Eq. 4 into Eq. 1 provides the final form of the integral for discharge

$$Q = \int_0^h \sqrt{2g(h-y)} \left[ 2 \frac{H}{R} \left( 1 - \sqrt{1 - \frac{y^2}{H^2}} \right) + t \right] dy \quad (5)$$

where all variables have been previously defined.

An explicit solution is not obtainable for Eq. 5 due to the complexity of the equation; therefore, trapezoidal numerical integration of Eq. 5 was used to determine an approximate solution of the definite integral (Jeffrey 1995). Eq. 6 provides the general expression for trapezoidal approximation of Eq. 5 using non-uniform intervals

$$\int_0^h f(y) dy \approx \frac{1}{2} \sum_{k=1}^N (y_{k+1} - y_k) (f(y_{k+1}) + f(y_k)) \quad (6)$$

Where  $k$  = integer for individual intervals; and  $N$  = total number of intervals. Eq. 7 provides the function equation  $f(y)$  for approximation of Eq. 5 using Eq. 6:

$$f(y) = \sqrt{2g(h-y)} \left[ 2 \frac{H}{R} \left( 1 - \sqrt{1 - \frac{y^2}{H^2}} \right) + t \right] \quad (7)$$

Through an optimization analysis comparing the implicit integral solution to the explicit trapezoidal approximation, the optimal intervals for the trapezoidal approximation were determined to be 0 to 0.603, 0.603 to 0.886, and 0.886 to 1.000 times the flow depth ( $h$ ). Eq. 8 provides the simplified expression for trapezoidal numerical approximation of Eq. 5 using Eq. 7 with the optimal intervals:

$$\begin{aligned} Q_{app} = & 0.3015h[f(0) + f(0.603h)] \\ & + 0.1415h[f(0.603h) + f(0.886h)] \\ & + 0.0570h[f(0.886h)] \end{aligned} \quad (8)$$

The trapezoidal approximation (Eq. 6) predicted the integral solution with a mean absolute percent error of 0.62%.

A key objective for the weir design is to convey a majority of the flow from the upper portion of the water column. Figure 4 shows the theoretical percent of total flow conveyed about a given vertical depth  $y$  versus the distance along the vertical depth ( $y$ ) for the example scenario. Approximately 50% of the flow is conveyed in the top one-third of the water column.

## 2.22 Weir Discharge Coefficient Analysis

A discharge coefficient ( $C_d$ ) was necessary to correct the theoretical flow equation for energy losses, velocity distribution, and streamline curvature. Three parameters were evaluated to determine the coefficient of discharge for the elliptical weir: (1) the discharge measured in the physical model ( $Q_{meas}$ ); (2) the discharge solved implicitly from the integral ( $Q_{int}$ ); and (3) the discharge calculated from the integral approximation ( $Q_{app}$ ). Initially, values for  $Q_{int}$  and  $Q_{app}$  were computed for each of physical model tests, where  $Q_{int}$  was computed from Eq. 5 using Maple™, a mathematics software program (Maplesoft™ 2013), and  $Q_{app}$  was computed using Eq. (8). Discharges predicted using the integral solution ( $Q_{int}$ ) were compared to measured discharges ( $Q_{meas}$ ) to evaluate the discharge coefficient. Measured discharges were predicted using discharges computed from implicitly solving Eq. 5 ( $Q_{int}$ ) with the discharge coefficient ( $C_d$ ) of 0.642. The predicted discharges had a mean absolute percent error of 5.11% for the entire data set and a mean absolute percent error of 3.49% for the data set excluding discharges lower than 2.83 L/s (0.10 cfs). The residual errors are evenly distributed at both high and low flows. This indicates that the effect of end contractions was encompassed within the constant discharge coefficient without the introduction of any bias associated with flow depth.

The integral approximation, Eq. 8, provides a solution that can be directly computed (explicit), which is preferable over the implicit integral technique for its ease of use. Discharge can be predicted as a function of the discharge computed using the integral approximation ( $Q_{app}$ ) and the discharge coefficient ( $C_d$ )

$$Q_{pred} = C_d Q_{app} \quad (9)$$

Where  $C_d = 0.642$ .

Discharges were predicted for the elliptical-weir data set using Eq. 9. The percent errors are elevated for the low discharges because the error is large relative to the magnitude of the

discharges; however, the magnitudes of the errors for the lower discharges are not generally greater than the errors for the remaining discharges. The mean absolute percent error for the entire data set is 5.20% and the mean absolute percent error for the data set excluding discharges lower than 2.83 L/s (0.10 cfs) is 3.55%.

### 2.23 Qualitative Observations of Debris Handling Characteristics

Qualitative debris handling tests were performed by introducing a number of neutrally buoyant items into the detained water volume as shown in Figure 12. While many of the smaller pieces of introduced debris slipped through the elliptical slot unimpeded, larger masses were caught in the slot. While these larger pieces did have to be cleared by hand, they did not completely block the elliptical slot, in every case leaving the top 1/3 – 1/2 open for flow. Initial sizing estimates indicated that the elliptical slot weir is preferable to an orifice plate for larger detention basins, but not for very small detention basins. This is due to the fact that for very small detention basins, the slot in the weir becomes unmanageably narrow. From the laboratory observations, any slot narrower than 3/8” would pose clogging issues and become a maintenance problem.



*Figure 12. Qualitative observations on debris handling indicate that the elliptical slot weir handles debris better than does an orifice plate with a well screen covering the water quality orifices.*

### 2.3 Field Installation

Two sites were selected for field installation of the elliptical slot weirs, those being the Northfield Detention Basin and the USPS Detention Basin (Figure 13). Using the slot sizing guidance produced by CSU, both of these detention basins were retrofitted with slot weirs.



Figure 13. Extended Detention basins at Northfield Stapleton where traditional water quality orifice plates were removed and replaced with elliptical slot weirs.

Detention Basin Alternative Outlet Design Study

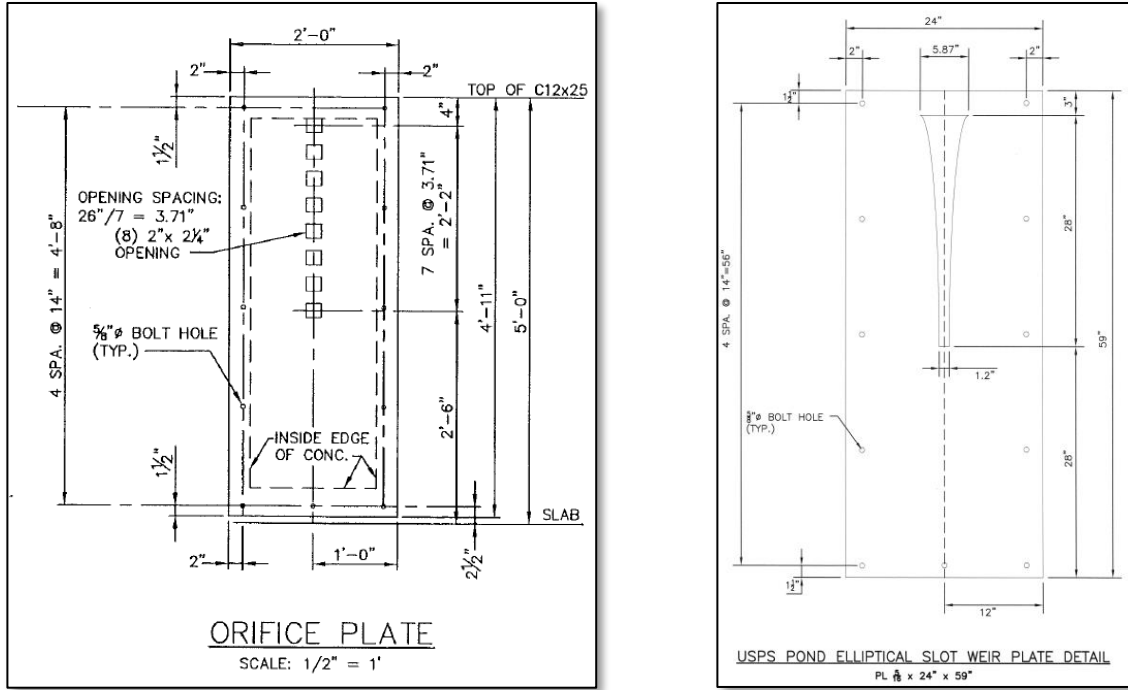


Figure 14. Fabrication details of (left) water quality orifice plate, and (right) elliptical slot weir for USPS Detention Basin.

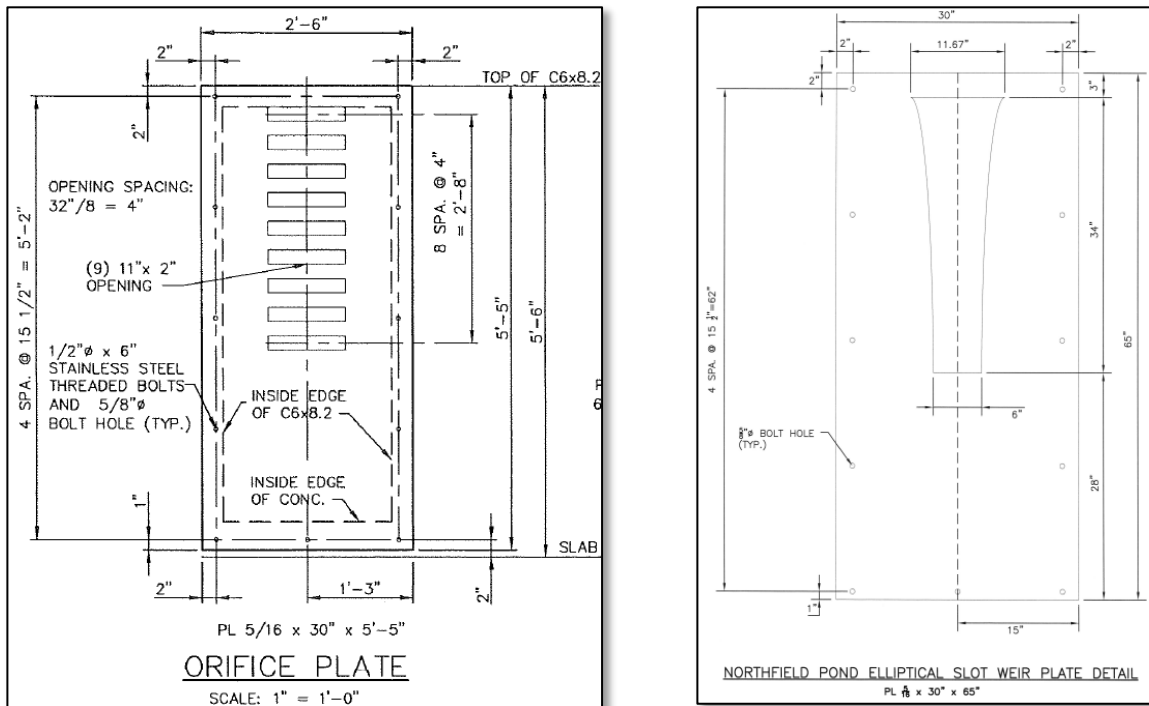


Figure 15. Fabrication details of (left) water quality orifice plate, and (right) elliptical slot weir for Northfield Detention Basin.

Detention Basin Alternative Outlet Design Study



Figure 16. Actual installation of (left) water quality orifice plate, and (right) elliptical slot weir for the Northfield Detention Basin.



Figure 17. Levelogger™ pressure transducer installation over 2014 and 2015 rainfall seasons allowed testing of the elliptical slot weir in the field.

## Detention Basin Alternative Outlet Design Study

Each of the two sites were fitted with stilling wells for Levellogger™ pressure transducers. Data were collected for the two precipitation years of 2014 and 2015, in an effort to determine whether the weir sizing algorithm that had been adopted in the laboratory produced good drain time results in a real world setting. The data from these Levelloggers™ were analyzed in early 2016. The results are produced in Figures 18 and 19.

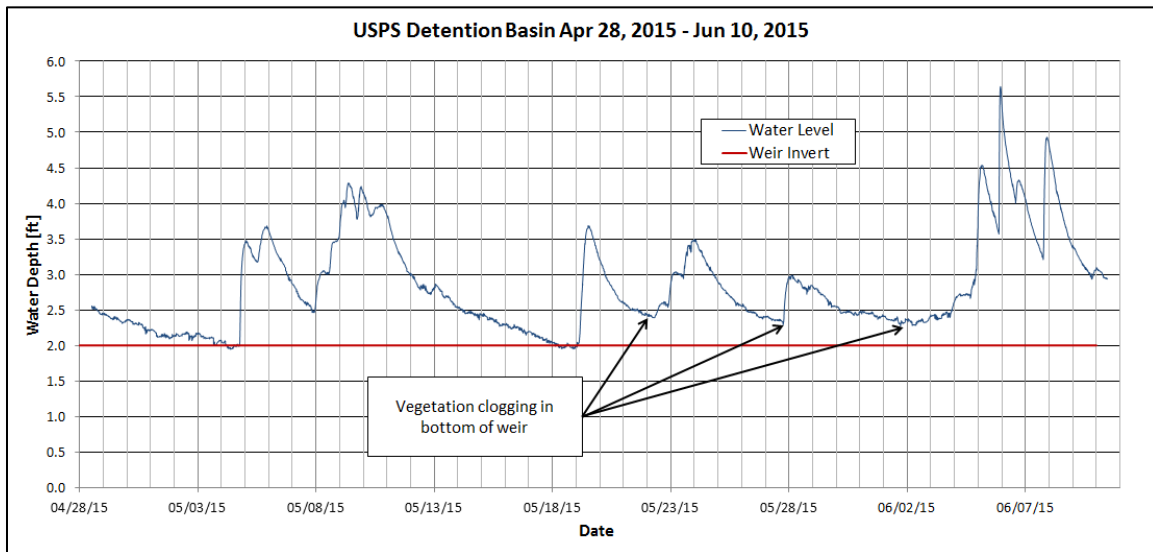


Figure 18. USPS detention basin storage levels during period of April 28, 2015 through June 10, 2015. The bottom 6 inches of the slot began to clog with cattails during the storm on May 19<sup>th</sup>.

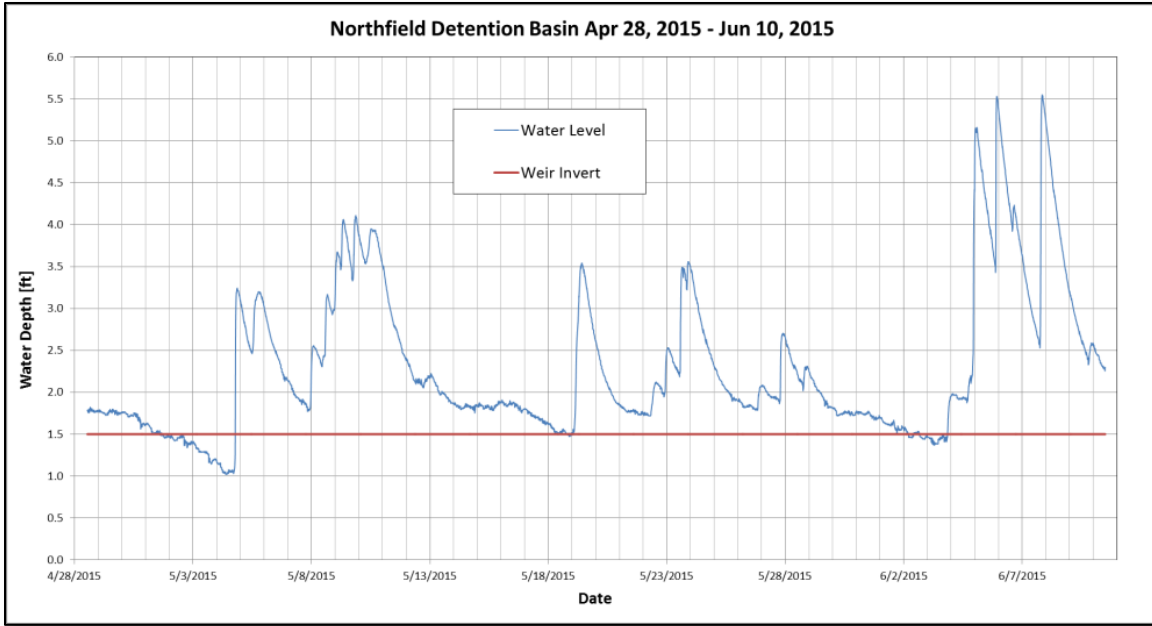


Figure 19. Northfield detention basin storage levels during period of April 28, 2015 through June 10, 2015.

Difficulties encountered during the monitoring period included the removal of the Northfield elliptical weir plate by the metropolitan district (and replacement with an orifice plate) during maintenance, subsequent leakage of the replacement plate, and clogging of the narrower weir slot at the USPS detention basin. Both of these detention basins have large permanent pools with heavy wetland vegetation cover. This creates maintenance issues regardless of what type of outlet plate is chosen. The graphs in Figures 18 and 19 indicate that, in the absence of clogging, the basins emptied the WQCV in approximately 40 hours, which was the goal of the design.

### 3. MAXIMIZED ORIFICE AREA ALTERNATIVE

The qualitative debris handling investigation in the CSU hydraulics laboratory and the two-year field testing made it clear that while the elliptical slot weir handles debris very well when the slot is wide (say greater than 1 inch), debris clogging becomes an issue as the slot grows more narrow. Based on these investigations, UDFCD does not recommend an elliptical slot weir having a slot width of less than 3/8-inch. This equates roughly to a WQCV of one acre-ft or larger, assuming a 40-hour drain time; or an excess urban runoff volume (EURV, refer to the USDCM Volume 3 for details on the EURV concept) of 1.6 acre-ft or larger, assuming a 60-hour drain time.

Understanding that most of CDOT's stormwater extended detention basins will not be large enough to qualify for the application of the elliptical slot weir, the orifice plate concept was re-evaluated to determine if there was a way to minimize clogging with that type of outlet configuration. As shown in Figure 2, the standard of practice as promulgated by UDFCD in the USDCM Volume 3 since 1999 was a column (or multiple columns) of water quality orifices spaced 4 inches vertically on center. In the USDCM, a well screen as shown in Figure 20 was specified for circular openings up to 2 inches in diameter and a bar grate as shown in Figure 21 was specified for larger orifices. The problem with this strategy was that 1) the well screen is prone to clogging, and 2) orifices larger than 2 inches in diameter were a rarity due to the close vertical spacing so the bar grate was seldom applicable.

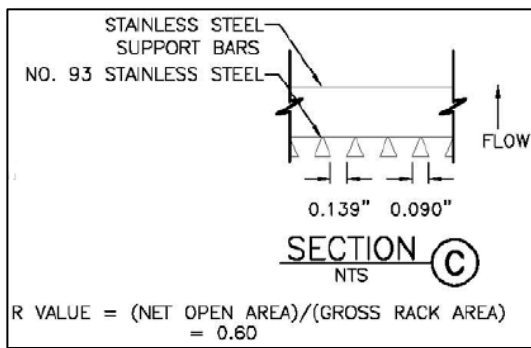


Figure 20. Well Screen from 1999 USDCV Vol 3.

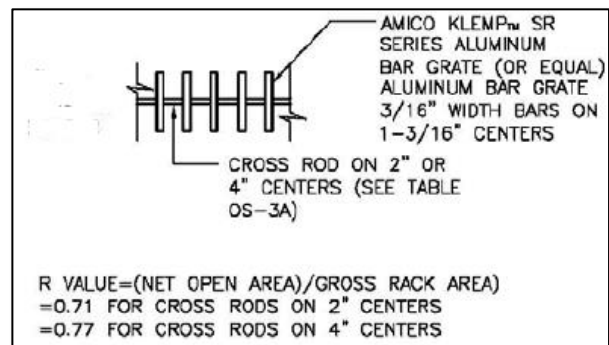


Figure 21. Bar Grate from 1999 USDCV Vol 3.

Figure 22 shows an all-too-common clogged well screen. The solution to the problem for these basins that are too small to warrant the application of the elliptical slot weir is to maximize the open area of each individual orifice such that the lower maintenance bar can be applied in lieu of grate the higher maintenance well screen.



*Figure 22. Typical frequent clogging issues associated with well screens  
(Grant Ranch Research Extended Detention Basin, Denver, CO 2009).*

From a hydraulic standpoint, the ideal scenario would be one water quality orifice at the bottom of the WQCV that would drain the entire volume in 40 hours. But from a water quality perspective, this results in the resuspension and release of more sediment as compared to a column of smaller orifices. Resuspension and an increased amount of sediment release is due to concentration of sediment and associated pollutants being larger toward the bottom of the WQCV. This causes the extended detention basin less effective. It was determined that three is the minimum number of orifices to properly drain the WQCV without releasing excessive sediment. The most recent update of the USDCM Volume 3 reflects this change in practice. UDFCD now recommends only three orifices to maximize the individual orifice area and avoid clogging of the orifice plate. A detail showing the recommended orifice configuration is provided in Figure 23.

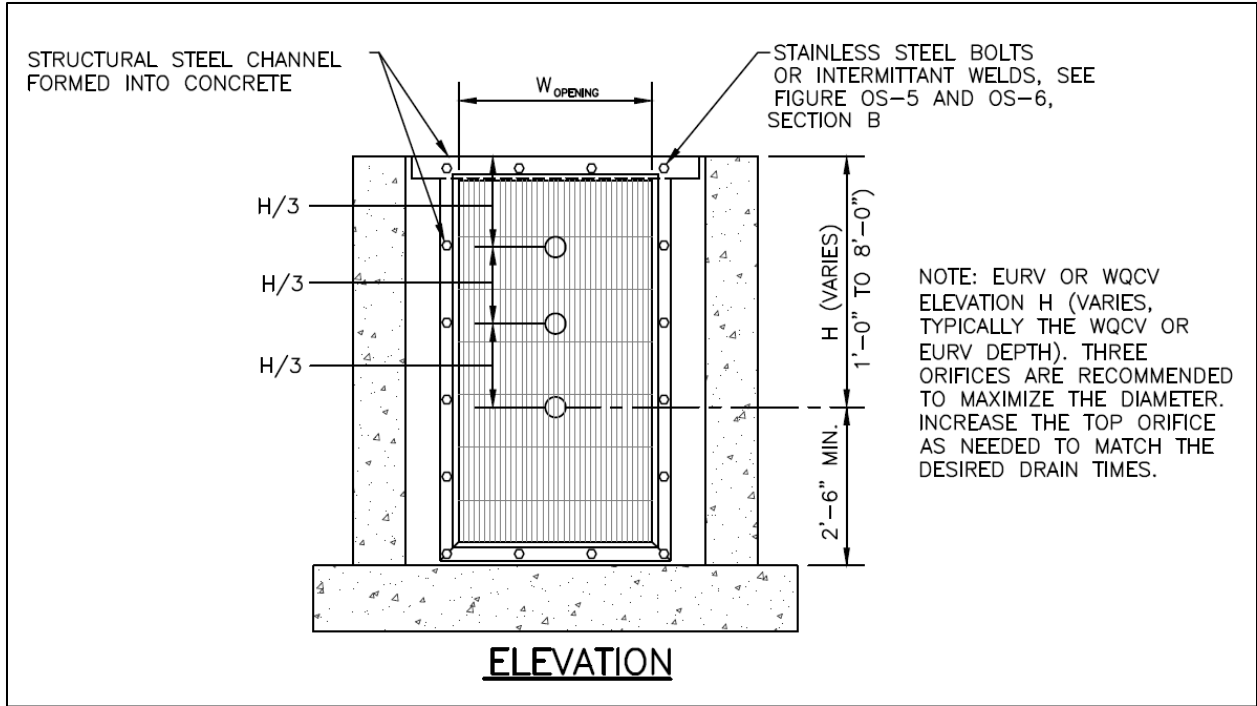


Figure 23. New practice of minimizing the number of water quality orifices while maximizing the area of each individual orifice is presented in the 2016 USDCM Volume 3 as Figure OS-4 in Fact Sheet T-12.

In the case of a detention basin incorporating the EURV and WQCV, the top orifice oftentimes will need to be enlarged such that the lower two orifices drain the WQCV in 40 hours and the top orifice works with the others to drain the EURV in less than 72 hours. The 72-hour rule will be discussed in Section 6 of this report.

#### 4. NEW SIZING GUIDANCE FOR OVERFLOW OUTLET

Detention basins that provide flood control in addition to stormwater quality management have outlet structures fitted with metering plates (either elliptical slot weirs or orifice plates). This is used to control the release of the EURV and/or WQCV, and have an overflow outlet to direct flows in excess of the EURV and/or WQCV into the outlet vault. This is where typically the 100-year volume is metered into the receiving system via a restrictor on the final discharge pipe, as shown in Figure 24.

## Detention Basin Alternative Outlet Design Study

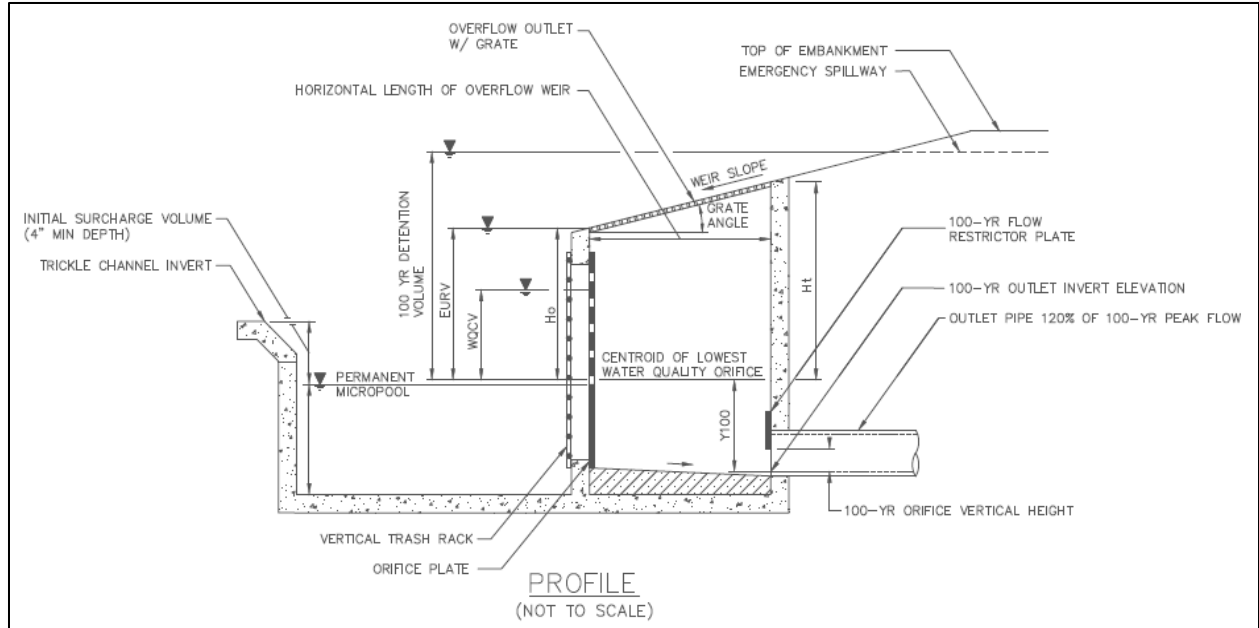


Figure 24. Section of detention basin outlet structure showing water quality plate and overflow outlet with grate.

The overflow outlet acts to regulate the flow of storm events larger than the EURV and/or WQCV but smaller than the 100-year event. When properly designed, these overflow outlets operate under weir flow and not orifice. The final metering of the design (e.g., 100-year) discharge from the detention basin should always be provided by an orifice plate covering the final discharge pipe inside the outlet box, and never from the overflow grate. There are two reasons for this strategy:

1. Orifice flow through the overflow indicates an excessive depth of ponding and a patently dangerous pinning/drowning hazard should a person slip or fall into the water, and
2. The overflow grate must be oversized to accommodate some level of clogging (UDFCD recommends a 50% clogging factor). Since the actual clogging condition cannot be assured, accurate metering cannot be achieved.

The hydraulic design of a detention basin requires knowledge of the discharge characteristics of the overflow outlet. If the outlet structure has a flat-topped (horizontal) overflow grate, then the classic weir and orifice equations can be used with area and perimeter reductions to account for the effects of the grate and assumed clogging thereof. If, however, the overflow grate is inclined in order to fit flush with the dam embankment, the discharge characteristics become much more complex and a different set of equations needs to be applied. Prior to this study, no standard

guidance was available to calculate the stage-discharge curves necessary for the hydraulic design of extended detention basins.

#### 4.1 Computational Fluid Dynamics (CFD) Modeling

In March 2012, UDFCD contracted with ARCADIS U.S., Inc. to apply computational fluid dynamics to estimate the stage-discharge relationship of various overflow outlets. The computational flow model was based on outlet boxes designed with a 3:1 H:V and 4:1 H:V sloped top, as shown in Figure 25.

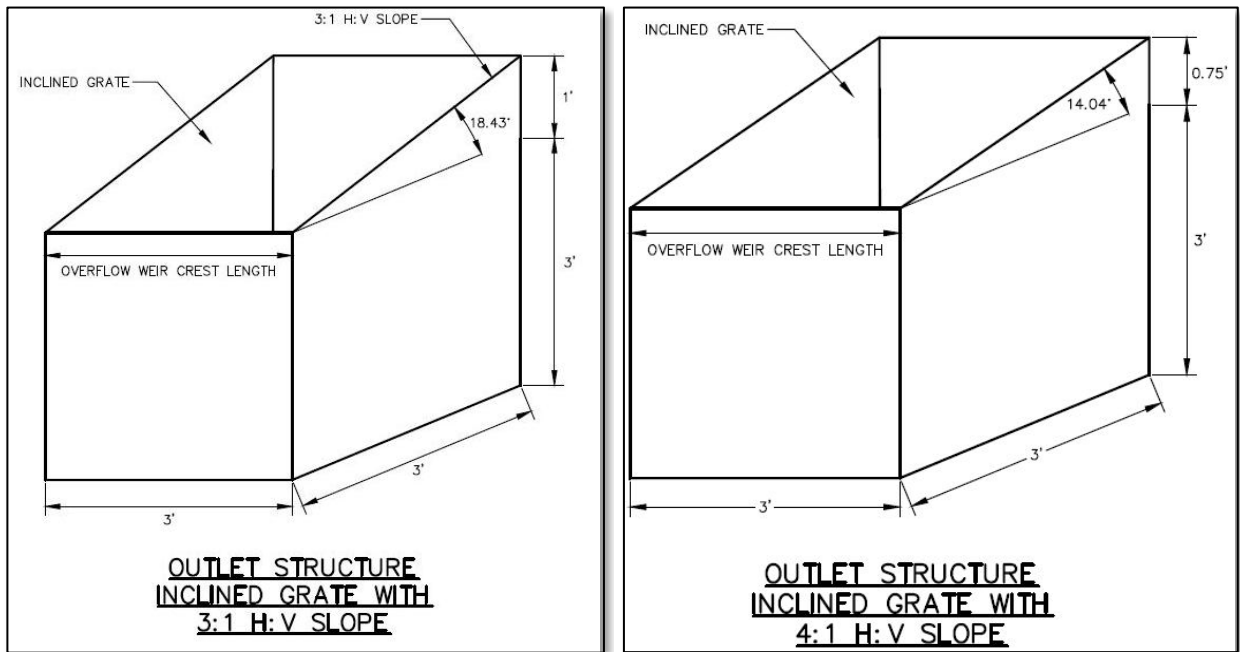


Figure 25. Basic model setup for 3:1 and 4:1 sloped overflow weirs in the CFD model.

The outlet box was modeled as being constructed into the dam embankment. The CFD model of the outlet box with 3:1 slide slopes was constructed as shown in Figure 26. The outlet box was a 3' x 3' square with the top tapered to provide a good match with the slope of the embankment. The outlet box top was cut at an angle of 18.43 degrees for the 3:1 slope and 14.04 degrees for the 4:1 slope.

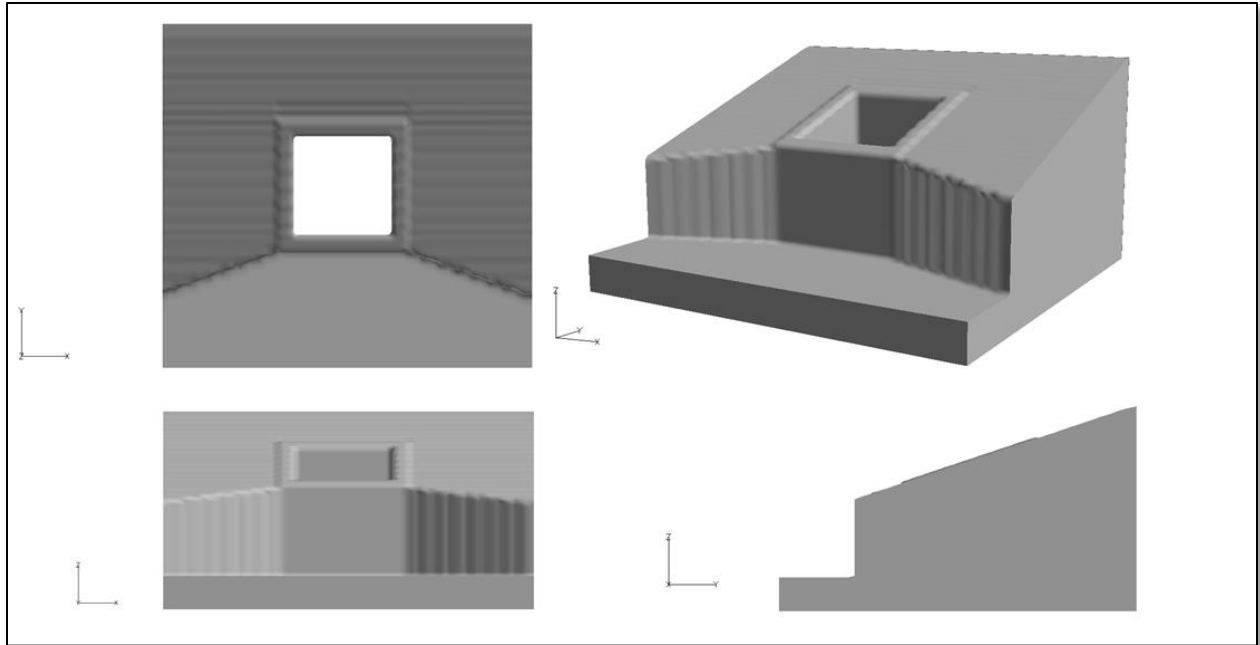


Figure 26. Outlet box model.

Based on the results provided by different grid sensitivity comparison tests, a mesh size of 1,200,000 control volumes (100 x 100 x 120) was selected to resolve the structure and to provide accurate results. In each of the calculations, water surface elevations were specified at each of the open boundaries, and flow left the domain through the bottom of the outlet box (continuative boundaries at the bottom). No-slip boundary conditions were specified at all solid walls, and the Renormalized Group (RNG) model was used for turbulence closure. A visualization of the model is shown in Figure 27.

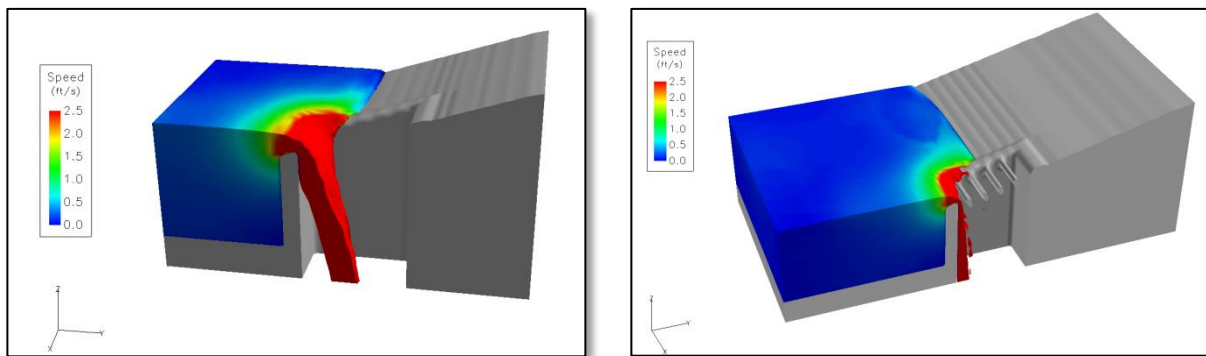


Figure 27. Water Surface Cutaway (colored by velocity, without grate and with grate)

Nine calculations were carried out for each configuration using the FLOW-3D<sup>®</sup> computer program. The results were used to determine rating curves for the outlet box over the range of water levels from 1 to 5 ft above the lower front edge of the weir. The model results were calculated using the 1,200,000 control volume mesh, the most recent release version 10 of FLOW-3D, and the RNG turbulence model, with the simulation results shown in Figure 28.

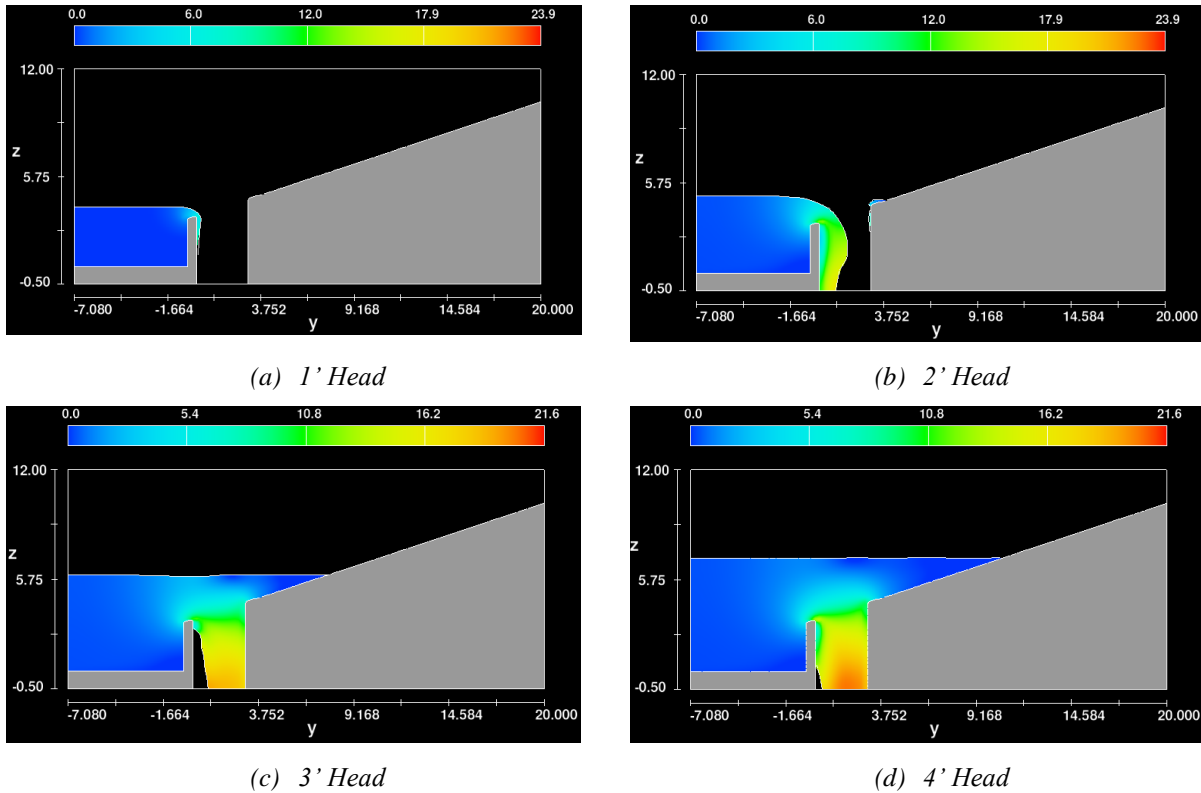


Figure 28. FLOW-3D<sup>®</sup> simulations with gradually-increasing water depths above the low front edge of the overflow weir.

The resulting rating curve for the outlet box with 3:1 top slope is shown in Figure 29 and the resulting rating curve for the outlet box with 4:1 top slope is shown in Figure 30. A side-by-side comparison is shown in Figure 31.

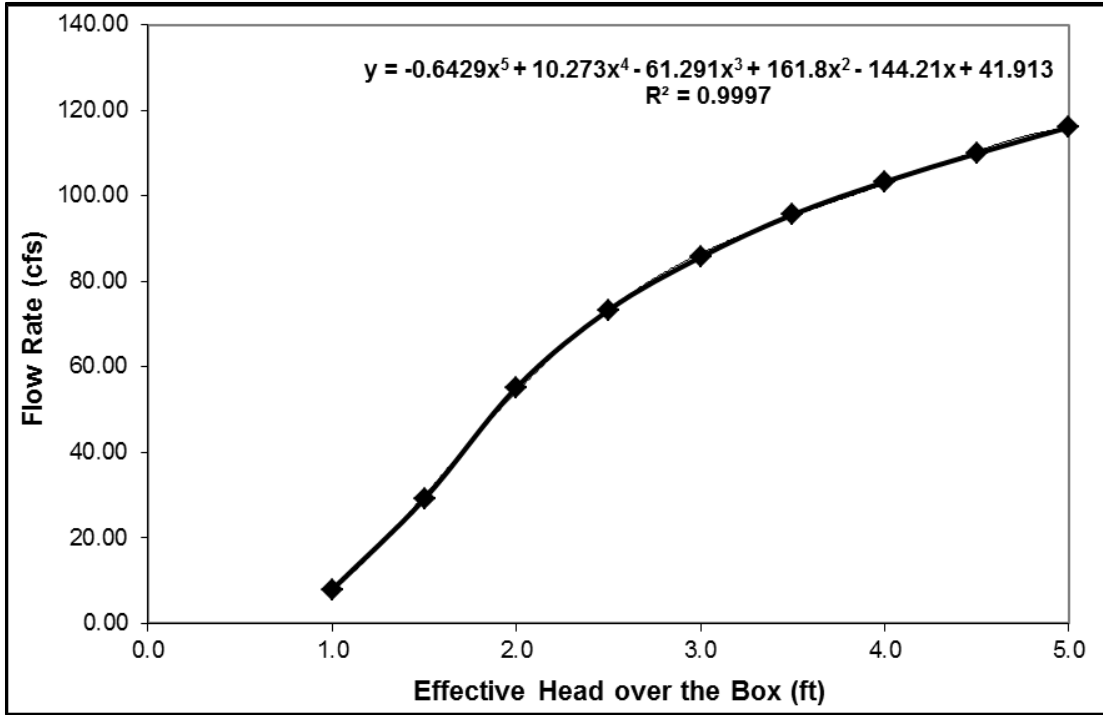


Figure 29. FLOW-3D® resulting rating curve for the outlet box with 3:1 H:V top slope (5<sup>th</sup> degree polynomial regression curve fit).

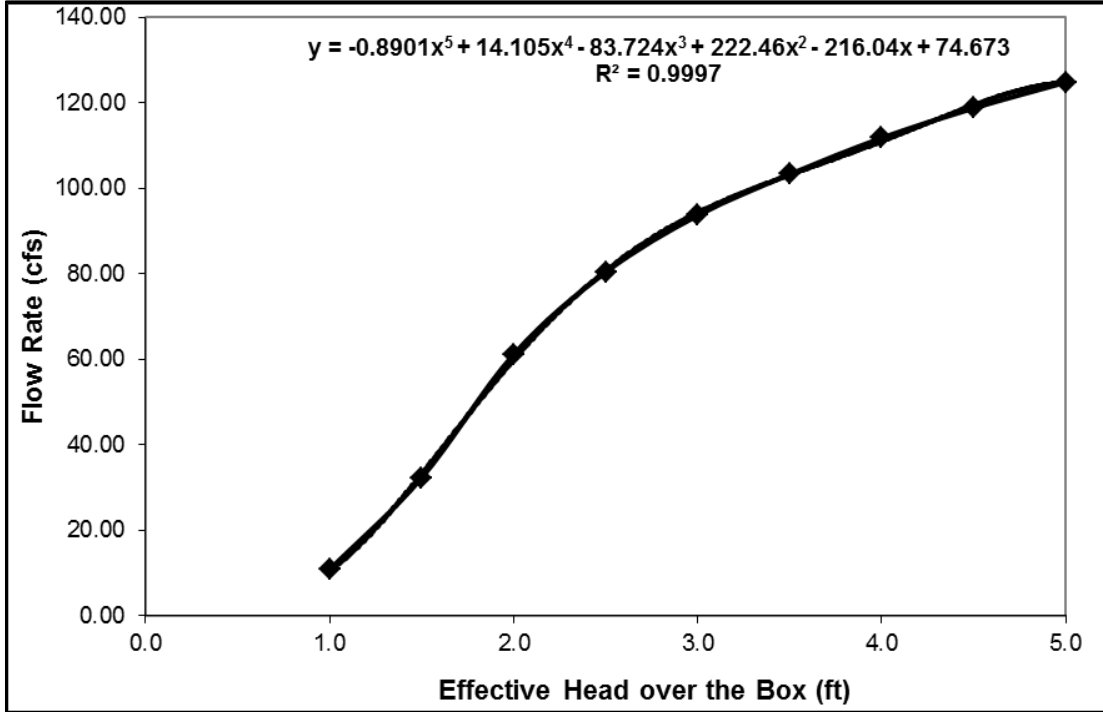


Figure 30. FLOW-3D® resulting rating curve for the outlet box with 4:1 H:V top slope (5<sup>th</sup> degree polynomial regression curve fit).

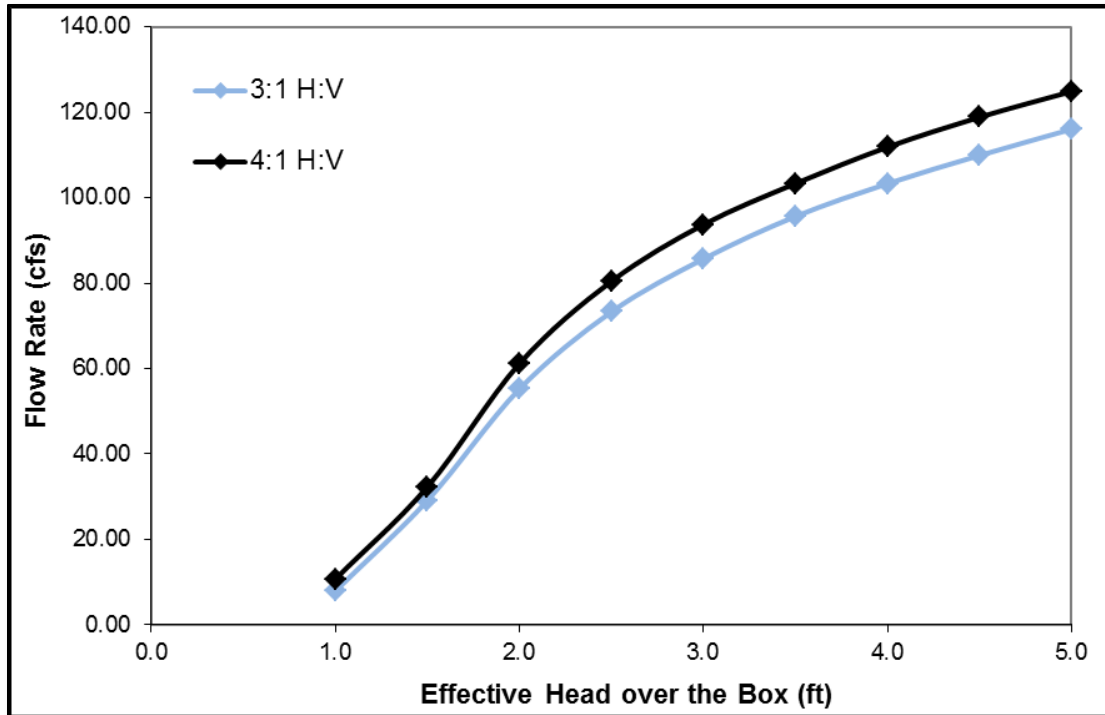


Figure 31. Side-by-side comparison of FLOW-3D<sup>®</sup> rating curves for the outlet box with 3:1 and 4:1 H:V top slopes.

Further analysis of the ARCADIS work indicated that the 5<sup>th</sup> degree polynomials shown in Figures 29 and 30 are inadequate to use for design since 1) the Y-intercept must go through the origin (flow at zero depth must equal zero), and 2) instability issues with high degree polynomial regression equations such as these result in negative flow rates at a very shallow depth.

#### 4.2 Guo’s Analysis by Comparing to CDOT Type C and D Grated Inlet Study

The hydraulics of the inlet grates commonly used for overflow outlets were studied in 2012 as part of a previous collaborative project between CDOT and UDFCD. CDOT Type C and D inlets were modeled at the CSU hydraulics laboratory, where a study was conducted to investigate the hydraulic performance of a 1/3-scaled model Type C grate with an inclined angle varied from zero to 30 degrees. The results of that study were reported by Guo et al. in the ASCE Journal of Irrigation and Drainage Engineering in April 2016 (Volume 140, Issue 6) and are summarized here. The hydraulic performance of a grate to a large degree depends on the ponding depth on the grate. When the water depth is too shallow to submerge the entire grate surface, the grate operates as a weir. When the grate area is completely submerged, the grate operates like an orifice. The transition from weir to orifice flow is called mixed flow (Guo et al. 2008). As shown

in Figure 32, a grate is formed with I-beam bars. The net opening ratio for a grate is defined as the clear opening area for water to flow through the grate surface as:

$$n = (1 - C \log) \frac{LB - L_b B}{LB} = (1 - C \log) \frac{L - L_b}{L} \quad (10)$$

Where  $n$  = net area opening ratio,  $C \log$  = clogging factor  $0 \leq C \log \leq 1.0$  due to debris,  $L$  = grate length,  $B$  = grate width, and  $L_b$  = cumulative width of bars on grate. Eq. 10 indicates that the grate's area opening ratio for an orifice flow is equal to the length opening ratio for a weir flow. The selection of clogging factor depends on the highway condition, and a decayed clogging factor is recommended for multiple grates.

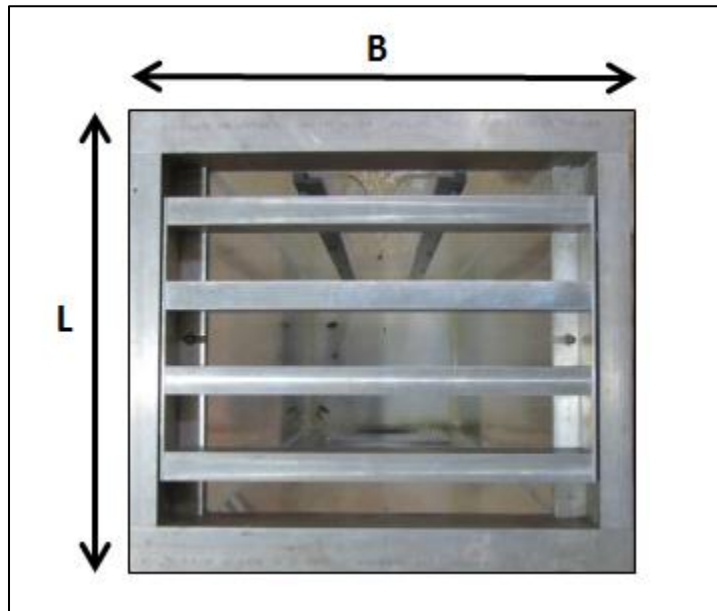


Figure 32. Grate dimensions.

The hydraulic capacity of a Type C grate is quantified according to its flow interception. The integral of flow interception is described as:

$$Q = nC_d \int \sqrt{2gh} dA \quad (11)$$

Where  $Q$  = flow rate,  $C_d$  = discharge coefficient,  $v$  = flow velocity,  $g$  = gravitational acceleration,  $dA$  = flow area, and  $h$  = headwater depth on  $dA$ . For a given water depth, the grate may operate like a weir or an orifice, whichever is less in flow interception. In this study, two sets of equations were derived to predict both the weir and the orifice flows. The discharge coefficients are respectively derived and then calibrated with the observed measurements.

#### 4.21 Weir Flow Capacity

As illustrated in Figure 33, the inclined angle is formed by the gate length,  $L$ , and its height,  $H_b$ . The coordination system  $(h,x)$  is set to describe the flow condition in which  $h$  = water depth variable measured downward from the water surface, and  $x$  = distance variable measured upward from the base width. Under a shallow water depth, the grate's wetted perimeter may operate like a weir. Water overtops the three submerged sides into the inlet box, including two inclined sides and the lower base width.

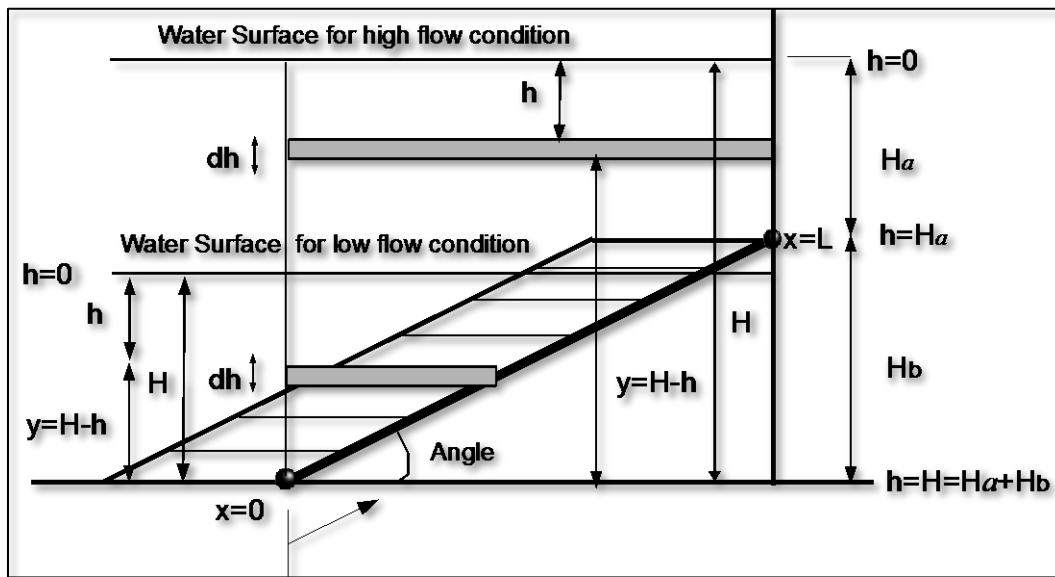


Figure 33. Weir Flow Overtopping Submerged Side along Grate.

Under a low flow condition as shown in Figure 33, only the lower portion of the grate is submerged. The infinitesimal flow area for a weir flow is derived as:

$$dA = (H - h) \cot \theta dh \quad \text{for } H < H_b \quad (12)$$

$$y = H - h \quad (13)$$

Where  $\theta$  = inclined angle,  $H$  = water depth,  $y$  = location of  $dA$  above the ground, and  $dh$  = infinitesimal thickness for flow area. The weir flow overtopping the wetted length along the grate's side is integrated from  $h=0$  to  $h=H$ . Aided by Eq. 12, Eq. 14 yields:

$$Q_{ws} = \frac{4}{15} n C_d \sqrt{2g} \cot \theta H^{\frac{5}{2}} \quad \text{for } H < H_b \quad (14)$$

Where  $Q_{ws}$  = side weir flow. Under a high water depth as illustrated in Figure 33, the integration limit is divided into two zones for mathematical convenience as:

$$H = H_b + H_a \quad (15)$$

Where  $H_a$  = surcharge depth above the top base of the grate. The infinitesimal areas for the weir flow in these two flow zones are respectively formulated as:

$$dA_1 = (H - h) \cot \theta \, dh \quad 0 < h < H_a \text{ for Zone 1} \quad (16)$$

$$dA_2 = L \cos \theta \, dh \quad H_a < h < H \text{ for Zone 2} \quad (17)$$

The weir flow overtopping the wetted length is integrated as:

$$Q_{ws} = nC_d \int_{h=0}^{h=H_a} \sqrt{2gh} L \cos \theta \, dh + nC_d \int_{h=H_a}^{h=H} \sqrt{2gh} (H - h) \cot \theta \, dh \quad (18)$$

Integrating Eq. 18 yields:

$$Q_{ws} = \frac{4}{15} nC_d \sqrt{2g} \cot \theta (H^{5/2} - H_a^{5/2}) \quad (19)$$

Re-arranging Eq. 19 yields:

$$Q_{ws} = \frac{4}{15} nC_d \sqrt{2g} L \cos \theta H^{\frac{3}{2}} \left[ \frac{H^{\frac{5}{2}}}{H^{\frac{3}{2}} H_b} - \frac{(H - H_b)^{\frac{5}{2}}}{H^{\frac{3}{2}} H_b} \right] \quad \text{for } H > H_b \quad (20)$$

At  $H = H_b$ , Eq. 20 agrees with Eq. 14. The total flow collected into the inlet box is the sum of the weir flows overtopping the two wetted sides along the grate and the lower base width of the grate. The weir flow,  $Q_{WB}$ , over the lower base is computed as:

$$Q_{WB} = \frac{2}{3} nC_d \sqrt{2g} B H^{\frac{3}{2}} \quad (21)$$

In which  $Q_{WB}$  = flow overtopping the low base width. The total weir flow is the sum as:

$$Q_w = 2Q_{ws} + Q_{WB} \quad (22)$$

In which  $Q_w$  = total interception for weir flow

#### 4.22 Orifice Flow Capacity

When the grate surface area operates under orifice flow as illustrated in Figure 34, the integration of the orifice flow into the inlet box is separately conducted for the low and high water depth conditions.

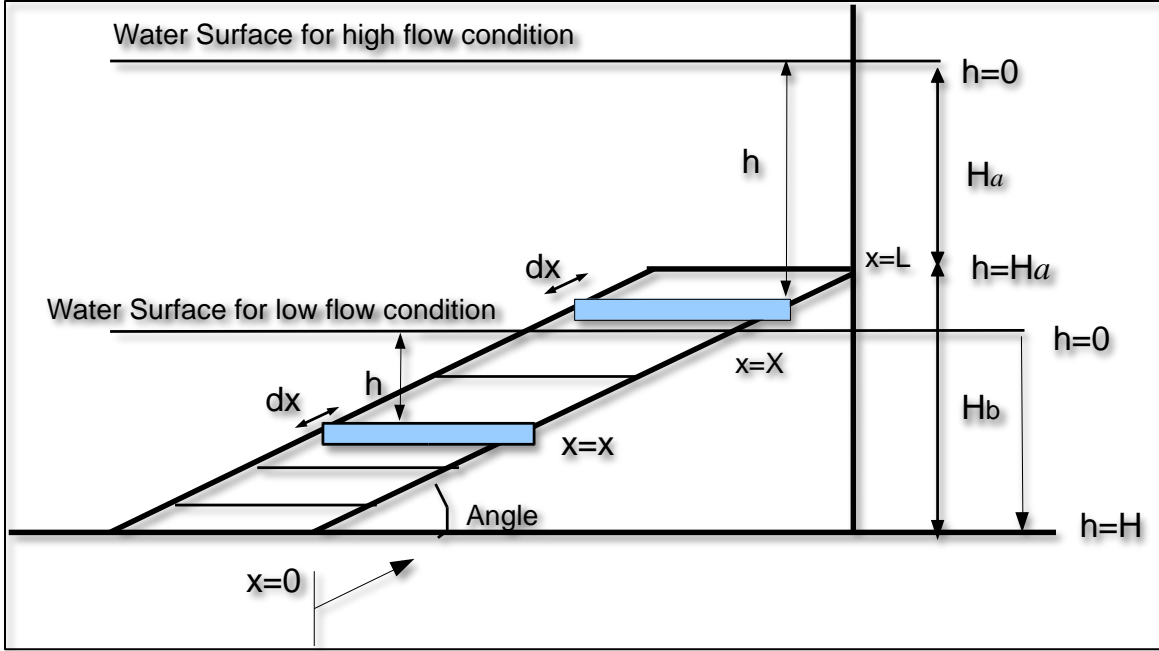


Figure 34. Orifice Flow through Submerged Area on Grate.

For  $H < H_b$ , the infinitesimal flow area for orifice flow in Figure 34 is defined as:

$$dA = n B \cos \theta dx \quad (23)$$

The head water depth,  $h$ , can be related to the wetted length,  $x$ , along grate's side as:

$$h = \left(1 - \frac{x}{X}\right)H \quad (24)$$

Where  $X$  = wetted length that varies between  $0 \leq X \leq L$ ,  $x$  = integration variable that varies between  $0 \leq x \leq X$ . Under a low flow condition,  $H \leq H_b$ , the orifice flow through the submerged surface area on the grate is integrated from  $x=0$  to  $x=X$  as:

$$Q_o = \frac{2}{3} n C_d B H \cot \theta \sqrt{2gH} \quad \text{for } H \leq H_b \quad (25)$$

When  $\theta=0$ , Eq. 25 is reduced to a horizontal orifice as:

$$Q_o = \frac{2}{3} n C_d B L \sqrt{2gH} \quad \text{for } H_b = 0 \text{ and } \theta=0 \quad (26)$$

Under a high flow condition, the entire grate surface area is submerged. The headwater is related to the wetted length along the grate as:

$$h = H - \frac{x}{L}(H - H_a) = H - \frac{x}{L}H_b \quad (27)$$

For mathematical convenience, the flow depth is divided into two zones for numerical integration as: (1) above the top of the grate and (2) below the top of the grate. The orifice flow under a high water depth is integrated from  $x=0$  to  $x=L$  as:

$$Q_o = \frac{2}{3} n C_d B L \cos \theta \sqrt{2gH} \left[ \frac{H^{\frac{3}{2}}}{H_b \sqrt{H}} - \frac{(H - H_b)^{\frac{3}{2}}}{H_b \sqrt{H}} \right] \quad \text{for } H > H_b \quad (28)$$

At  $H = H_b$ , Eq. 28 agrees with Eq. 25. Comparing with the conventional approach, the orifice and weir coefficients can be related to the discharge coefficient as:

$$C_o = \frac{2}{3} C_d \quad (29)$$

$$C_w = \frac{4}{15} C_d \sqrt{2g} \quad (30)$$

In which  $C_o$  = orifice coefficient and  $C_w$  = weir coefficient. Using the orifice and weir coefficients, the governing equations for various flow conditions are summarized as follows.

For  $H \leq H_b$ , the orifice and weir flows are respectively estimated as:

$$Q_o = n C_o B H C \cot \theta \sqrt{2gH} \quad \text{for low orifice flow} \quad (31)$$

$$Q_w = 2n C_w C \cot \theta H^{\frac{5}{2}} + n C_w B H^{\frac{3}{2}} \quad \text{for low weir flow} \quad (32)$$

For  $H \geq H_b$ , the orifice and weir flows are respectively estimated as:

$$Q_o = n C_o B L C \cos \theta \sqrt{2gH} \left[ \frac{H^{\frac{3}{2}}}{H_b \sqrt{H}} - \frac{(H - H_b)^{\frac{3}{2}}}{H_b \sqrt{H}} \right] \quad \text{for high orifice flow} \quad (33)$$

$$Q_w = 2n C_w L C \cos \theta H^{\frac{3}{2}} \left[ \frac{H^{\frac{5}{2}}}{H^{\frac{3}{2}} H_b} - \frac{(H - H_b)^{\frac{5}{2}}}{H^{\frac{3}{2}} H_b} \right] + n C_w B H^{\frac{3}{2}} \quad \text{for high weir flow} \quad (34)$$

For a given water depth, the interception capacity through an inclined grate is dictated by weir or orifice flows, whichever is less as:

$$Q_c = \min (Q_w, Q_o) \text{ for a given water depth} \quad (35)$$

In which  $Q_c$  = flow interception through grate. On the contrary, for a given design flow, the required headwater depth,  $H$ , acting on an inclined grate is determined as:

$$H = \max (H_w, H_o) \text{ for a given design flow} \quad (36)$$

Where  $H_w$  = headwater for weir flow,  $H_o$ = headwater for orifice flow, and  $H$ = design headwater. The equations developed by Guo et al. are summarized in Table 2.

Table 2. Summary of equations by Guo et al. for calculating discharge through CDOT Type C and D median inlets.

Flow Type	Flow Overtopping Two Sides of Inclined Grate	Flow overtopping the Lower Base Width	Condition
Orifice	$Q_o = \frac{2}{3}nC_dBHCot\theta\sqrt{2gH} = \frac{2}{3}nC_dBXCos\theta\sqrt{2gH}$ <p>Subject to: <math>X = \frac{H}{Sin\theta} &lt; L</math></p>		$H < H_b$ Un-submerged
Weir	$Q_{ws} = \frac{4}{15}nC_d\sqrt{2g}Cot\theta H^{\frac{5}{2}} = \frac{4}{15}nC_dXCos\theta\sqrt{2g}H^{\frac{3}{2}}$ <p>subject to: <math>X = \frac{H}{Sin\theta} &lt; L</math></p> $Q_w = 2Q_{ws} + Q_{wb}$	$Q_{wb} = \frac{2}{3}nC_d\sqrt{2g}BH^{3/2}$	$H < H_b$ Un-submerged
Orifice	$Q_o = \frac{2}{3}nC_dBLCos\theta\sqrt{2gH}\left[\frac{H^{\frac{3}{2}}}{H_b\sqrt{H}} - \frac{(H - H_b)^{\frac{3}{2}}}{H_b\sqrt{H}}\right]$ <p>In case of <math>\theta=0</math> and <math>H_b=0</math>, then</p> $Q_o = \frac{2}{3}nC_dBL\sqrt{2gH} \text{ if } \theta = 0$		$H \geq H_b$ Submerged
Weir	$Q_{ws} = \frac{4}{15}nC_d\sqrt{2g}LCos\theta H^{\frac{3}{2}}\left[\frac{H^{\frac{5}{2}}}{H^{\frac{3}{2}}H_b} - \frac{(H - H_b)^{\frac{5}{2}}}{H^{\frac{3}{2}}H_b}\right]$ <p>In case of <math>\theta=0</math> and <math>H_b=0</math>, then</p> $Q_{ws} = \frac{2}{3}nC_dL\sqrt{2g}H^{\frac{3}{2}}$ $Q_w = 2Q_{ws} + Q_{wb}$	$Q_{wb} = \frac{2}{3}nC_d\sqrt{2g}BH^{3/2}$	$H \geq H_b$ Submerged

### 4.3 Physical Modeling at the USBR Hydraulics Lab

In December 2012, UDFCD contracted with the U.S. Bureau of Reclamation (USBR) Hydraulics Laboratory in Lakewood, Colorado to perform physical modeling of the overflow weir and grate in different configurations. The results of that study were published by Heiner in 2014 and are summarized here. The purpose of this effort was to verify that the equations developed by Guo (see Section 4.2).

### 4.31 Model Setup

A model box approximately 25-ft wide, 45-ft long and 4-ft deep was configured to simulate an extended detention basin. One end of the box contained a 12-inch diameter inlet pipe and a 6-inch thick rock baffle to evenly distribute the flow entering the model. The opposite end of the box contained several configurations of the overflow outlet structure with and without grating, as shown in Figure 35.

The outlet structure was modeled at a geometric scale of 1:3, which means model dimensions are one-third of the prototype dimensions. Since hydraulic performance for open channel flow depends primarily on gravitational and inertial forces, Froude law scaling was used to establish a relationship between the model and prototype. Froude law scaling causes the ratio of gravitational to inertial forces to be equal in the model and prototype; stated in another way, the Froude numbers of the model and prototype are kept equal to one another.

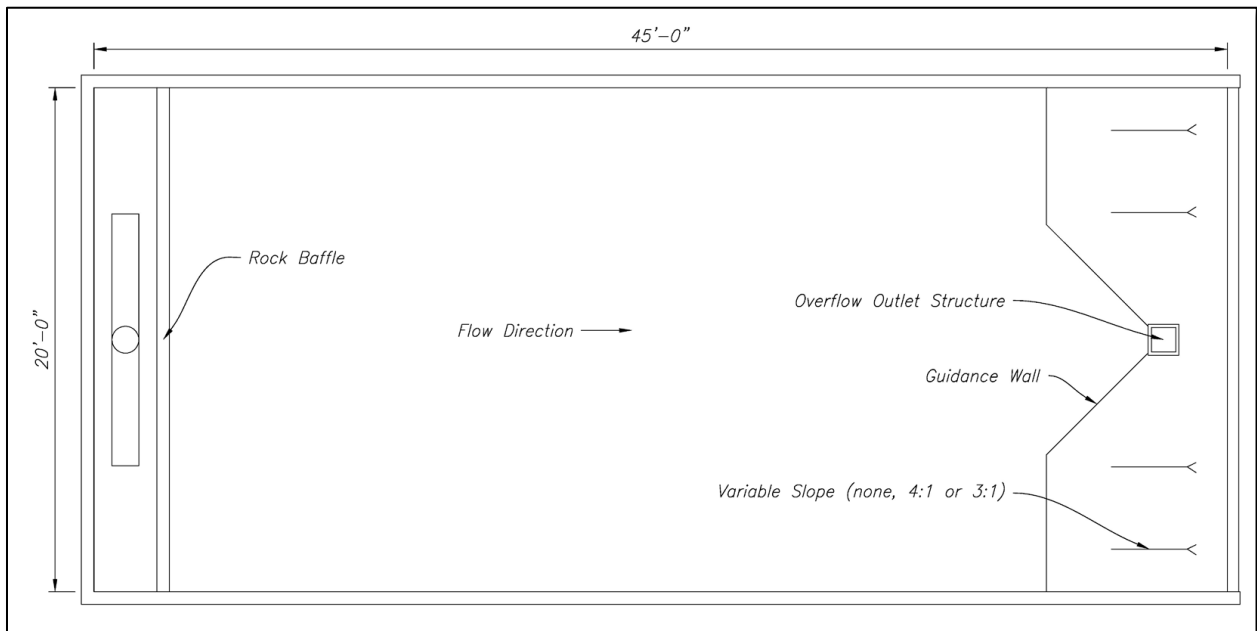


Figure 35. Physical model layout of an extended detention basin (EDB, model scale)

Froude law similitude produces the following relationships between model (m) and prototype (p), as:

$$\text{Length Ratio: } L_r = L_m/L_p = 1:3 \quad (37)$$

$$\text{Velocity Ratio: } V_r = V_m/V_p = L_r^{1/2} = 1:1.732 \quad (38)$$

$$\text{Discharge Ratio: } Q_r = Q_m/Q_p = L_r^{5/2} = 1:15.59 \quad (39)$$

Three different grates were tested, including a Standard CDOT Type C grate (Figure 36a), a CDOT close-mesh grate (Figure 36b), and a “No Grate” scenario (Figure 36c) where only the grate frame, which was a rectangular opening approximately 41 inches by 35 inches, was tested. Each grate configuration was tested at slopes of 3:1 (H:V), 4:1, and 1:0 horizontal (no slope). The two sloped configurations were modeled as though the outlet structure was constructed into the dam embankment as this is the typical reason for the sloped top. The flat-topped outlet was modeled as a free standing structure as this configuration is common in the field.



(a) CDOT Type C grate

(b) Type C close-mesh grate

(c) No grate

Figure 36. Types of grates tested in USBR hydraulics lab 1/3-scale model.

Table 3 contains a summary of the test configurations modeled and indicates where surrounding topography was set at the same slope as the overflow outlet structure and grate (Figure 37), as opposed to a no slope with no topography configuration (Figures 38 and 39). Most test configurations modeled the flow passing through the overflow outlet portion of the outlet works. One final configuration was modeled that tested no slope with no topography and included a complete outlet structure with water quality orifice plate and 100-yr orifice (Figure 40) restricting flow downstream of the overflow outlet. The water quality orifice plate was modeled as both the standard configuration with a series of orifice holes and as an alternative elliptical weir (Figure 41).

Table 3 - Summary of test configurations that were modeled

<b>Slope</b>	<b>Grate</b>	<b>Surrounding Topography</b>
3:1 (H:V)	Standard CDOT Type C	YES
3:1 (H:V)	CDOT Close Mesh	YES
3:1 (H:V)	None	YES
4:1 (H:V)	Standard CDOT Type C	YES
4:1 (H:V)	CDOT Close Mesh	YES
4:1 (H:V)	None	YES
Horizontal	Standard CDOT Type C	NO
Horizontal	CDOT Close Mesh	NO
Horizontal	None	NO

Each model configuration was tested by completing the following steps:

1. Establish a specific flow rate measured by a calibrated Venturi meter accurate to  $\pm 0.25$  percent (USBR 1989) into the model box.
2. Allow the flow to stabilize for the necessary amount of time so that no change in water surface in the EDB is noticed for at least 5 minutes.
3. Obtain the water surface elevation (stage) above the lower edge of the inlet using both a calibrated laboratory ultrasonic sensor and a point gauge (redundant measurements for consistency).
4. Record both the stage and flow.
5. Repeat steps 1-4 to create a complete rating curve that identifies any transitions between weir and orifice flow.

Inflow and stage were recorded and plotted to generate stage-discharge relationships for each configuration. Collected data were then compared to the provided rating equations by Guo in Section 4.2.



*Figure 37. Model setup for 3:1 (H:V) and 4:1 (H:V) grate slope testing.*



*Figure 38. Model setup for horizontal grate testing.*



*Figure 39. Close-up of horizontal grate testing.*



*Figure 40. 100-year restrictor plate covering the final discharge pipe inside the outlet structure.*

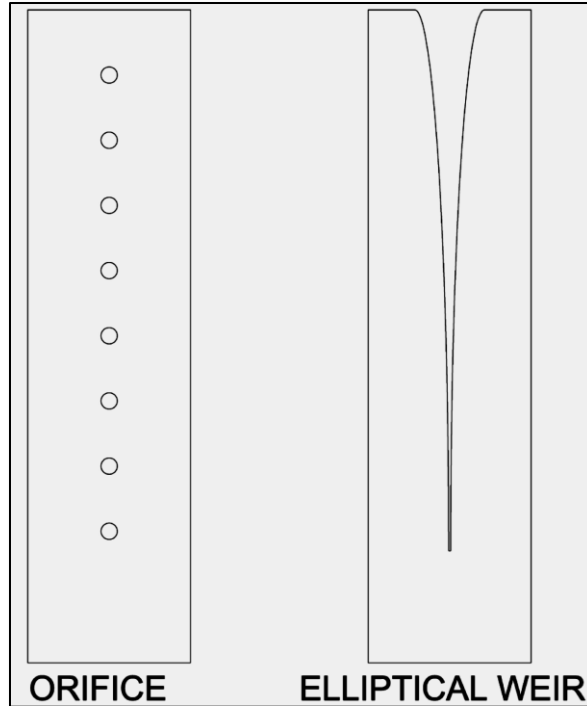


Figure 41. Water quality orifice plate configurations tested in the complete EDB model.

#### 4.32 Model Results

Figure 42 shows data collected at the 1:0 (H:V) (no slope, aka horizontal) configuration for each of the three tested grates. Figure 43 shows data collected at the 4:1 (H:V) slope configuration for each of the three tested grates. Figure 44 shows data collected at the 3:1 (H:V) slope configuration for each of the three tested grates. Each figure plots stage above the lowest edge of the overflow outlet structure in ft on the x-axis and discharge through the overflow outlet in cfs on the y-axis.

Figure 45 provides data collected on the complete EDB with micropool, water quality orifice, horizontal overflow outlet, and 100-year controlling orifice. This plot also shows stage (ft) above the lowest edge of the overflow outlet structure on the x-axis and discharge through the overflow outlet in cfs on the y-axis. All three grates were tested with a series of orifice holes in the water quality plate. One test was conducted with the orifice holes being replaced with an elliptical weir which releases a significantly larger discharge for a given head.

### Detention Basin Alternative Outlet Design Study

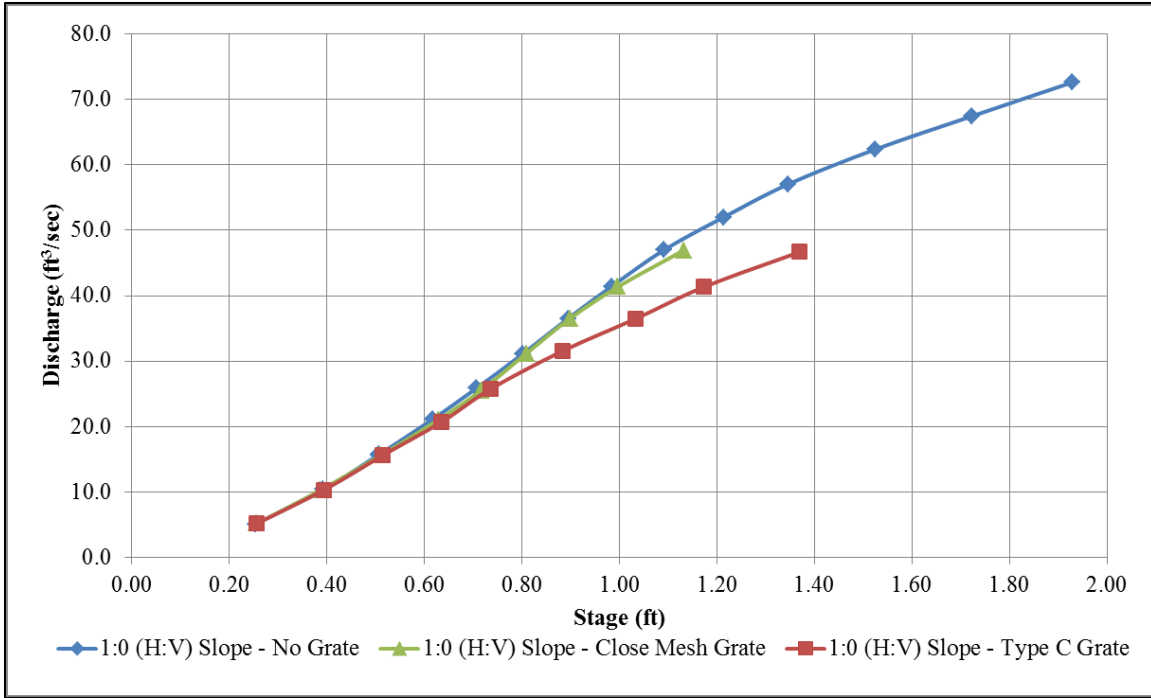


Figure 42. Data collected in the 1:0 (H:V) slope configuration for each grate (prototype dimensions).

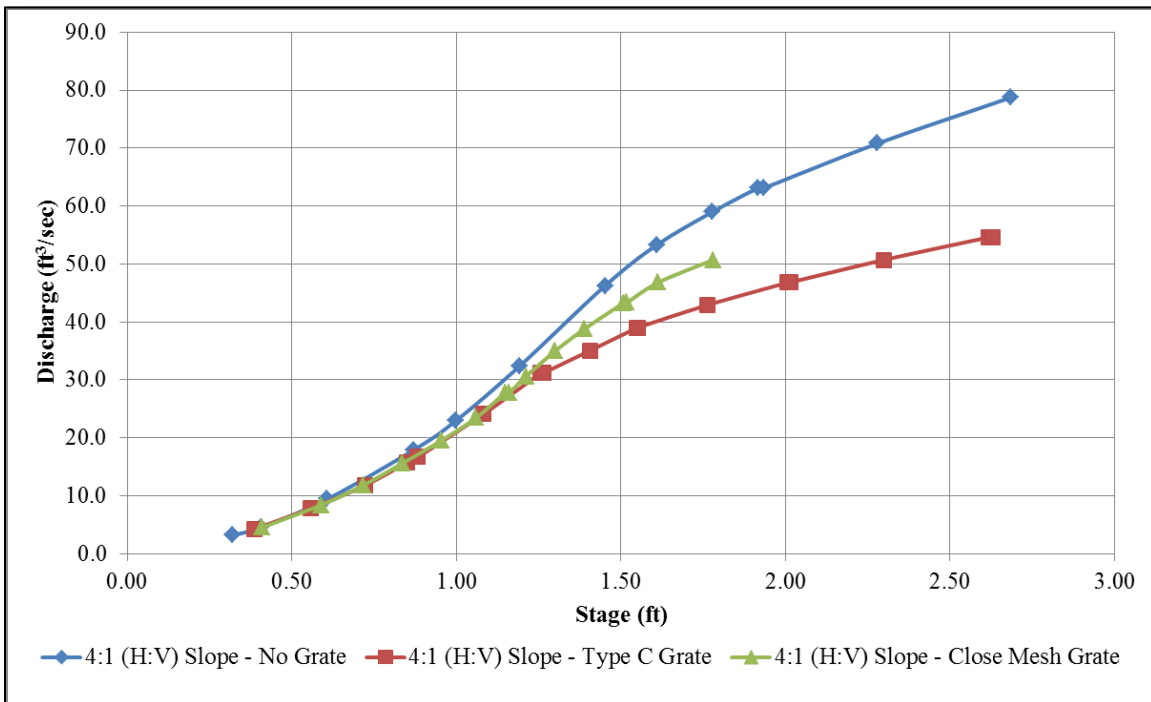


Figure 43. Data collected in the 4:1 (H:V) slope configuration for each grate (prototype dimensions).

Detention Basin Alternative Outlet Design Study

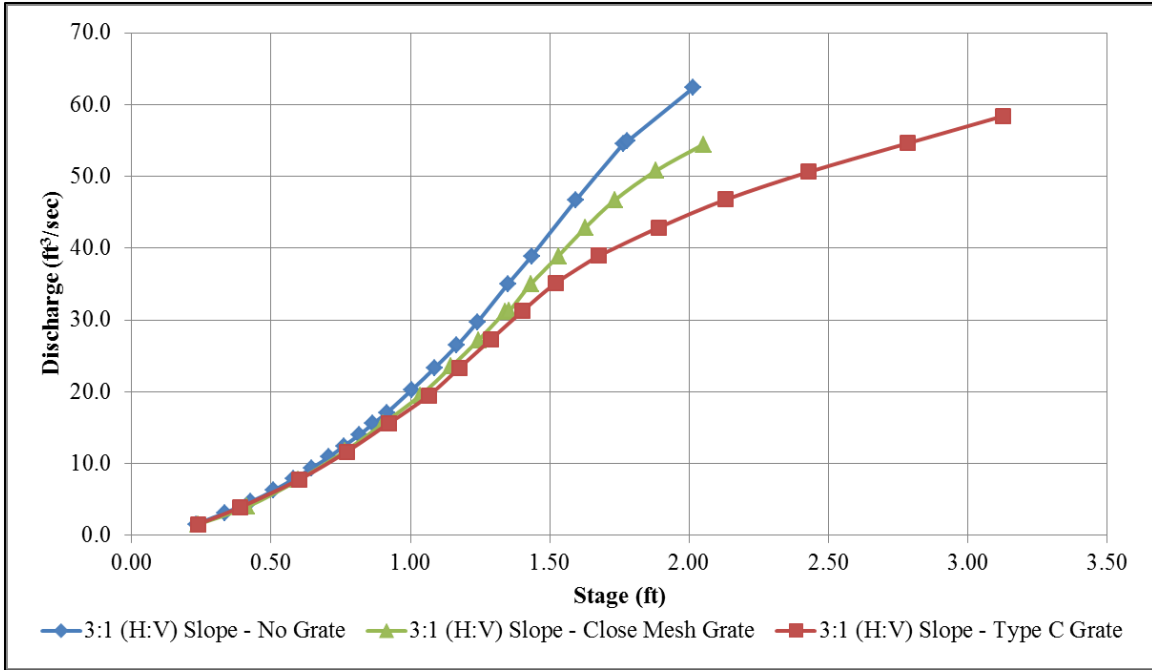


Figure 44. Data collected in the 3:1 (H:V) slope configuration for each grate (prototype dimensions).

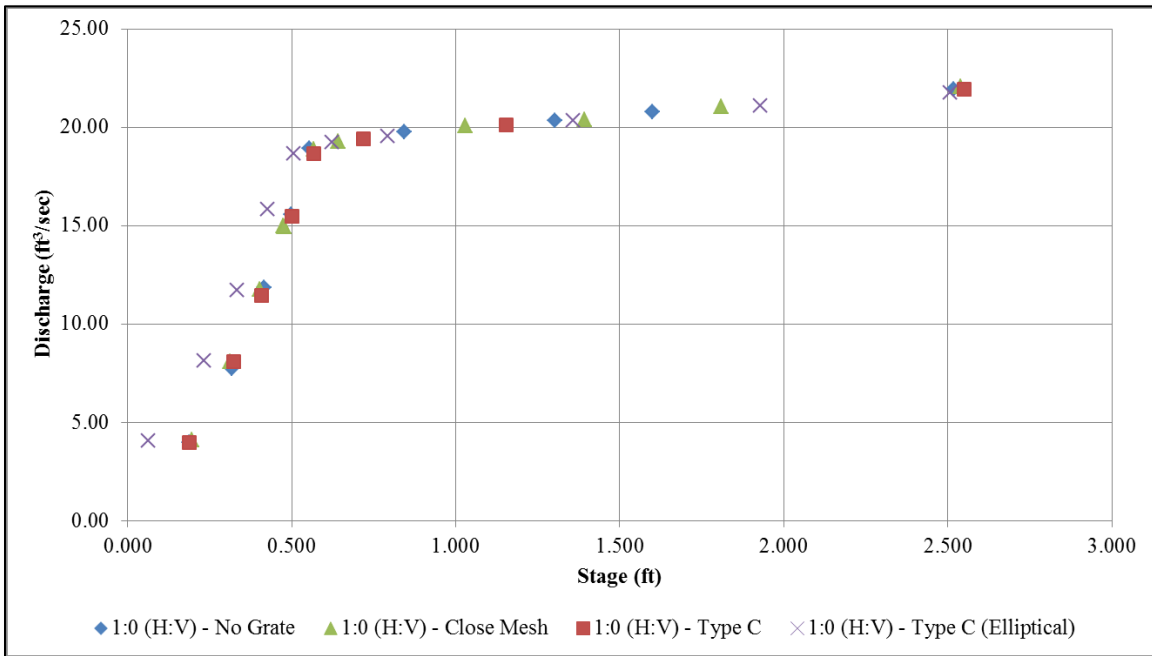


Figure 45. Data collected on the complete EDB with micropool and 1:0 (H:V) slope overflow outlet structure. Water quality plates and the 100-year controlling orifice were installed for each configuration tested.

Each scenario was compared to equations by Guo provided in Table 2 to determine if the equations generated rating curves consistent with the physical model. The shape of the stage-discharge curve observed in the model makes it apparent that flow control varies from weir flow at low heads to transitional (mixed flow) at intermediate heads, and finally orifice flow at high heads. Approximate bounds of these zones are illustrated in Figure 46. Zones will change slightly depending on the geometry and configuration of the outlet structure and overflow weir.

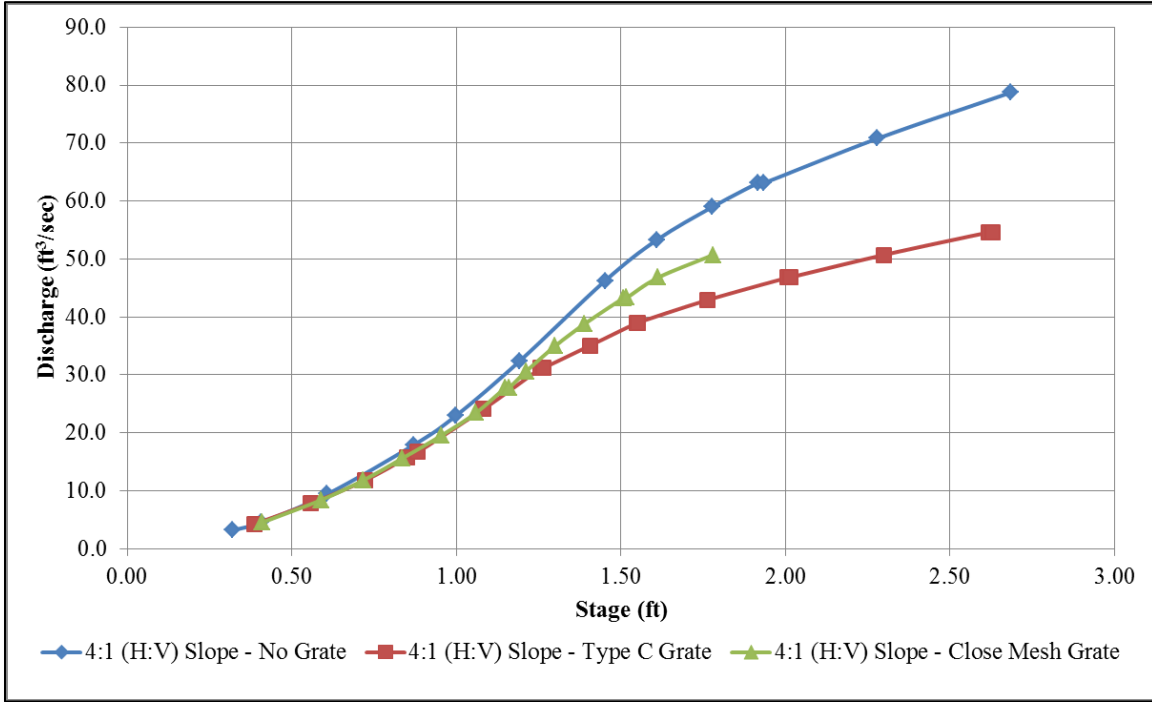


Figure 46. Approximate boundary zones for weir flow, mixed flow and orifice flow.

When flows were in the mixed flow zone they became unstable and the stage in the EDB would fluctuate significantly with a constant inflow. Figure 47 shows this phenomenon, which was present at all configurations. Data was collected for each configuration until the stage oscillations were noticed. As can be seen in Figures 42 through 44, oscillations occurred at different head and discharge for each configuration.

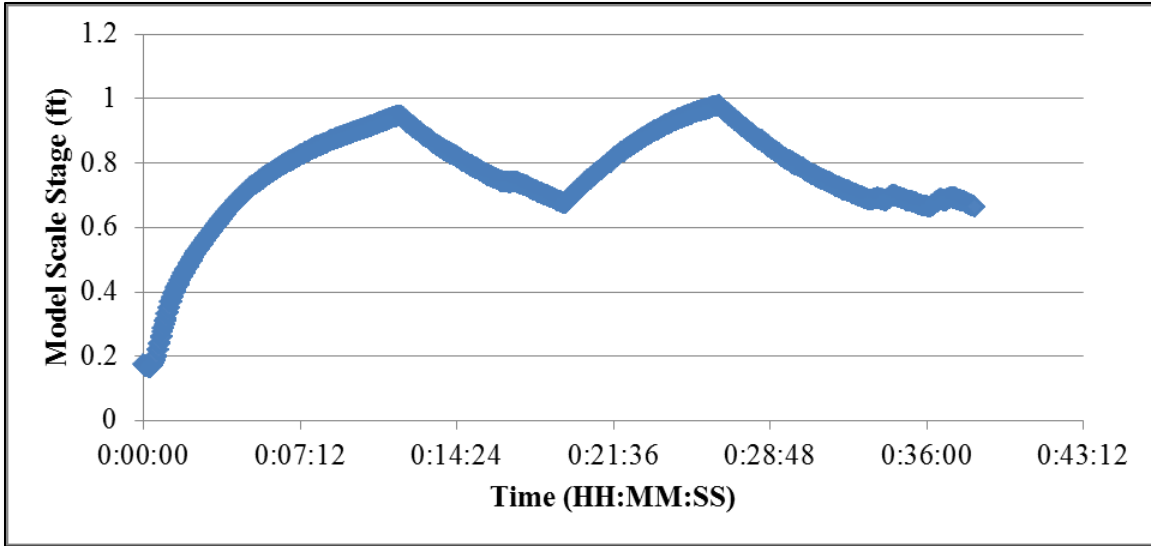


Figure 47. Sample flow oscillations that occurred when flows entered mixed zone for the 4:1 slope with standard CDOT Type C grate.

The USBR analyzed the data to determine if a single new equation or set of equations of consistent form could be generated that would accurately describe the flow through the overflow outlet works for all structure configurations. The data was plotted in TableCurve 2D and TableCurve 3D, utilizing different dependent and independent variables. No single relationship was found that accurately described the overflow outlet discharge for all configurations tested. It was determined that it would be difficult if not impossible to develop a new equation that would accurately describe the flow through the overflow outlet in all zones (weir, mixed, and orifice) for all slopes, especially with the limited data that were collected during this modeling effort.

Calculating the discharge through the overflow outlet in all three zones (weir, mixed, and orifice) was determined to be unnecessary from a practical perspective. When installed, the outlet structure typically employs a 100-yr orifice that restricts the flow downstream of the overflow outlet and prevents the overflow outlet from ever functioning as the flow control in the transitional or orifice mode. It was therefore determined that modeling a complete EDB would adequately verify how the overflow outlet and the 100-yr orifice combine to control the flow. As shown in Figure 45, the complete model of the EDB confirmed that flow would be restricted by the 100-yr orifice prior to the overflow outlet entering the mixed flow or orifice flow zones; the overflow outlet is in the weir flow zone for the entire range in which it controls the flow.

The 100-yr orifice installed downstream of the overflow outlet performs several valuable functions for the EDB:

1. First and foremost, this improves the safety of the outlet structure by minimizing the possibility of a drowning by becoming pinned to the grate as the result of the suction force accompanying greater ponding depths and orifice flow. This pinning phenomenon was reported by Guo and Jones in the ASCE Journal of Irrigation and Drainage Engineering in February 2010.
2. The flow rate from the EDB must be limited to the 100-yr flow so that open channels or piping systems downstream of the EDB outlet are not overwhelmed.
3. The 100-yr orifice makes calculating the flow from the overflow outlet less complicated because the flow would remain primarily in the weir flow zone. Discharge calculations from the EDB would transfer to using the 100-yr orifice before utilizing the overflow outlet as an orifice.
4. The 100-yr orifice would prevent the overflow outlet from reaching an unstable oscillating water surface with associated unstable outflows that could not be accurately calculated from the EDB stage.

The limiting action of the 100-year orifice on the overflow outlet is shown as the blue line in in Figure 48.

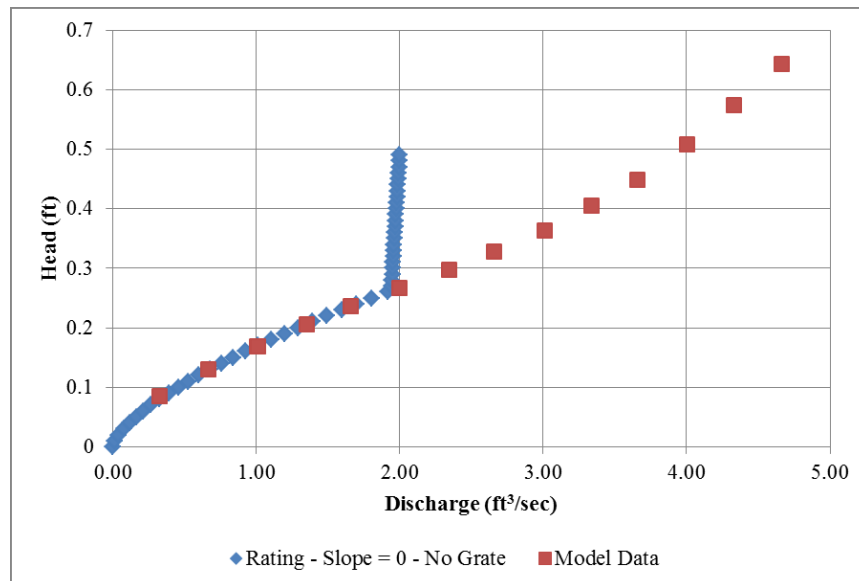


Figure 48. Final calculated stage discharge plot showing the flow from the 100-year orifice acting with the overflow in blue and the overflow outlet acting alone in red, using data for a 1:0 (H:V) slope with no grate.

Flows entering the outlet structure become very turbulent between the overflow outlet and the 100-yr orifice. Under these circumstances, it was necessary to determine whether using a standard orifice discharge coefficient of 0.61 would yield accurate discharge calculations from the 100-yr orifice. Data from the physical model were used to determine that the coefficient in the model was 0.60. When calculating flow from the 100-yr orifice, head relative to the center of the orifice was used.

When calculating flow through an overflow outlet, a clogging factor is recommended by UDFCD which is a reduction factor to represent typical clogging. To this clogging factor, an additional factor is added to represent the reduction in area caused by the grates. For the USBR study, it was determined that it would be more appropriate to use a discharge coefficient to account for the reduction in flow caused by the grate and have a separate clogging factor to account for debris clogging. By creating custom discharge coefficients from the physical model data for each grate and slope, the physical model data were able to be matched to the weir equations provided by Guo in Table 2. Discharge coefficients for each slope and grate are shown in Table 4. These discharge coefficients are used in the equations presented in Table 5 (adapted from Guo) to calculate the flow from the overflow outlet structure; variable locations are shown in Figure 49.

Table 4. Discharge coefficients for each slope and grate.

<b><u>100-yr Orifice Coefficient</u></b>	
0.60	100-yr orifice
<b><u>Overflow Outlet Coefficient, <math>C_d</math></u></b>	
0.64	1:0 (H:V) Slope - No Grate
0.62	1:0 (H:V) Slope - Close Mesh
0.60	1:0 (H:V) Slope - Type C
0.68	4:1 (H:V) Slope - No Grate
0.63	4:1 (H:V) Slope - Close Mesh
0.62	4:1 (H:V) Slope - Type C
0.68	3:1 (H:V) Slope - No Grate
0.60	3:1 (H:V) Slope - Close Mesh
0.58	3:1 (H:V) Slope - Type C

Table 5. Equations to determine discharge from the EDB overflow outlet, adapted from Guo et al.

Flow Type	Equation
100-yr orifice	$Q_o = C_o A_o \sqrt{2gH}$
Flat Weir	$Q_{Flat} = \frac{2}{3} n C_d (2B + 2L) \sqrt{2g} H^{\frac{3}{2}}$
Sloped Un-Submerged Weir ( $H < H_b$ )	$Q_{WS} = \frac{4}{15} n C_d \sqrt{2g} \cot(\theta) H^{\frac{5}{2}}$ $Q_{WB} = \frac{2}{3} n C_d \sqrt{2g} B H^{\frac{3}{2}}$ $Q_W = 2Q_{WS} + Q_{WB}$
Sloped Submerged Weir ( $H \geq H_b$ )	$Q_{WS} = \frac{4}{15} n C_d \sqrt{2g} L \cos(\theta) \left[ \frac{H^{\frac{5}{2}} - (H - H_b)^{\frac{5}{2}}}{H_b} \right]$ $Q_{WB} = \frac{2}{3} n C_d \sqrt{2g} B H^{\frac{3}{2}}$ $Q_W = 2Q_{WS} + Q_{WB}$

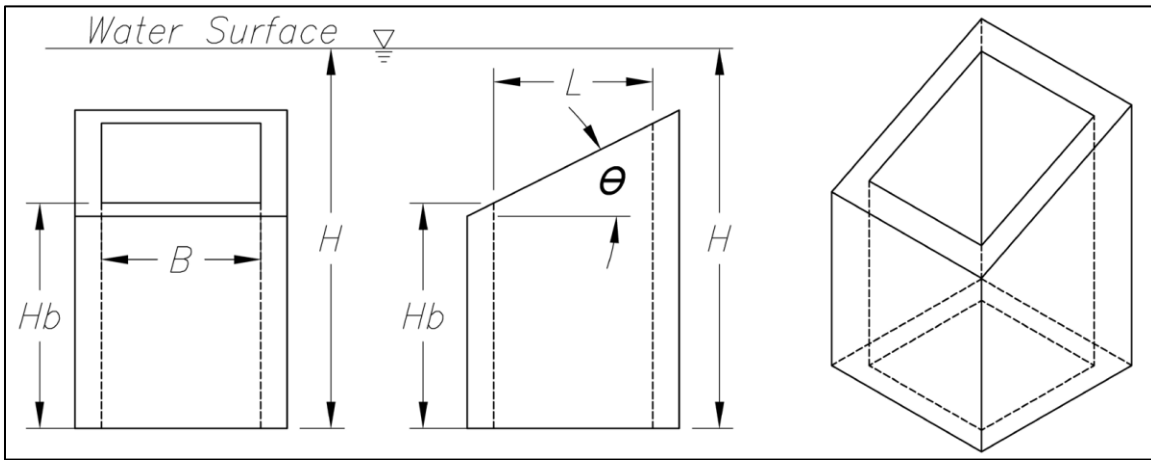


Figure 49. Locations of variables used in Table 5 equations.

The USBR used Guo’s weir-flow equations to calculate flow over only three sides of the overflow outlet, based on the assumption that flow over the top edge is considered negligible because the head acting on this section is limited by the overland flow across the ground surface.

For the 1:0 (H:V) horizontal case, this assumption is not realistic because flow can enter equally from all four sides. This is the result of these outlets typically not being installed in the bank of the EDB and do not have surrounding topography. When modeling the complete EDB, two different water quality orifice options were tested: a series of orifice holes and an elliptical weir configuration. The elliptical weir configuration is desirable from a debris standpoint because the orifice holes have a tendency to clog when floating debris enters the EDB, however, the elliptical slot will be prone to clogging if the width of the slot is insufficient to pass small debris (a minimum slot of 3/8-inch (0.375-inch) is recommended) . Figure 45 shows at higher depths of ponding, the elliptical weir will release more flow from the EDB than the orifice configuration, but that at lower depths of ponding, the opposite condition is true. In theory, this should result in better water quality from the elliptical slot weir as compared to the orifice plate since the discharge curve more closely follows the gradation-based settling velocity curve as defined by Stokes Law. Significant water quality testing would be necessary to demonstrate this theory however, and that was not included in the scope of this project.

## **5. DEVELOPMENT OF NEW DESIGN SOFTWARE**

Directly as the result of the work completed by ARCADIS, CSU, and the USBR, major improvements were made to the UD-Detention and UD-FSD design workbooks. In their new state, these freeware design workbooks are powerful software tools for CDOT and its consultants to apply to the hydrologic and hydraulic design of extended detention basins, bioretention BMPs, sand filtration BMPs, constructed treatment wetlands, and retention ponds. These workbooks apply regression equations to user-inputted watershed data to size a suite of inflow hydrographs representing common probabilistic recurrence intervals. These inflow hydrographs are then routed through a modeled facility using the Modified Puls reservoir routing method, allowing the user to experiment with different control volumes and outlet configurations in order to achieve the desired drain times and target maximum discharge rates.

### **5.1 Mathematical Model of a Detention Basin**

In order to apply the Modified Puls reservoir routing method to a detention facility, two things are essential:

1. A stage-storage or stage-area table or equation, and

2. A stage-discharge table or equation.

For final design, the stage-area data set is readily available from the grading plans, but in the planning or conceptual design stage, the engineer must make some basic assumptions regarding the volume and shape of the basin. To this end, a set of equations and methods to model proposed detention basins, with stage-storage relationships that produce realistic draining characteristics, were developed. In addition to the UD-Detention and UD-FSD design workbooks, these methods can be used in other reservoir routing programs such as HEC-HMS and HEC-1; TR-20/TR-55; HEC-RAS unsteady flow; SWMM (including PC-SWMM and XP-SWMM); ICPR, PondPack, HydroCAD, and Hydraflow. These methods are appropriate for modeling proposed flood and/or stormwater quality detention basins in watershed planning studies. The mathematical model of a detention basin includes the initial surcharge volume, the basin floor volume, and the main basin volume. The sum of all these is the total basin volume. The initial surcharge volume is represented as:

$$ISV = 0.003WQCV A_{ISV} = \frac{ISV}{ISD} \quad (40)$$

$$L_{ISV} = \sqrt{A_{ISV}} \quad (41)$$

$$W_{ISV} = \sqrt{A_{ISV}} \quad (42)$$

Where  $ISV$  is the initial surcharge volume ( $\text{ft}^3$ ),  $A_{ISV}$  is  $ISV$  surface area ( $\text{ft}^2$ ),  $ISD$  is the initial surcharge depth (ft, typically 0.33 to 0.50), and  $L_{ISV}$  and  $W_{ISV}$  are the length and width of the  $ISV$  (ft). The basin floor volume is expressed as:

$$L_{floor} = L_{ISV} + \frac{H_{floor}}{S_{TC}} + H_{floor}(S_{main}) \quad (43)$$

$$W_{floor} = W_{ISV} + \frac{H_{floor}}{R_{L,W}(S_{TC})} \quad (44)$$

$$A_{floor} = L_{floor}(W_{floor}) \quad (45)$$

$$V_{floor} = \frac{H_{floor}}{3} \left( A_{ISV} + A_{floor} + \sqrt{A_{ISV}(A_{floor})} \right) \quad (46)$$

Where  $L_{floor}$  and  $W_{floor}$  (ft) are the length and width of the basin floor section at the point where the top of the basin floor section meets the toe of the basin main section,  $H_{floor}$  is the depth of the basin floor section (ft),  $S_{TC}$  is the trickle channel slope (ft/ft),  $S_{main}$  is the side slope of the basin main section (H:V; e.g., 4 if the H:V ratio is 4:1),  $R_{L,W}$  is the basin length-to-width ratio (e.g., 2 if

the basin length is twice the basin width),  $A_{floor}$  is top area of the basin floor section (ft<sup>2</sup>), and  $V_{floor}$  is volume of the basin floor section (ft<sup>3</sup>). The main basin volume is represented as:

$$L_{main} = L_{floor} + 2H_{main}(S_{main}) \quad (47)$$

$$W_{main} = W_{floor} + 2H_{main}(S_{main}) \quad (48)$$

$$A_{main} = L_{main}(W_{main}) \quad (49)$$

$$V_{main} = \frac{H_{main}}{3} \left( A_{main} + A_{floor} + \sqrt{A_{main}(A_{floor})} \right) \quad (50)$$

Where  $L_{main}$  and  $W_{main}$  (ft) are the length and width of the main basin section at the point at the top of the basin,  $H_{main}$  is the depth of the main basin section (ft),  $A_{main}$  is top area of the main basin section (ft<sup>2</sup>), and  $V_{main}$  is volume of the main basin section (ft<sup>3</sup>). The total basin volume is the sum of the individual volumes:

$$V_{total} = ISV + A_{ISV}(D_{TC}) + V_{floor} + V_{main} \quad (51)$$

Where  $V_{total}$  is the total basin volume (ft<sup>3</sup>) and  $D_{TC}$  is the depth of the trickle channel (ft).

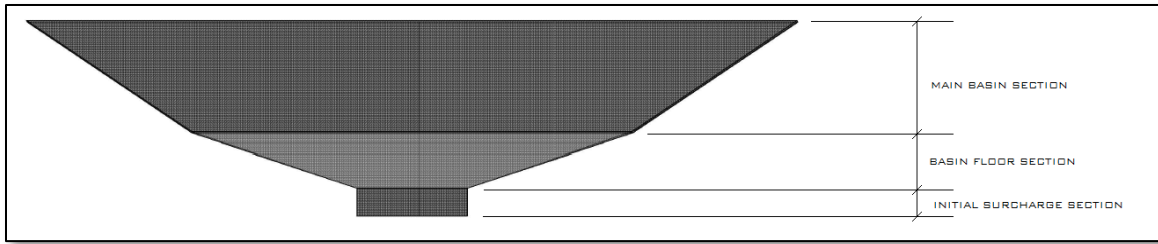


Figure 50. Front view of detention basin model.

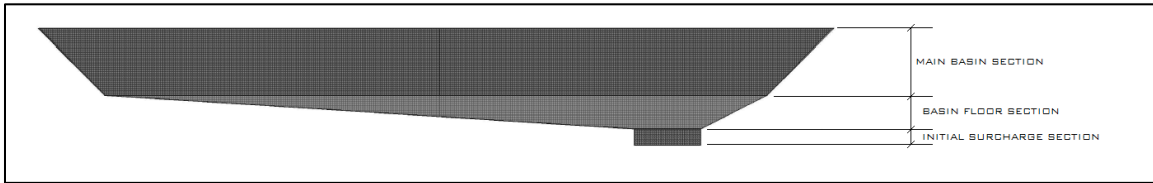


Figure 51. Side view of detention basin model.

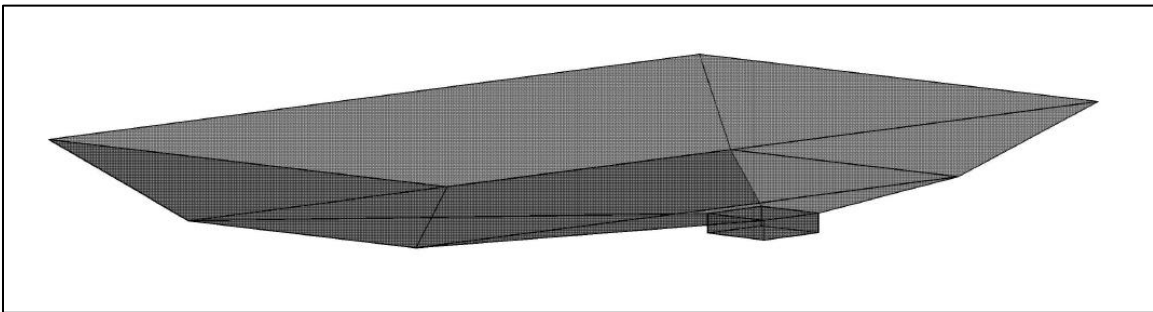


Figure 52. Axonometric projection of detention basin model.

## 5.2 Sizing of Runoff Volumes and Required Storage Volumes

The runoff volume equations developed in this memorandum were based on Colorado Urban Hydrograph Procedure (CUHP 2005, v1.4.4) modeling and one-hour rainfall depths in the Rainfall chapter of the USDCM. CUHP is a Snyder-based unit hydrograph program that temporally distributes the one-hour rainfall depth into a design storm to create runoff hydrographs for the 2-, 5-, 10-, 25-, 50-, 100, and 500-year recurrence intervals as well as the WQCV- and EURV-sized storms. CUHP was used to evaluate over 2,000 subcatchments from recent UDFCD master planning studies. Watershed characteristics (e.g., size, shape, slope, location of centroid, and imperviousness) were taken directly from the master planning studies. Various combinations of Soil Type (A, B, and C/D) were evaluated for each subcatchment.

By performing a multiple regression analysis on those CUHP subcatchments, equations were developed for the 2-, 5-, 10-, 25-, 50-, 100- and 500-yr return periods for each hydrologic soil group and combined to provide the following watershed runoff equations:

$$V_{Runoff\_2yr} = P_1A[(0.084I^{1.440})A\% + (0.084I^{1.173})B\% + (0.084I^{1.094})CD\%] \quad (52)$$

$$V_{Runoff\_5yr} = P_1A[(0.084I^{1.350})A\% + (0.077I + 0.007)B\% + (0.070I + 0.014)CD\%] \quad (53)$$

$$V_{Runoff\_10yr} = P_1A[(0.085I^{1.220})A\% + (0.069I + 0.016)B\% + (0.061I + 0.024)CD\%] \quad (54)$$

$$V_{Runoff\_25yr} = P_1A[(0.082I + 0.004)A\% + (0.055I + 0.031)B\% + (0.048I + 0.038)CD\%] \quad (55)$$

$$V_{Runoff\_50yr} = P_1A[(0.078I + 0.009)A\% + (0.049I + 0.038)B\% + (0.044I + 0.043)CD\%] \quad (56)$$

$$V_{Runoff\_100yr} = P_1A[(0.073I + 0.015)A\% + (0.043I + 0.045)B\% + (0.038I + 0.050)CD\%] \quad (57)$$

$$V_{Runoff\_500yr} = P_1A[(0.064I + 0.025)A\% + (0.036I + 0.053)B\% + (0.031I + 0.058)CD\%] \quad (58)$$

Where  $V_{Runoff\_#yr}$  is the runoff volume for the given return period (acre-feet),  $P_1$  is the one-hour rainfall depth (inches),  $A$  is the contributing watershed area (acres),  $I$  is the percentage imperviousness (expressed as a decimal), and  $A\%$ ,  $B\%$ , and  $CD\%$  are the percent of each hydraulic soil group (also expressed as a decimal). It should be noted that these equations are a mix of linear and power functions, and as shown in these equations, a watershed's runoff volume for a given return period is a function of the watershed's area, imperviousness, and soil type.

In order to develop estimated storage volume equations, the UD-FSD workbook was used to model full spectrum detention basins. UD-FSD v.1.09 was run for watershed areas of 5-, 10-, 20-, 40-, 60-, and 100-acres at 33%, 67%, and 100% imperviousness. Design storms included the 2-, 5-, 10-, 25-, 50-, and 100-year return period. Hydrologic soil groups A, B, and C/D were evaluated separately. WQCV drain times of 40 hours, 24 hours, and 12 hours were also evaluated (resulting in a total of 972 model runs). The resulting maximum required storage volumes were divided by the corresponding runoff hydrograph volume and those ratios were recorded.

For each return period, the average storage/runoff ratio was plotted vs. imperviousness for each of the three hydrologic soil groups and a power regression was applied as shown in Figure 53 for the 100-year return period. Similar power regression plots were developed for the other five return periods also.

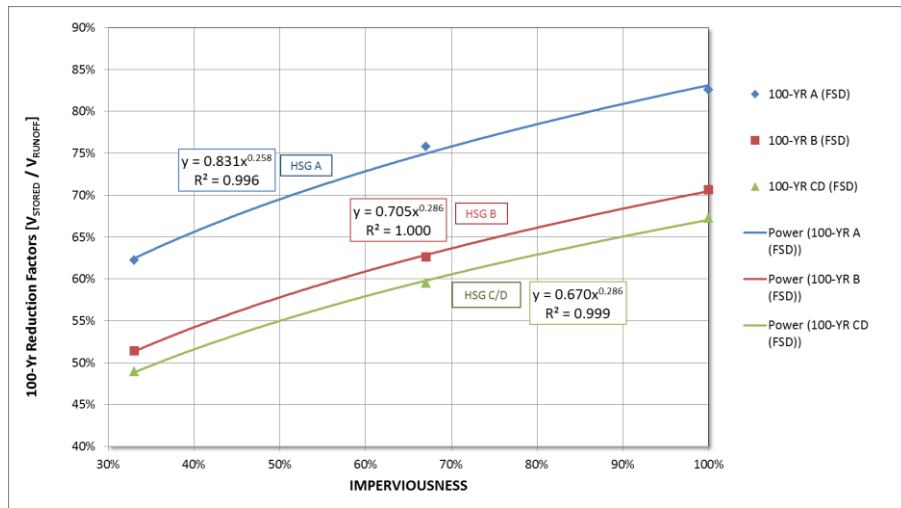


Figure 53. 100-yr Power regression equations for ratio of stored volume to runoff volume as a function of hydrologic soil group and imperviousness.

The resulting storage/runoff ratio equations were then multiplied by the runoff volume equations (converted to watershed inches instead of acre-feet as expressed in Equations 52-58) to develop new storage volume equations. The resulting storage volume equations (in acre-feet) are shown in Equations 59 through 64. The same process was repeated for WQCV drain times of 24 hours and 12 hours. The results were almost identical since the WQCV is such a small percentage of the total detention volume. Therefore, the equations developed for the 40-hour WQCV drain time are considered suitable for all WQCV drain times.

$$V_{Storage\_2yr}(ac - ft) = P_1A[(0.081I^{1.458})A\% + (0.080I^{1.183})B\% + (0.080I^{1.104})CD\%] \quad (59)$$

$$V_{Storage\_5yr}(ac - ft) = P_1A[(0.081I^{1.368})A\% + (0.075I^{1.098} + 0.007I^{0.098})B\% + (0.066I^{1.226} + 0.013I^{0.226})CD\%] \quad (60)$$

$$V_{Storage\_10yr}(acft) = P_1A[(0.082I^{1.237})A\% + (0.063I^{1.254} + 0.015I^{0.254})B\% + (0.052I^{1.371} + 0.021I^{0.371})CD\%] \quad (61)$$

$$V_{Storage\_25yr}(ac - ft) = P_1A[(0.075I^{1.246} + 0.004I^{0.246})A\% + (0.045I^{1.409} + 0.025I^{0.409})B\% + (0.036I^{1.438} + 0.029I^{0.438})CD\%] \quad (62)$$

$$V_{Storage\_50yr}(ac - ft) = P_1A[(0.067I^{1.291} + 0.008I^{0.291})A\% + (0.036I^{1.368} + 0.028I^{0.368})B\% + (0.031I^{1.346} + 0.030I^{0.346})CD\%] \quad (63)$$

$$V_{Storage\_100yr}(ac - ft) = P_1A[(0.061I^{1.258} + 0.012I^{0.258})A\% + (0.030I^{1.286} + 0.032I^{0.286})B\% + (0.025I^{1.286} + 0.034I^{0.286})CD\%] \quad (64)$$

Where  $V_{STORAGE\_#yr}$  is the storage volume (acre-feet),  $P_1$  is the one-hour rainfall depth corresponding to the return period (in),  $A$  is the watershed area in acres,  $I$  is the percentage imperviousness (expressed as a decimal), and  $A\%$ , and  $B\&CD\%$  are the percent of each hydraulic soil group (expressed as a decimal). A comparison of the 100-yr runoff and storage volumes are shown in Figure 54.

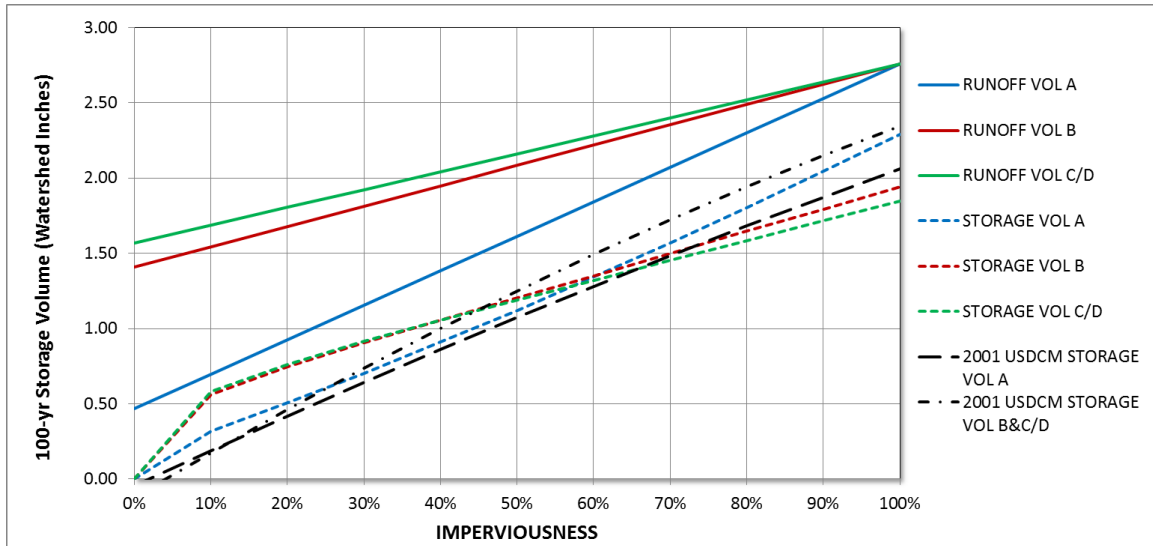


Figure 54. Plot of 100-yr runoff volumes and storage volumes.

### 5.3 Shaping of Inflow Hydrographs

As described in Section 5.2, the volume of the runoff inflow hydrograph is a function of the watershed size, imperviousness, and soil type. The shape this volume takes is primarily a

function of the CUHP design storm distribution, which, in turn is manipulated in CUHP according to the watershed shape factor and slope. In each of the UD-Detention and UD-FSD workbooks, there is a hidden library of over 16,000 inflow hydrographs. The program selects one of these hydrographs for each recurrence interval based on the user’s runoff volume input parameters. Because every inflow hydrograph in the hidden library was created in CUHP using default parameters of watershed shape factor ( $\text{length}^2 / \text{area}$ ) = 2 and watershed slope = 2%, it is necessary to reshape these hydrographs based on the modeled watershed’s specific shape factor and slope. The routine developed to achieve this was developed by running CUHP for watersheds of equal area, imperviousness, and soil type but varying the shape factor from 1 to 4 and varying the slope from 0.5% to 4%. The peak flow rate from each of these tests was then compared to the peak flow rate from CUHP with the default shape factor and slope parameters as a ratio of specific peak flow rate / default peak flow rate.

Plotting these ratios vs. shape factor of 1, 2, 3, and 4 for each slope or 0.5%, 1.0%, 1.5%, 2.0%, 2.5%, 3.0%, and 4.0% provided a family of seven curves for which further regression analysis could be performed in order to create the power regression equation of the form:

$$\text{Hydrograph Constant} = \alpha(\text{Shape}^\beta) \tag{65}$$

Where  $\alpha$  is the leading coefficient and  $\beta$  is the exponent of the power regression equation. The values for  $\alpha$  and  $\beta$  are shown in Table 6, the shape of the curves is shown in Figure 55, and the plots of  $\alpha$  and  $\beta$  are shown I Figure 56.

Table 6. Leading coefficient  $\alpha$  and exponent  $\beta$ .

<i>Slope</i>	$\alpha$	$\beta$
0.5	1.0013	-0.304
1.0	1.1093	-0.298
1.5	1.1706	-0.291
2.0	1.2138	-0.284
2.5	1.2391	-0.275
3.0	1.2695	-0.273
4.0	1.3118	-0.263

### Detention Basin Alternative Outlet Design Study

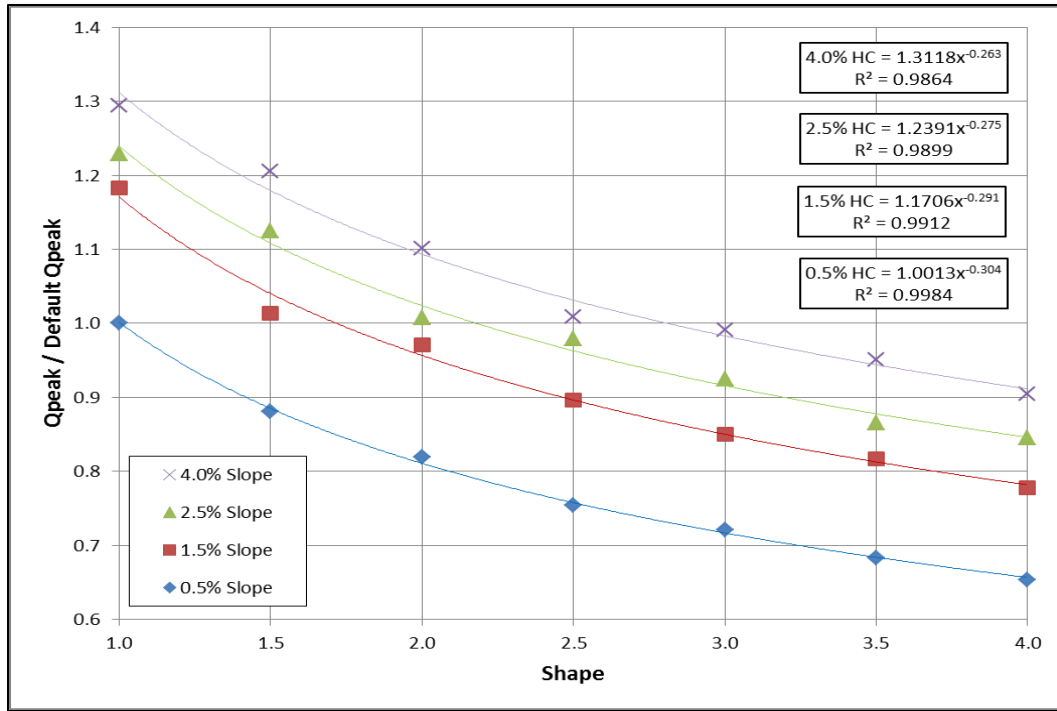


Figure 55. Plot of hydrograph constants vs. shape factors for various slopes.

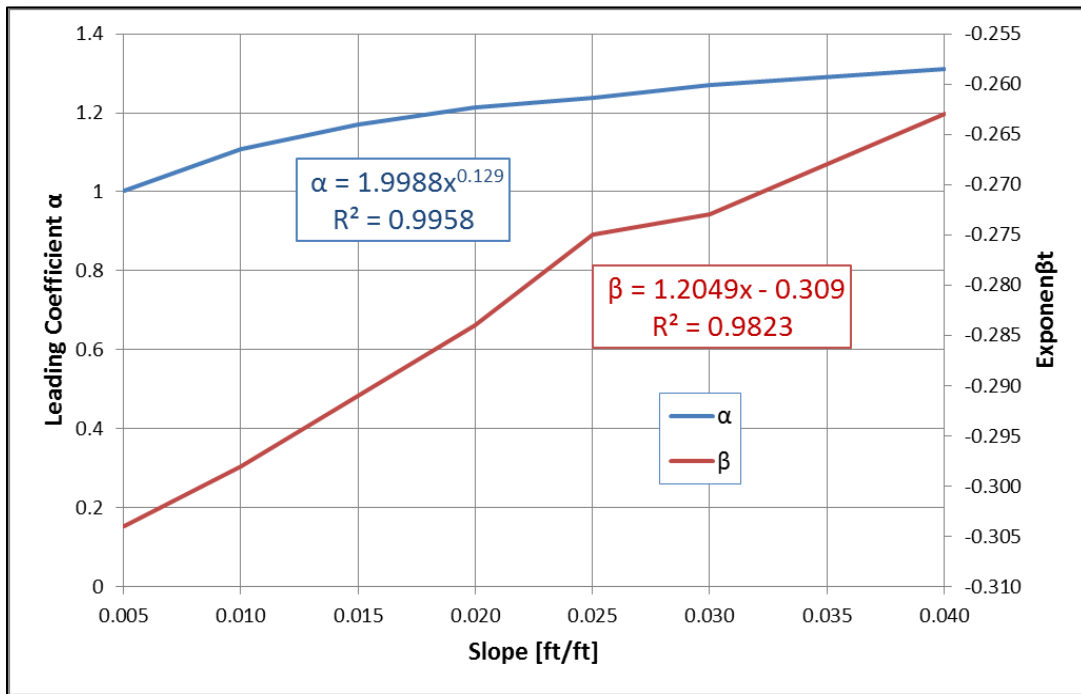


Figure 56. Plot of leading coefficient  $\alpha$  and exponent  $\beta$  vs. watershed slope.

Performing regression analysis on the curves of  $\alpha$  and  $\beta$  in Figure 56 provides a power equation to represent  $\alpha$  and  $\beta$  and a linear equation to represent  $\beta$ , as:

$$\alpha = 2.03(\text{Slope}^{0.13}) \tag{66}$$

$$\beta = 1.2(\text{Slope}) - 0.31 \tag{67}$$

Combining Eqs. 66 and 67 with Eq. 65 provides the final form of the hydrograph constant:

$$\text{Hydrograph Constant} = 2.03(\text{Slope}^{0.13})(\text{Shape}^{(1.2(\text{Slope})-0.31)}) \tag{68}$$

To make the shape adjustment to each of the recurrence interval inflow hydrographs while conserving the volume of those hydrographs, the UD-Detention and UD-FSD programs multiply each incremental flow rate by the hydrograph constant while dividing the standard 5-minute time step by the same hydrograph constant. Watersheds shorter and/or steeper than those with the default shape factor of 2 and slope of 2% will produce higher flow rates at each time step with a shorter standard time step, while the opposite condition will occur with longer and/or flatter watersheds, as demonstrated in Figure 57.

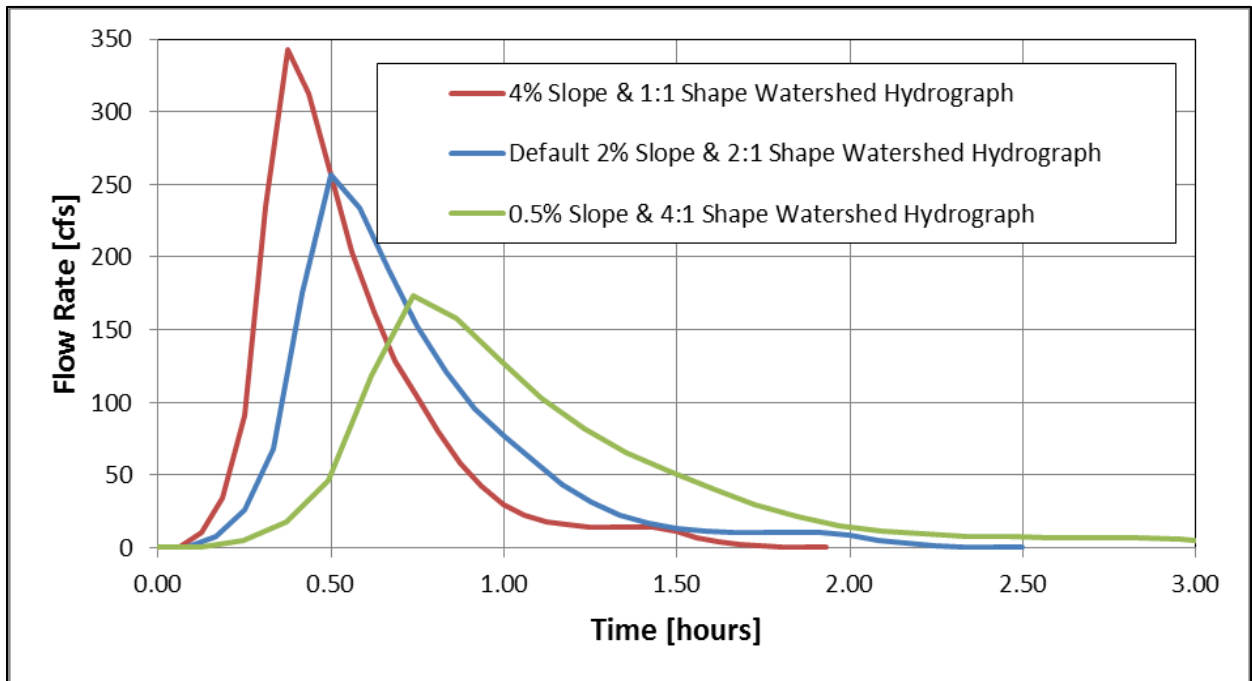


Figure 57. These three hydrographs have different flow rates at each time step based on watershed shape factor and slope, but all have the same volume (i.e., the area under the curve) based on the watershed area, imperviousness, and soil.

#### 5.4 Using the UD-Detention Workbook Model

UDFCD has created three design workbooks to assist CDOT and others in a simplified design method for extended detention basins. The SDI (Statutory Detention and Infiltration) Design Data workbook was specifically created to allow CDOT and others to demonstrate statutory compliance with the new Colorado state law described in Section 6. UD-FSD provides tools to design a full spectrum detention (FSD) basin only. UD-Detention can be used for FSD basins but can also be used for EDBs, bioretention BMPs, sand filter BMPs, constructed treatment wetlands, and retention ponds. It is the most versatile of the three workbooks and also the most complicated, and for those reasons this section will cover the UD-Detention model. Once familiar with the UD-Detention model, the other two workbooks will be easily understood. The UD-Detention workbook is an extremely powerful design tool, featuring nearly 7,000 lines of Visual Basic programming code to aid the designer in creating a stormwater management facility.

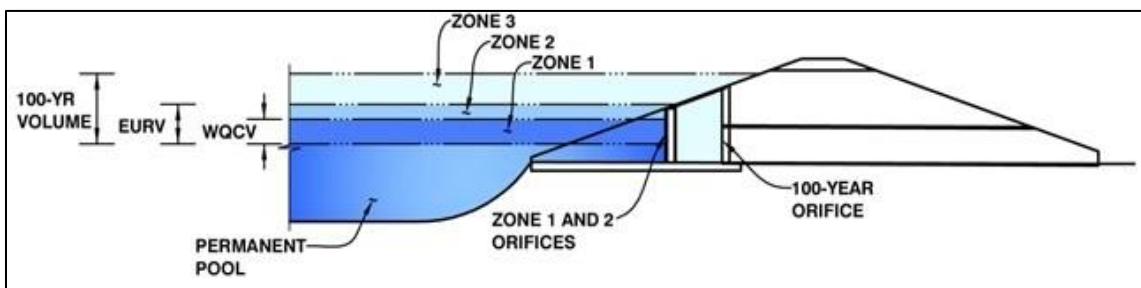


Figure 58. UD-Detention figure showing the three design zones.

#### 5.41 Basin Worksheet

The UD-Detention workbook has two main worksheets, the Basin sheet and the Outlet Structure sheet. The Basin worksheet allows the user to size the storage volume of the basin based on mathematical model described in Section 5.1, Equations 40 through 51 and the runoff and required storage volumes presented in Section 5.2, Equations 52 through 64. In order for this process to initiate, the user must enter basic stormwater treatment type parameters and watershed

parameters as shown in Figure 61, and stormwater treatment facility parameters as shown in Figure 62.

There are two dropdown menus on the Basin worksheet; the “Select BMP Type” dropdown menu shown in Figure 59, and the “Location for 1-hr Rainfall Depths” dropdown menu shown in Figure 60. The choices for the latter dropdown are all within the UDFCD boundary area, but there is an option to select “User Input” from this dropdown and then manually enter the appropriate one-hour rainfall depths. From NOAA Atlas 14 in the user input rainfall depth cells.

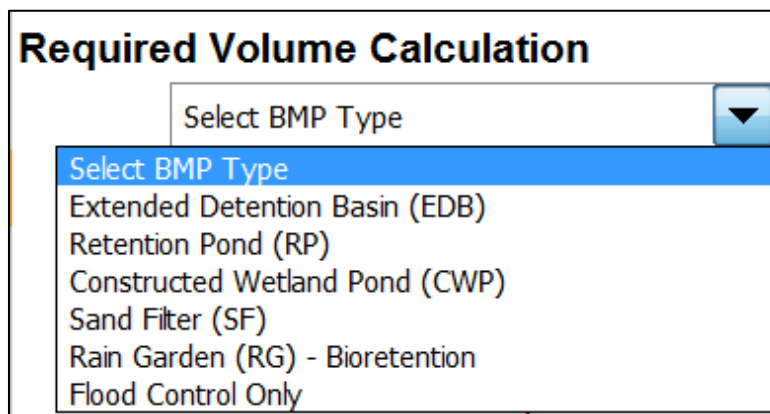


Figure 59. “Select BMP Type” dropdown menu.

Location for 1-hr Rainfall Depths =		User Input
Water Quality Capture Volume (WC)		UDFCD Default
Excess Urban Runoff Volume (EU)		Aurora - Town Center at Aurora
2-yr Runoff Volume (P1 = 0.9)		Aurora Reservoir
5-yr Runoff Volume (P1 = 1.3)		Boulder - University of Colorado
10-yr Runoff Volume (P1 = 1.5)		Brighton - Brighton City Hall
25-yr Runoff Volume (P1 = 1.9)		Broomfield - Broomfield City Manager
50-yr Runoff Volume (P1 = 2.2)		Commerce City
100-yr Runoff Volume (P1 = 2.5)		D.I.A.
500-yr Runoff Volume (P1 = 3.2)		Denver - Capitol Hill
Approximate 2-yr Detention Volume		Eldorado Springs
Approximate 5-yr Detention Volume		Front Range Airport
Approximate 10-yr Detention Volume		Golden - School of Mines
Approximate 25-yr Detention Volume		Greenwood Village - Greenwood Village City Hall
		Highlands Ranch - Highlands Ranch Mansion
		Ken Caryl - Chatfield High School
		Lakewood - Lakewood Cultural Center
		Littleton - Arapahoe Community College
		Morrison - Red Rocks Amphitheater
		Parker - Parker Town Court
		Roxborough Park
		Sedalia
		Thornton - Thornton City Office
		Westminster - Westminster City Hall
		User Input

Figure 60. "Location for 1-hr Rainfall Depths" dropdown menu.

Detention Basin Alternative Outlet Design Study

Required Volume Calculation		
Extended Detention Basin (EDB) ▼	<b>EDB</b>	
Watershed Area =	50.00	acres
Watershed Length =	2,087	ft
Watershed Slope =	0.020	ft/ft
Watershed Imperviousness =	50.00%	percent
Percentage Hydrologic Soil Group A =	0.0%	percent
Percentage Hydrologic Soil Group B =	0.0%	percent
Percentage Hydrologic Soil Groups C/D =	100.0%	percent
Desired WQCV Drain Time =	40.0	hours
Location for 1-hr Rainfall Depths =	Commerce City ▼	
Water Quality Capture Volume (WQCV) =	0.859	acre-feet
Excess Urban Runoff Volume (EURV) =	2.365	acre-feet
2-yr Runoff Volume (P1 = 0.95 in.) =	1.869	acre-feet
5-yr Runoff Volume (P1 = 1.36 in.) =	3.332	acre-feet
10-yr Runoff Volume (P1 = 1.56 in.) =	4.251	acre-feet
25-yr Runoff Volume (P1 = 1.99 in.) =	6.169	acre-feet
50-yr Runoff Volume (P1 = 2.24 in.) =	7.280	acre-feet
100-yr Runoff Volume (P1 = 2.6 in.) =	8.970	acre-feet
500-yr Runoff Volume (P1 = 3.23 in.) =	11.870	acre-feet
Approximate 2-yr Detention Volume =	1.768	acre-feet
Approximate 5-yr Detention Volume =	2.674	acre-feet
Approximate 10-yr Detention Volume =	2.835	acre-feet
Approximate 25-yr Detention Volume =	3.452	acre-feet
Approximate 50-yr Detention Volume =	4.009	acre-feet
Approximate 100-yr Detention Volume =	4.958	acre-feet

Optional User Input  
1-hr Precipitation

	inches

Figure 61. User-entered treatment type and watershed design parameters (blue cells) and calculated results (white cells) in the UD-Detention Basin sheet.

Detention Basin Alternative Outlet Design Study

Stage-Storage Calculation		
Zone 1 Volume (WQCV)	0.859	acre-feet
Zone 2 Volume (EURV - Zone 1)	1.506	acre-feet
Zone 3 Volume (100-year - Zones 1 & 2)	2.593	acre-feet
Total Detention Basin Volume =	4.958	acre-feet
Initial Surcharge Volume (ISV) =	112	ft <sup>3</sup>
Initial Surcharge Depth (ISD) =	0.33	ft
Total Available Detention Depth ( $H_{total}$ ) =	8.00	ft
Depth of Trickle Channel ( $H_{TC}$ ) =	0.50	ft
Slope of Trickle Channel ( $S_{TC}$ ) =	0.005	ft/ft
Slopes of Main Basin Sides ( $S_{main}$ ) =	4	H:V
Basin Length-to-Width Ratio ( $R_{L/W}$ ) =	2	
Initial Surcharge Area ( $A_{ISV}$ ) =	337	ft <sup>2</sup>
Surcharge Volume Length ( $L_{ISV}$ ) =	18.4	ft
Surcharge Volume Width ( $W_{ISV}$ ) =	18.4	ft
Depth of Basin Floor ( $H_{FLOOR}$ ) =	0.96	ft
Length of Basin Floor ( $L_{FLOOR}$ ) =	213.7	ft
Width of Basin Floor ( $W_{FLOOR}$ ) =	114.1	ft
Area of Basin Floor ( $A_{FLOOR}$ ) =	24,386	ft <sup>2</sup>
Volume of Basin Floor ( $V_{FLOOR}$ ) =	8,806	ft <sup>3</sup>
Depth of Main Basin ( $H_{MAIN}$ ) =	6.21	ft
Length of Main Basin ( $L_{MAIN}$ ) =	263.4	ft
Width of Main Basin ( $W_{MAIN}$ ) =	163.8	ft
Area of Main Basin ( $A_{MAIN}$ ) =	43,137	ft <sup>2</sup>
Volume of Main Basin ( $V_{MAIN}$ ) =	206,893	ft <sup>3</sup>
Calculated Total Basin Volume ( $V_{total}$ ) =	<b>4.958</b>	acre-feet

Figure 62. User-entered stormwater treatment facility design parameters (blue cells) and calculated results (white cells) in the UD-Detention Basin sheet.

In the UD-Detention workbook, the blue cells are for user input parameters and the white cells are calculated values. After the necessary design parameters are entered as shown in Figures 61 and 62, the program creates a stage-area-volume table of the proposed facility, as shown in Figures 63 through 64.

## Detention Basin Alternative Outlet Design Study

Depth Increment =	0.1	ft							
Stage - Storage Description	Stage (ft)	Optional Override Stage (ft)	Length (ft)	Width (ft)	Area (ft <sup>2</sup> )	Optional Override Area (ft <sup>2</sup> )	Area (acre)	Volume (ft <sup>3</sup> )	Volume (ac-ft)
<b>Micropool</b>	0.00		18.4	18.4	337		0.008		
<b>ISV</b>	0.33		18.4	18.4	337		0.008	111	0.003
	0.40		18.4	18.4	337		0.008	132	0.003
	0.50		18.4	18.4	337		0.008	165	0.004
	0.60		18.4	18.4	337		0.008	199	0.005
	0.70		18.4	18.4	337		0.008	233	0.005
	0.80		18.4	18.4	337		0.008	266	0.006
	0.90		30.0	24.1	722		0.017	311	0.007
	1.00		50.4	34.1	1,717		0.039	429	0.010
	1.10		70.8	44.1	3,119		0.072	667	0.015
	1.20		91.2	54.1	4,930		0.113	1,067	0.024
	1.30		111.6	64.1	7,149		0.164	1,667	0.038
	1.40		132.0	74.1	9,776		0.224	2,510	0.058
	1.50		152.4	84.1	12,811		0.294	3,636	0.083
	1.60		172.8	94.1	16,254		0.373	5,086	0.117
	1.70		193.2	104.1	20,104		0.462	6,900	0.158
<b>Floor</b>	1.79		213.6	114.1	24,363		0.559	9,120	0.209
	1.80		213.6	114.1	24,363		0.559	9,120	0.209
	1.90		214.5	114.9	24,647		0.566	11,572	0.266
	2.00		215.3	115.7	24,911		0.572	14,050	0.323
	2.10		216.2	116.6	25,203		0.579	16,806	0.386
	2.20		217.0	117.4	25,470		0.585	19,340	0.444
	2.30		217.8	118.2	25,738		0.591	21,900	0.503
	2.40		218.6	119.0	26,008		0.597	24,487	0.562
	2.50		219.4	119.8	26,278		0.603	27,102	0.622
	2.60		220.2	120.6	26,550		0.610	29,743	0.683
	2.70		221.0	121.4	26,824		0.616	32,412	0.744
	2.80		221.8	122.2	27,098		0.622	35,108	0.806
<b>Zone 1 (WQCV)</b>	2.89		222.5	122.9	27,346		0.628	37,558	0.862
	2.90		222.6	123.0	27,374		0.628	37,831	0.868
	3.00		223.4	123.8	27,651		0.635	40,583	0.932
	3.10		224.2	124.6	27,929		0.641	43,362	0.995
	3.20		225.0	125.4	28,209		0.648	46,168	1.060
	3.30		225.8	126.2	28,490		0.654	49,003	1.125
	3.40		226.6	127.0	28,772		0.661	51,867	1.191
	3.50		227.4	127.8	29,056		0.667	54,758	1.257
	3.60		228.2	128.6	29,340		0.674	57,678	1.324
	3.70		229.0	129.4	29,627		0.680	60,626	1.392
	3.80		229.8	130.2	29,914		0.687	63,603	1.460
	3.90		230.6	131.0	30,202		0.693	66,609	1.529
	4.00		231.4	131.8	30,492		0.700	69,644	1.599
	4.10		232.2	132.6	30,784		0.707	72,707	1.669
	4.20		233.0	133.4	31,076		0.713	75,800	1.740
	4.30		233.8	134.2	31,370		0.720	78,923	1.812
	4.40		234.6	135.0	31,665		0.727	82,074	1.884
	4.50		235.4	135.8	31,961		0.734	85,256	1.957
	4.60		236.2	136.6	32,259		0.741	88,467	2.031
	4.70		237.0	137.4	32,557		0.747	91,707	2.105
	4.80		237.8	138.2	32,858		0.754	94,978	2.180
	4.90		238.6	139.0	33,159		0.761	98,279	2.256
	5.00		239.4	139.8	33,462		0.768	101,610	2.333
<b>Zone 2 (EURV)</b>	5.05		239.8	140.2	33,613		0.772	103,287	2.371
	5.10		240.2	140.6	33,766		0.775	104,971	2.410
	5.20		241.0	141.4	34,071		0.782	108,363	2.488
	5.30		241.8	142.2	34,377		0.789	111,785	2.566
	5.40		242.6	143.0	34,685		0.796	115,239	2.646
	5.50		243.4	143.8	34,994		0.803	118,723	2.725
	5.60		244.2	144.6	35,305		0.810	122,238	2.806
	5.70		245.0	145.4	35,616		0.818	125,784	2.888
	5.80		245.8	146.2	35,929		0.825	129,361	2.970
	5.90		246.6	147.0	36,243		0.832	132,969	3.053
	6.00		247.4	147.8	36,559		0.839	136,610	3.136
	6.10		248.2	148.6	36,876		0.847	140,281	3.220
	6.20		249.0	149.4	37,194		0.854	143,985	3.305
	6.30		249.8	150.2	37,513		0.861	147,720	3.391
	6.40		250.6	151.0	37,834		0.869	151,487	3.478
	6.50		251.4	151.8	38,156		0.876	155,287	3.565
	6.60		252.2	152.6	38,479		0.883	159,119	3.653
	6.70		253.0	153.4	38,803		0.891	162,983	3.742
	6.80		253.8	154.2	39,129		0.898	166,879	3.831
	6.90		254.6	155.0	39,456		0.906	170,808	3.921
	7.00		255.4	155.8	39,784		0.913	174,770	4.012
	7.10		256.2	156.6	40,114		0.921	178,765	4.104
	7.20		257.0	157.4	40,445		0.928	182,793	4.196
	7.30		257.8	158.2	40,777		0.936	186,854	4.290
	7.40		258.6	159.0	41,110		0.944	190,949	4.384
	7.50		259.4	159.8	41,445		0.951	195,076	4.478
	7.60		260.2	160.6	41,781		0.959	199,238	4.574
	7.70		261.0	161.4	42,118		0.967	203,433	4.670
	7.80		261.8	162.2	42,457		0.975	207,661	4.767
	7.90		262.6	163.0	42,796		0.982	211,924	4.865
<b>Zone 3 (100-year)</b>	8.00		263.4	163.8	43,137		0.990	216,221	4.964

Figure 63. Stage-area-volume table created by UD-Detention program based on user inputs.

## Detention Basin Alternative Outlet Design Study

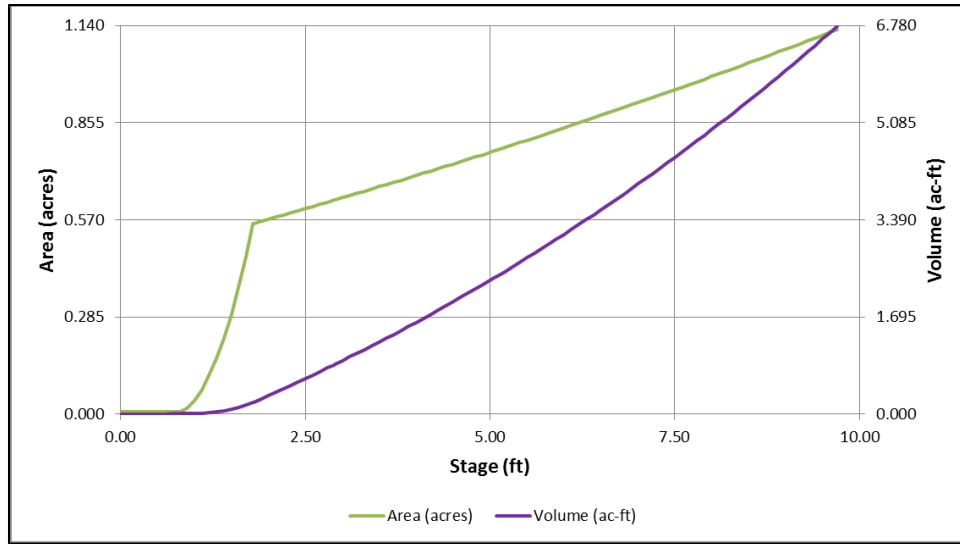


Figure 64. Graphical representation of tabulated data in Figure 63 prepared by UD-Detention program based on user inputs.

Once the required information has been entered in the Basin worksheet, the calculations automatically create the stage-area-volume table based on the required storage volume, the given maximum depth, basin slope, side slopes, and length-to-width ratio. There will be cases where no mathematical solution is available that can satisfy all of the given constraints. When this happens, the program will notify the user as shown in Figure 65. The user can then select “Yes” and allow the program to incrementally flatten the detention basin trickle channel slope until a mathematical solution is available, or the user can select “No” and manually change any of the aforementioned design constraint parameters.

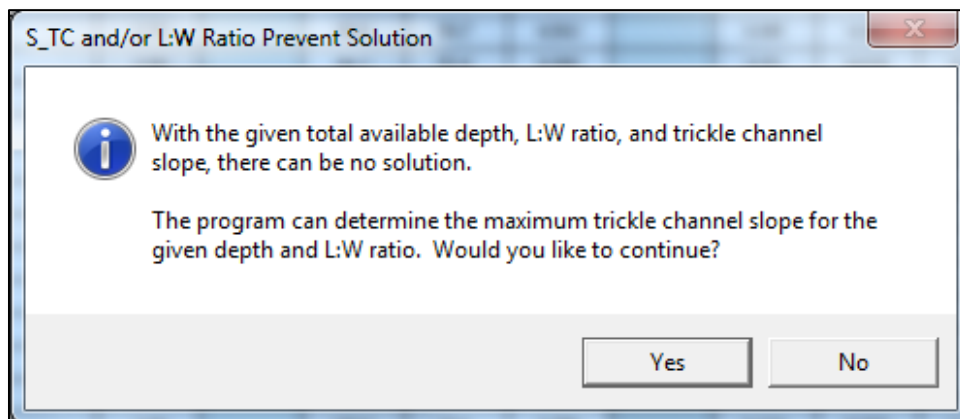


Figure 65. Example of built-in automation assists the user in sizing the storage volume.

### 5.42 Outlet Structure Worksheet

When the Basin worksheet user inputs have been satisfied and the program has been run, the user can proceed to the Outlet Structure worksheet. This worksheet is divided into 9 visible and 2 hidden (but optionally viewable) sections, including:

1. Basic information as to how the three zones will be drained,
2. Information specific to the EURV and/or WQCV orifice plate or elliptical slot weir,
3. Optional additional information regarding up to sixteen water quality drain orifices,
4. Optional vertical orifice information,
5. Overflow outlet weir and grate information,
6. 100-year (or other design event) orifice and restrictor plate information,
7. Emergency spillway information,
8. Routed hydrograph results,
9. Optional user-defined inflow hydrograph table,
10. Hidden (but optionally viewable) stage-storage-discharge result table, and
11. Hidden (but optionally viewable) Modified Puls reservoir routing table.

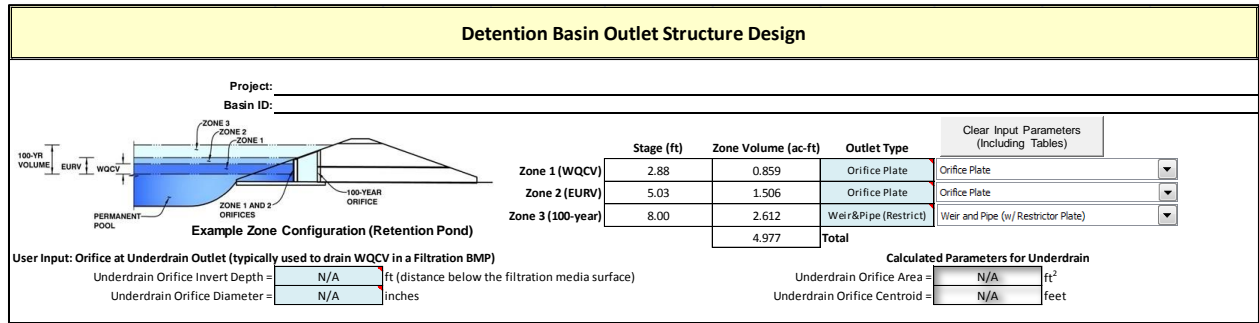


Figure 66. Outlet Structure Worksheet Section 1, showing user selections for Zones 1, 2, and 3.

Because EDB was selected as the BMP treatment method on the Basin worksheet in Figure 66, the underdrain user input (blue) cells are left blank.

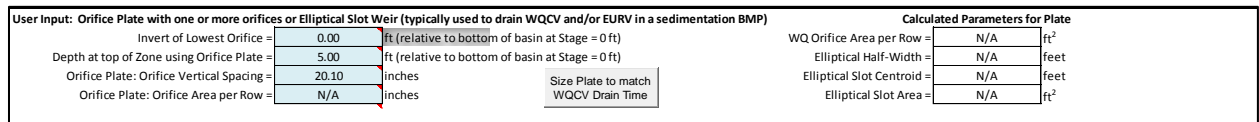


Figure 67. Outlet Structure Worksheet Section 2, showing user selections for water quality orifice placement and sizing in order to drain zones 1 and 2.

Detention Basin Alternative Outlet Design Study

In Figure 67, previous selection of the elliptical slot weir in Section 1 had resulted in a slot with a gap of less than 0.375 inches, which would have been prone to clogging. The user then selected the orifice plate consisting of 3 orifices spaced 20.1 inches on center vertically. The Area per Row value is N/A because the user overrode the top orifice area as shown in Figure 68.

User Input: Stage and Total Area of Each Orifice Row (numbered from lowest to highest)							
	Row 1 (required)	Row 2 (optional)	Row 3 (optional)	Row 4 (optional)	Row 5 (optional)	Row 6 (optional)	Row 7 (optional)
Stage of Orifice Centroid (ft)	0.00	1.67	3.33				
Orifice Area (sq. inches)	4.19	4.19	12.00				
	Row 9 (optional)	Row 10 (optional)	Row 11 (optional)	Row 12 (optional)	Row 13 (optional)	Row 14 (optional)	Row 15 (optional)
Stage of Orifice Centroid (ft)							
Orifice Area (sq. inches)							

Figure 68. Outlet Structure Worksheet Section 3, showing the stage and area of the three water quality (EURV and WQCV) draining orifices.

In Figure 68, note that the user overrode the top orifice area in order to drain the storage volumes in compliance with the new Colorado statutory requirements (described in Section 6 of this report). Typically, only the first three rows will be used for the three required water quality orifices. The other 13 rows are solely for the purpose of analyzing an existing facility designed before the current recommendations became operative.

User Input: Vertical Orifice (Circular or Rectangular)			Calculated Parameters for Vertical Orifice		
	Not Selected	Not Selected		Not Selected	Not Selected
Invert of Vertical Orifice =	N/A	N/A	ft (relative to bottom of basin at Stage = 0 ft)	Vertical Orifice Area =	N/A
Depth at top of Zone using Vertical Orifice =	N/A	N/A	ft (relative to bottom of basin at Stage = 0 ft)	Vertical Orifice Centroid =	N/A
Vertical Orifice Diameter =	N/A	N/A	inches		

Figure 69. Outlet Structure Worksheet Section 4, showing the optional vertical orifice input and calculation cells.

Figure 69 shows Section 4, where the user can add a vertical orifice to assist in shaping the drawdown curve to meet the design intent. The vertical orifice is optional and for most EDBs will not be used.

User Input: Overflow Weir (Dropbox) and Grate (Flat or Sloped)			Calculated Parameters for Overflow Weir		
	Zone 3 Weir	Not Selected		Zone 3 Weir	Not Selected
Overflow Weir Front Edge Height, H <sub>o</sub> =	5.00	N/A	ft (relative to bottom of basin at Stage = 0 ft)	Height of Grate Upper Edge, H <sub>g</sub> =	7.00
Overflow Weir Front Edge Length =	8.00	N/A	feet	Over Flow Weir Slope Length =	8.25
Overflow Weir Slope =	4.00	N/A	H:V (enter zero for flat grate)	Grate Open Area / 100-yr Orifice Area =	9.22
Horiz. Length of Weir Sides =	8.00	N/A	feet	Overflow Grate Open Area w/o Debris =	46.18
Overflow Grate Open Area % =	70%	N/A	% grate open area / total area	Overflow Grate Open Area with Debris =	23.09
Debris Clogging % =	50%	N/A	%		

Figure 70. Outlet Structure Worksheet Section 5, showing the design parameter inputs and calculations for the overflow outlet and grate.

In Figure 70, the user inputs the design parameters for the overflow outlet and grate in the blue cells, while preliminary calculations are completed in the white cells. The work by Guo et al., as discussed in Section 4.2 of this report, provided the mathematical expressions to calculate the flow through an inclined overflow outlet grate.

User Input: Outlet Pipe w/ Flow Restriction Plate (Circular Orifice, Restrictor Plate, or Rectangular Orifice)			Calculated Parameters for Outlet Pipe w/ Flow Restriction Plate				
	Zone 3 Restrictor	Not Selected		Zone 3 Restrictor	Not Selected		
Depth to Invert of Outlet Pipe =	3.00	N/A	ft (distance below bottom of basin at Stage = 0 ft)	Outlet Orifice Area =	5.01	N/A	ft <sup>2</sup>
Outlet Pipe Diameter =	36.00	N/A	inches	Outlet Orifice Centroid =	1.12	N/A	feet
Restrictor Plate Height Above Pipe Invert =	24.00		inches	Restrictor Plate on Pipe =	1.91	N/A	radians
			Size Outlet Plate to match 90% of Predevelopment 100-year Peak Runoff Rate				

Figure 71. Outlet Structure Worksheet Section 6, showing the design parameter inputs and calculations for the 100-year (or other design event) orifice.

Figure 71 shows Section 6, where the user can size the 100-year (or other design event) orifice. An optional button can be clicked to run a sizing program that will automatically size the 100-year restrictor plate or orifice plate in order to meter the design flow at 90% of the estimated predeveloped flow rate. This estimated flow rate is explained in a technical memorandum titled “*Determination of Watershed Predeveloped Peak Unit Flow Rates as the Basis for Detention Basin Design*” and posted on the UDFCD web site at [www.udfcd.org](http://www.udfcd.org). This orifice is in the bottom of the outlet structure and acts as the final flow control to prevent downstream flooding during the design event.

User Input: Emergency Spillway (Rectangular or Trapezoidal)			Calculated Parameters for Spillway		
Spillway Invert Stage =	9.10	ft (relative to bottom of basin at Stage = 0 ft)	Spillway Design Flow Depth =	0.97	feet
Spillway Crest Length =	67.00	feet	Stage at Top of Freeboard =	11.07	feet
Spillway End Slopes =	4.00	H:V	Basin Area at Top of Freeboard =	1.25	acres
Freeboard above Max Water Surface =	1.00	feet			
			Size Emergency Spillway to pass Developed 100-yr Peak Runoff Rate		

Figure 72. Outlet Structure Worksheet Section 7, showing the design parameter inputs and calculations for the emergency spillway. A 500-year inflow hydrograph is supplied to be routed through this spillway.

Figure 72 shows Section 7, the input cells and preliminary calculations for the emergency spillway. This spillway is typically sized to pass the undetained 100-year inflow hydrograph at a depth of one foot. An optional button can be clicked to run a sizing program that will automatically size the spillway to meet these design constraints.

## Detention Basin Alternative Outlet Design Study

Routed Hydrograph Results									
	WQCV	EURV	2 Year	5 Year	10 Year	25 Year	50 Year	100 Year	500 Year
Design Storm Return Period									
One-Hour Rainfall Depth (in)	0.53	1.07	0.95	1.34	1.64	2.02	2.32	2.61	3.29
Calculated Runoff Volume (acre-ft)	0.859	2.365	1.869	3.283	4.469	6.262	7.540	9.005	12.091
OPTIONAL Override Runoff Volume (acre-ft)									
Inflow Hydrograph Volume (acre-ft)	0.859	2.365	1.868	3.283	4.469	6.256	7.540	9.002	12.086
Predevelopment Unit Peak Flow, q (cfs/acre)	0.00	0.00	0.02	0.32	0.54	1.02	1.29	1.61	2.24
Predevelopment Peak Q (cfs)	0.0	0.0	0.8	16.1	27.1	50.9	64.4	80.5	112.0
Peak Inflow Q (cfs)	19.1	52.4	41.4	73.1	99.8	139.9	168.7	201.3	269.8
Peak Outflow Q (cfs)	0.4	1.1	0.9	8.4	25.1	54.8	72.5	75.5	114.0
Ratio Peak Outflow to Predevelopment Q	N/A	N/A	N/A	0.5	0.9	1.1	1.1	0.9	1.0
Structure Controlling Flow	Plate	Plate	Plate	Overflow Gate 1	Overflow Gate 1	Overflow Gate 1	Outlet Plate 1	Outlet Plate 1	Spillway
Max Velocity through Gate 1 (fps)	N/A	N/A	N/A	0.2	0.5	1.2	1.5	1.6	1.7
Max Velocity through Gate 2 (fps)	N/A	N/A	N/A	N/A	N/A	N/A	N/A	N/A	N/A
Time to Drain 97% of Inflow Volume (hours)	40	66	60	69	69	69	69	69	69
Time to Drain 99% of Inflow Volume (hours)	40	66	60	69	69	70	70	70	70
Maximum Ponding Depth (ft)	2.79	4.85	4.21	5.58	6.15	6.77	7.16	7.93	9.40
Area at Maximum Ponding Depth (acres)	0.62	0.76	0.72	0.81	0.85	0.90	0.93	0.99	1.11
Maximum Volume Stored (acre-ft)	0.798	2.220	1.748	2.794	3.268	3.810	4.176	4.904	6.441

Figure 73. Outlet Structure Worksheet Section 8, the final output table showing the design parameter inputs and calculations for the emergency spillway. A 500-year inflow hydrograph is supplied to be routed through this spillway.

In Figure 73, all of the results from the preliminary calculations and the hidden Modified Puls reservoir routing tables are reported in Section 8 for the user’s analysis. If the results are satisfactory, the work is complete. If the results are not satisfactory, the user can go back to any of the preceding sections and modify those inputs to adjust the results in this table.

Detention Basin Outlet Structure Design										
Reset hydrographs to default values from workbook		Outflow Hydrograph Workbook Filename:								
Storm Inflow Hydrographs		<input type="checkbox"/> Use relative path name					Export Outflow Hydrographs to a blank workbook for later use in a downstream UD-Detention Workbook			
The user can override the calculated inflow hydrographs from this workbook with inflow hydrographs developed in a separate program.										
	SOURCE	WORKBOOK	WORKBOOK	WORKBOOK	WORKBOOK	WORKBOOK	WORKBOOK	WORKBOOK	WORKBOOK	WORKBOOK
Time Interval	TIME	WQCV [cfs]	EURV [cfs]	2 Year [cfs]	5 Year [cfs]	10 Year [cfs]	25 Year [cfs]	50 Year [cfs]	100 Year [cfs]	500 Year [cfs]
5.00 min	0:00:00	0.00	0.00	0.00	0.00	0.00	0.00	0.00	0.00	0.00
	0:05:00	0.03	0.08	0.06	0.10	0.13	0.17	0.19	0.21	0.26
Hydrograph Constant	0:10:00	1.00	2.43	2.00	3.17	4.01	5.15	5.89	6.66	8.14
	0:15:00	2.48	6.38	5.13	8.61	11.35	15.29	18.00	20.99	27.03
1.000	0:20:00	6.85	17.39	14.05	23.29	30.47	40.69	47.68	55.36	70.85
	0:25:00	17.26	44.13	35.58	59.30	77.90	104.50	122.77	142.86	183.58
	0:30:00	19.10	52.42	41.38	73.09	99.79	139.94	168.69	201.30	269.79
	0:35:00	16.33	45.83	36.01	64.22	88.20	124.65	151.13	181.68	246.68
	0:40:00	13.20	37.40	29.34	52.44	72.11	102.09	123.87	148.91	202.28
	0:45:00	10.58	29.91	23.48	41.89	57.55	81.42	98.71	118.53	160.68
	0:50:00	8.33	23.64	18.54	33.17	45.65	64.71	78.54	94.39	128.17
	0:55:00	6.60	18.71	14.68	26.21	36.06	51.12	62.06	74.59	101.32
	1:00:00	5.43	15.18	11.95	21.18	29.10	41.26	50.08	60.18	81.72
	1:05:00	3.91	11.20	8.76	15.81	21.96	31.46	38.41	46.42	63.57
	1:10:00	2.93	8.32	6.53	11.66	16.07	22.84	27.78	33.47	45.67
	1:15:00	2.04	5.88	4.59	8.31	11.54	16.53	20.18	24.38	33.38
	1:20:00	1.48	4.21	3.30	5.91	8.15	11.60	14.11	17.01	23.21
	1:25:00	1.15	3.26	2.55	4.56	6.29	8.93	10.86	13.06	17.77
	1:30:00	0.94	2.64	2.08	3.69	5.07	7.18	8.71	10.47	14.20
	1:35:00	0.84	2.32	1.83	3.22	4.41	6.23	7.55	9.05	12.24
	1:40:00	0.80	2.21	1.74	3.07	4.19	5.88	7.10	8.49	11.43
	1:45:00	0.78	2.16	1.70	3.00	4.08	5.72	6.90	8.25	11.09
	1:50:00	0.78	2.16	1.70	3.00	4.08	5.71	6.88	8.21	11.03
	1:55:00	0.78	2.16	1.70	3.00	4.08	5.71	6.88	8.21	11.03
	2:00:00	0.51	1.49	1.16	2.13	2.99	4.32	5.29	6.43	8.86
	2:05:00	0.30	0.88	0.68	1.24	1.73	2.49	3.05	3.71	5.13
	2:10:00	0.17	0.50	0.39	0.72	1.00	1.45	1.78	2.16	2.99
	2:15:00	0.09	0.27	0.21	0.39	0.54	0.78	0.96	1.17	1.61
	2:20:00	0.04	0.13	0.10	0.19	0.27	0.40	0.50	0.61	0.86
	2:25:00	0.01	0.04	0.03	0.06	0.09	0.15	0.19	0.23	0.34
	2:30:00	0.00	0.00	0.00	0.00	0.00	0.01	0.02	0.03	0.05
	2:35:00	0.00	0.00	0.00	0.00	0.00	0.00	0.00	0.00	0.00

Figure 74. Outlet Structure Worksheet Section 9, the optional user-input inflow hydrograph table.

Figure 74 shows Section 9, the optional user-input inflow hydrograph table. If the user chooses not to allow the program to select from the hidden library of over 16,000 inflow hydrographs, custom inflow hydrographs may be entered in this table. A limitation with this option is that all of the hydrographs entered must have a common time interval. The heading at the top of each column changes from “Workbook” to “User” when the hydrograph in that column does not exactly match the hydrograph from the hidden library.

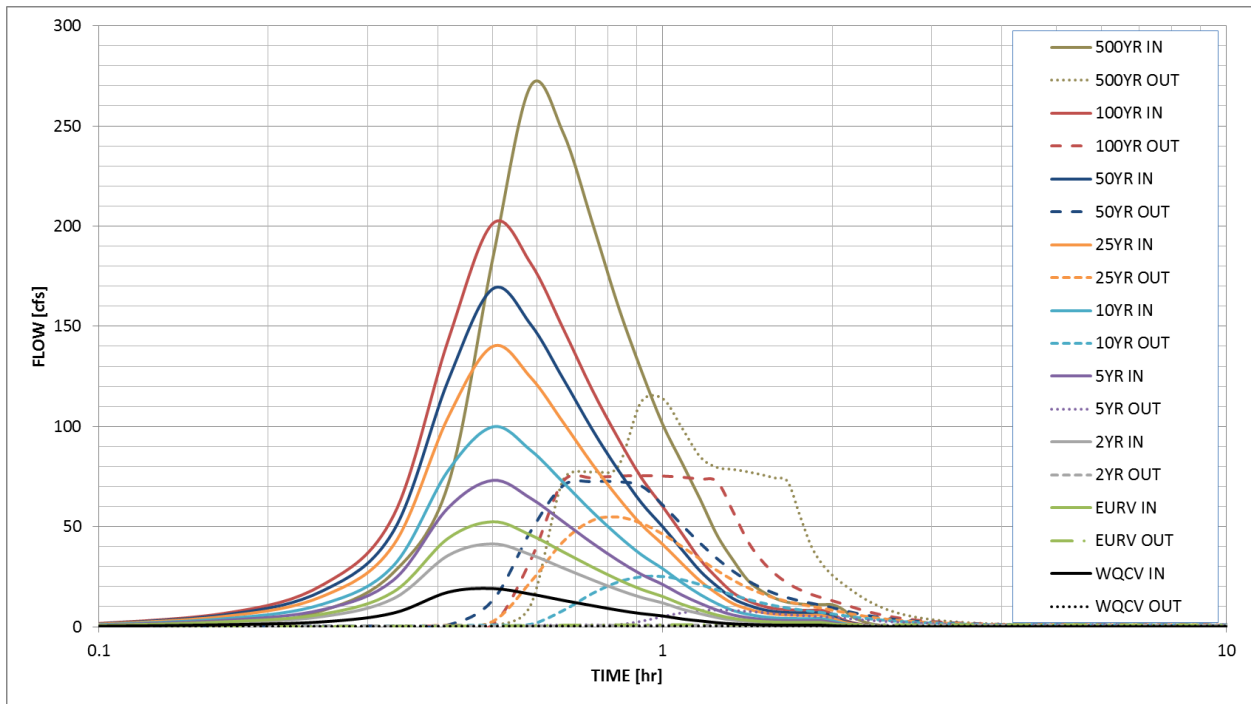


Figure 75. The Outlet Structure Worksheet includes graphs detailing the performance of the stormwater management facility, such as this graph depicting the inflow hydrographs and the resulting detained outflow hydrographs from the facility. Note that the abscissa axis scale is logarithmic.

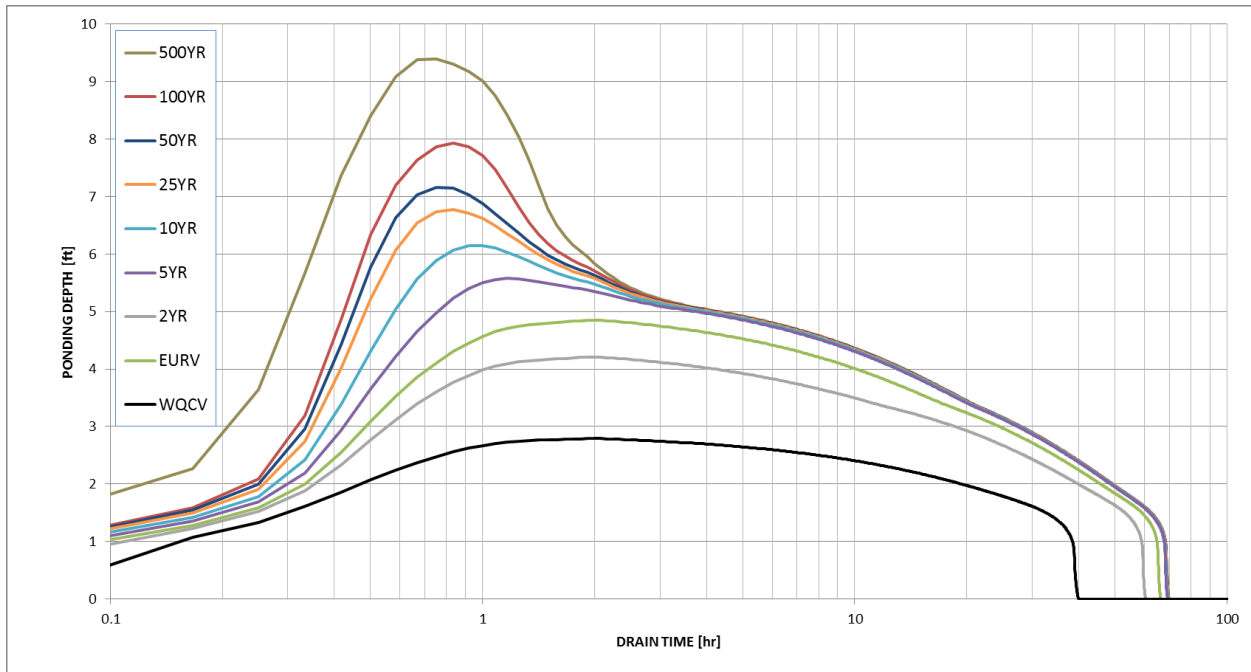


Figure 76. This Outlet Structure Worksheet graph depicts the ponding depth over time in the stormwater management facility for seven recurrence intervals plus the WQCV- and EURV-sized storms. Note that the abscissa axis scale is logarithmic.

Due to the complexity and magnitude of Section 10 (the stage-storage-discharge table), and Section 11 (the Modified Pulse reservoir routing tables), they cannot be shown as Figures in this report. While by default, the figures are hidden in the Outlet Structure Worksheet. The buttons below Section 8 (the routed results table) can allow the user to click and to make them visible for inspection and/or exporting to another application. Figure 75 shows the built-in graphing of the final inflow and outflow hydrographs, while Figure 76 shows the built-in graphing of the stormwater management facility’s ponding depth over time—information critical to demonstrate compliance with the new Colorado state statute as described in the next section.

## 6. RELEVANT NEW STATUTORY REQUIREMENTS

Senate Bill 15-212 was signed into law by Governor Hickenlooper in May 2015 and became effective on August 5, 2015 as Colorado Revised Statute (CRS) §37-92-602 (8). This statute provides legal protection for any regional or individual site stormwater detention and infiltration facility in Colorado, provided the facility meets the following criteria:

1. It is owned or operated by a governmental entity or is subject to oversight by a governmental entity (e.g., required under an MS4 permit).
2. It continuously releases or infiltrates at least 97% of all of the runoff from a rainfall event that is less than or equal to a 5-year storm within 72 hours after the end of the event.
3. It continuously releases or infiltrates as quickly as practicable, but in all cases releases or infiltrates at least 99% of the runoff within 120 hours after the end of events greater than a 5-year storm.
4. It operates passively and does not subject the stormwater runoff to any active treatment process (e.g., coagulation, flocculation, disinfection, etc.).
5. If it is in the Fountain Creek (tributary to the Arkansas River) watershed it must be required by or operated in compliance with an MS4 permit.

The statute specifies that runoff treated in stormwater detention and infiltration facilities shall not be used for any other purpose by the owner/operator/overseer (or that entity's assignees), shall not be released for subsequent diversion or storage by the owner/operator/overseer (or that entity's assignees), and shall not be the basis for a water right or credit.

There are specific notification requirements that apply to all new stormwater detention and infiltration facilities, including individual site facilities built by private parties as a development requirement. For any stormwater detention and infiltration facility constructed after August 5, 2015 and seeking protection under the new statute, the "entity that owns, operates, or has oversight for" shall, prior to operation of the facility, provide notice to all parties on the substitute water supply plan notification email list maintained by the State Engineer. This notice must include the following:

1. The location.
2. The approximate surface area at design volume.
3. Data that demonstrate that the facility has been designed to comply with the release rates described in Items 2 and 3 above.

The Colorado Division of Water Resources (DWR) maintains seven email lists, one for each of the seven major watersheds in Colorado (these coincide with the seven DWR Divisions). UDFCD worked with DWR and the Colorado Stormwater Council to develop a simple data sheet and an online map-based compliance portal website that will allow all municipalities and counties in Colorado to easily upload this required notification information. The website application will then automatically send email notifications to the proper recipients, relieving public works staff of the emailing burden while also minimizing the volume of email going out to the email list recipients.

The notification requirement applies only to new stormwater facilities (constructed after August 5, 2015), which the statute provides a “rebuttable presumption” of non-injury to water rights. This rebuttable presumption is contestable but only by comparison to the runoff that would have been generated from the undeveloped land condition prior to the development necessitating the stormwater facility.

Stormwater facilities in existence before August 5, 2015 are defined in the statute as materially non-injurious to water rights and do not require notification. Additionally, the State issued a memorandum on February 11, 2016 indicating that construction BMPs and non-retention BMPs do not require notice pursuant to SB-212 and are allowed at the discretion of the Division Engineer, and that green roofs are allowable as long as they intercept only precipitation that falls within the perimeter of the vegetated area and do not intercept or consume concentrated flow nor store water below the root zone. The DWR Statement can be found here:

<http://water.state.co.us/DWRIPub/Documents/DWR%20Storm%20Water%20Statement.pdf>

The compliance portal can be found here:

<https://maperture.digitaldataservices.com/gyh/?viewer=cswdif>

A tutorial YouTube video and a list of frequently asked questions (FAQs) can also be accessed from that website. UDFCD has worked closely with CDOT’s water quality staff toward making this process as streamlined as possible.

## 7. CONCLUSION

The purpose of this study was to examine alternative outlet designs for extended detention, particularly the concept of the elliptical slot weir. Traditional design of water quality outlets involved orifice plates with small orifices spaced four inches on center vertically. While the four-inch spacing was initially promulgated in the 1999 Urban Storm Drainage Criteria Manual Volume 3, this was intended to be a minimum dimension and not a standard spacing. But as frequently happens with design criteria, what were intended to be minimums become standards. To protect these small orifices, a well screen was recommended with a large open area compared to the sum of all the water quality orifices. Unfortunately, the well screen was not much better with regard to clogging than were the unprotected orifices.

Through the work with ARCADIS and subsequent work at the Colorado State University Hydraulics Laboratory, design parameters and mathematical equations were created, predicting the flow rate through the elliptical slot weir as a function of ponding depth. At CSU, additional qualitative testing was done to demonstrate the debris handling characteristics of the elliptical slot weir. The admittedly subjective observation of this qualitative testing was that the elliptical slot weir handles debris (particularly plastic bags and straw) better than do orifice plates of equal flow capacity.

The elliptical slot weir is very efficient. With a flow pattern characterized by higher flows at greater ponding depths and lower flows at lower ponding depths performed efficiently as compared to the traditional orifice plate. This is hypothesized to result in better sediment (and associated adsorbed pollutants of concern) removal since it matches more closely the sediment gradation-based settling velocities as defined by Stokes Law. However, the demonstration of this hypothesis was not included in the scope of this effort and it would likely take years of intensive water quality sampling to confirm or disprove this.

What this study did determine is that, while the elliptical slot weir drains and handles debris as well or better than does its orifice plate counterpart, it is too efficient for smaller detention basins, oftentimes resulting in a very narrow and clog-prone slot. The qualitative debris handling investigation in the CSU hydraulics laboratory and the two-year field testing at the Northfield

and U.S. Postal Service detention basins made it clear that while the elliptical slot weir handles debris very well when the slot is wide (say greater than one inch), debris clogging becomes an issue as the slot grows more narrow. Based on these investigations, UDFCD does not recommend an elliptical slot weir having a slot width of less than 3/8-inch. This equates roughly to a WQCV of one acre-ft or larger, assuming a 40-hour drain time; or an excess urban runoff volume (EURV, refer to the USDCM Volume 3 for details on the EURV concept) of 1.6 acre-ft or larger, assuming a 60-hour drain time. Of course, the depth of the storage volume also plays a significant role in the width of the slot.

Upon making these conclusions, the focus of the study turned to answering the question of how best to gravity drain the water quality volume when the elliptical slot width did not meet the minimum criterion. This resulted in the recommendation of limiting the number of water quality orifices to no more than three. These orifices are to be spaced at stage zero,  $H/3$ , and  $2H/3$ , where  $H$  is the maximum ponding depth of the EURV or the WQCV. When the number of orifice is limited to three (as opposed to the traditional three per foot of depth), the size of each orifice becomes larger and therefore less prone to clogging. This also facilitates the application of a bar grate instead of a well screen, which is also less prone to clogging.

This study also took advantage of the availability of the CSU and the USBR hydraulics laboratories to evaluate the stage-discharge characteristics of the overflow outlet structure. Previously, the researchers and CDOT had worked with Dr. James Guo of the University of Colorado on a physical modeling study of CDOT Type C and D grated inlets used in highway medians. With this modeling, Guo developed mathematical expressions to define the stage-discharge characteristics of those inlets. Guo's work was extended to this study as the same grates are commonly used to pass flow through the overflow outlet portion of the detention basin outlet structure. Questions did remain to whether the results from the previous study were truly transferrable to this study so additional work with the USBR confirmed Guo's previous work with some modifications to the orifice and weir coefficients for grate slopes of zero (horizontal), 3:1 (H:V), and 4:1 (H:V).

In order to standardize the elements learned through this research, the development of new design software was undertaken, including research to:

1. Create a mathematical model of a detention basin,
2. Create equations to approximate runoff volumes and required storage volumes,
3. Create a method to shape inflow hydrographs based on the watershed slope and shape factor.

This work in turn led to the creation of three new design workbooks, namely:

1. SDI-Design-Data,
2. UD-FSD,
3. UD-Detention.

The first workbook, SDI-Design-Data.xlsm, is simply a tool that can be used in conjunction with the new compliance website for Colorado Revised Statute (CRS) 37-92-602(8) to demonstrate compliance with the statute. The second workbook, UD-FSD.xlsm facilitates the design of full spectrum detention basins only. For the design of all other stormwater management facilities, the UD-Detention workbook is a very powerful and easy to use design aid that will help the design engineer complete a preliminary volume sizing and outlet configuration to drain the various recurrence interval inflow hydrographs appropriately. UD-Detention can also be used with a grading plan to complete the final analysis of the performance of the facility.

UDFCD is committed to the maintenance and upkeep of these three design aid workbooks and is currently in the process of creating tutorial videos that will be made freely available at [www.udfcd.org](http://www.udfcd.org).

## Detention Basin Alternative Outlet Design Study

## REFERENCES

- ARCADIS (2011). "Calculation of Rating Curves for Three Elliptical Slot Weirs," Internal technical report to UDFCD.
- ARCADIS (2012). "Calculation of Rating Curve for Outlet Box with 3:1 Side Slope," Internal technical report to UDFCD.
- ARCADIS (2012). "Calculation of Rating Curve for Outlet Box with 4:1 Side Slope," Internal technical report to UDFCD.
- ASCE Manual of Practice No. 87 and WEF Manual of Practice No. 23, (1998). "Urban Runoff Quality Management," American Society of Civil Engineers, New York.
- CDOT (2004) "Drainage Design Manual," Colorado of Department of Transportation, Denver, Colorado.
- Comport, B.C., Cox, A. L., and Thornton C. (2010). "Performance Assessment of Grate Inlets for Highway Median Drainage," submitted to UDFCD, Denver, Colorado.
- Flow Science, Inc. (1997), "Sensitivity of Computational Results to Different Computers," FSI-97-TN46, Santa Fe, NM.
- Guo, James C.Y. and MacKenzie, Ken, and Mommandi, A. (2009) "Sump Inlet Hydraulics," ASCE Journal of Hydraulic Engineering, Vol 135, No 11, Nov 2009.
- Guo, James C.Y. (2000). "Design of Grate Inlets with a Clogging Factor," Advances in Environmental Research, Vol 4, Elsevier Science, Ireland.
- Guo, James C.Y. (1999). "Street Hydraulics and Inlet Sizing," published by WRP Company, Littleton, Colorado.
- Guo, James C.Y. (2012). "Off-stream Detention Design for Stormwater Management," ASCE Journal of Irrigation and Drainage Engineering, Vol. 138, No. 4, April 1.
- Guo, James, C.Y., and Jones, Jonathan (2010). "Pinning Force during Closure Process at Blocked Pipe Entrance," ASCE Journal of Irrigation and Drainage Engineering, Vol. 136, No. 2, February 2010.
- Guo, James, C.Y., Urbonas, B., and MacKenzie, Ken (2014). "Water Quality Capture Volume for Storm Water BMP and LID Designs," ASCE Journal of Irrigation and Drainage Engineering, Vol. 19, Issue 4, April 2014.
- Guo, James C.Y. (2004). "Hydrology-Based Approach to Storm Water Detention Design Using New Routing Schemes," ASCE Journal of Hydrologic Engineering, Vol 9, No. 4, July/August
- Guo, James C.Y. (1999). "Detention Basin Sizing for Small Urban Catchments," ASCE Journal of Water Resources Planning and Management, Vol 125, No.6, Nov.
- Guo, James C.Y. and Urbonas, B. (1996). "Maximized Detention Volume Determined by Runoff Capture Rate," ASCE Journal of Water Resources Planning and Management, Vol 122, No 1, Jan.
- HEC 22 (2002) "Urban Drainage Design Manual , US Department of Transportation, Federal Highway Administration, Washington D.C., Virginia.
- Heiner, B.J. (2014). "Physical Modeling of Overflow Outlets for Extended Detention Stormwater Basins," U.S. Department of the Interior Bureau of Reclamation Hydraulic Laboratory Technical Memorandum PAP-1105.

## Detention Basin Alternative Outlet Design Study

MacKenzie, Ken (2010). "Full-Spectrum Detention for Stormwater Quality Improvement and Mitigation of the Hydrologic Impact of Development: A Regionally Calibrated Empirical Design Approach." Master's Degree Thesis, Civil Engineering, University of Colorado Denver, Colorado

MacKenzie, Ken and Stawski, Jason (2014). "Modeling Detention Basins." Urban Drainage and Flood Control District, Denver, Colorado. <http://www.udfcd.org>

MacKenzie, Ken and Rapp, Derek (2015). "Determination of Watershed Predeveloped Peak Unit Flow Rates as the Basis for Detention Basin Design." Urban Drainage and Flood Control District, Denver, Colorado. <http://www.udfcd.org>

USDCM (2016). "Urban Storm Drainage Criteria Manual." Volumes 1 and 2, Urban Drainage and Flood Control District, Denver, Colorado. <http://www.udfcd.org>

UDFCD (2010). "Urban Drainage Criteria Manual." Volume 3, Urban Drainage and Flood Control District, Denver, Colorado. <http://www.udfcd.org>

U.S. Bureau of Reclamation (USBR) (1989). "Hydraulics Laboratory Techniques." U.S. Government Printing Office, Washington D.C

U.S. Department of Commerce, National Oceanic and Atmospheric Administration (NOAA) (2013). "Precipitation-Frequency Atlas of the United States Volume 8 Version 2.0: Midwestern States." U.S. Government Printing Office, Washington D.C